LONDON, METEOROLOGICAL OFFICE.

Met.O.15 Internal Report No.45.

The interpretation of NO2 absorption measured in twilight sky spectra using a multiple scattering model. By McMAHON,B.B.

London,Met.Off.,Met.O.15 Intern.Rep.No.45, 1982,31cm.Pp.36,46 pls.34 Refs.

An unofficial document - not to be quoted in print.

METEOROLOGICAL OFFICE
London Road, Bracknell, Berks.

MET.O.15 INTERNAL REPORT

No. 45

THE INTERPRETATION OF NO_2 ABSORPTION MEASURED IN TWILIGHT SKY SPECTRA USING A MULTIPLE SCATTERING MODEL

by

B B McMAHON

June 1982

Cloud Physics Branch (Met.O.15)

Contents

1. Introduction

Nitrogen dioxide (NO_2) is believed to play an important role in a catalytic chain of reactions which have a controlling effect on stratospheric ozone (Crutzen 1970). Attempts have been made by several workers to measure the atmospheric abundance of the gas by absorption spectroscopy. Most of these measurements were made in the 435-450 nm spectral region, exploiting characteristic structure in the NO_2 absorption cross section to determine the atmospheric abundance from direct solar or twilight sky spectra. Ground, balloon and aircraft-based observing platforms have been employed. Table 1 summarises some of the column NO_2 measurements reported to date. The few observations of the detailed vertical NO_2 distribution (including in-situ measurements) are reviewed elsewhere (Drummond & Jarnot 1978). Reported values of the total vertical column vary from 5×10^{15} to a few $\times 10^{17}$ molecules cm^{-2} and from 1×10^{15} to a few $\times 10^{17}$ molecules cm^{-2} for the stratospheric component. These latter values are obviously of greater interest to modellers of stratospheric ozone photochemistry.

Noxon (1979(a)) with the aid of a computer scattering model, attempted to deduce the stratospheric NO_2 column and 'centre of mass' altitude from a series of ground-based measurements of zenith sky NO_2 absorption over the twilight period. The physical principle involved is similar to that underlying the more familiar Götz 'Umkehr' effect, but there are important differences which will be examined later in the report. On the basis of such sky measurements Noxon reported, somewhat controversially, the existence of a very sharp gradient in stratospheric NO_2 across the boundary of the northern winter circum-polar vortex (Noxon 1979(b)).

The obvious advantages of ground-based stratospheric measurements are their cheapness and convenience compared with aircraft or balloon-based remote or in-situ measurements. Harrison (1979) and Brewer, McElroy & Kerr (1973, 1974) also investigated the possibility of remotely sensing stratospheric NO_2 from the ground, the former utilising Noxon's model results and the latter utilising a single scattering model.

This report examines in some detail the problem of interpreting twilight sky NO_2 absorption, making use of a multiple scattering model of the atmosphere developed specially for the purpose. Model results are compared

with those of other workers and the validity of some of their assumptions and subsequent conclusions tested. The effect on sky absorption of assuming different temperature profiles is also examined. Some preliminary measurements of twilight sky NO_2 absorption, made using the absorption spectroscopy technique at Beaufort Park are interpreted on the basis of model results, and consideration is given to the effects of cloud and large boundary-layer NO_2 concentrations on the absorption measured. Earlier measurements made at Beaufort Park used the direct solar beam, and included a significant tropospheric contribution to the total NO_2 column (McMahon & Simmons 1980 (a), (b)). Ambiguities in interpreting the data arose due to advection of tropospheric NO_2 across the absorbing path.

2. The Measurement of Twilight Sky NO_2 Absorption

The principal sources of atmospheric attenuation in the 435-450 nm wavelength interval are Rayleigh scattering, aerosol scattering, some slight water vapour absorption, ozone absorption (in the wings of the Chappuis band) and nitrogen dioxide (NO_2) absorption. When a ratio is taken of a twilight sky spectrum with a sky spectrum obtained near midday, and sufficient care is taken to ensure wavelength agreement between spectra, the resulting (ratio) spectrum can be analysed for NO_2 absorption, In the present case, spectra were obtained using the scanning spectrometer and data-gathering systems described in an earlier report (McMahon & Simmons 1980(a)). During scanning the spectral intensity was continously normalized with respect to the signal from a broad-band channel (30 nm wide) centred on the spectral wavelength, which scanned at the same rate. The simplified optical arrangement shown in Fig 1 illustrates how this was achieved. Normalization provided an automatic correction for any linear trend in intensity across the spectrum, and compensated well for the gradual secular change in the sky intensity which occurs at twilight. Partial compensation for rapid changes in intensity due to cloud interference was also achieved using this technique. To a good approximation, therefore, ratio spectra were free from the roughly linear effects of Rayleigh and aerosol scattering as well as the linear components of the effects due to other sources of attenuation, such as NO_2 absorption. Neglecting ozone and water vapour absorption, which is usually justifiable, the effective amount of NO_2 (n^{eff}) responsible for the absorption in a ratio spectrum was found by regression, (after first taking the natural logarithm and subtracting the mean value), against the NO_2 absorption cross-section spectrum expressed as a deviation from the best-fit line. The shape of the cross-section spectrum was determined using a carefully purefied NO_2 sample and measuring its absorption with the spectrometer. Wilkerson et al's (1974) cross-sections were used to quantify the spectra. Thus NO_2 was measured by its differential absorption with wavelength; the absolute absorption was not directly measured.

Strictly, the NO_2 absorption thus measured represents a difference between that present in the twilight spectrum and in the midday spectrum, but for reasons which will be explained later, the absorption present in a midday sky spectrum will usually be relatively small. Further, it is the variation of absorption over the twilight period which is of real interest here, and not the absolute value.

Noxon (1979(a), (b), (c)) also measured differential NO_2 absorption in twilight sky spectra, but his method of data analysis was somewhat simpler.

Fig 2 illustrates Noxon's approach to measuring differential absorption. He connected the 437 nm and 448 nm region of his ratio spectra with a straight line and found the difference between that line and the value at 439.5 nm. The corresponding difference in the absorption cross-section ($\Delta\sigma$) was assumed by Noxon to be 2.5×10^{-19} cm^2 (Hall & Blacet, 1952). This straight line method was designed to be insensitive to linear variations in intensity with wavelength, as was the method adopted in the present study. Noxon defined a quantity called the differential absorption (ZN) to be the percentage deviation of the ratio spectrumfrom the above line at 439.5 nm. It is easily shown that

$$ZN = (1 - \exp(-\Delta\sigma\, n^{eff})).100 \qquad (1)$$

where n^{eff} is the effective amount of NO_2, in molecules cm^{-2}, found from the regression analysis of ratio spectra described above. The absolute absorption (AA) due to NO_2 at 439.5 nm is given by

$$AA = \exp(-\sigma n^{eff}) \qquad (2)$$

where σ is the NO_2 cross-section at 439.5 nm.
Substituting for n^{eff} into (1) gives

$$ZN = (1 - AA^{\frac{\Delta\sigma}{\sigma}}).100 \qquad (3)$$

This relationship between ZN and AA was used in the model studies described in section 5(ii) in which Hall & Blacet's (1952) value for $\Delta\sigma$ was assumed, allowing direct quantitative comparison of model results with Noxon's model results. However, since Wilkerson et al's (1974) NO_2 cross-sections were used in the experimental determination of n^{eff}, it was necessary to use their value for $\Delta\sigma$ at 439.5nm (2.4×10^{-19} cm^2) to convert from n^{eff} to ZN (using equation 1).

3. Physics of Twilight Sky NO_2 Absorption

3(i) The Götz Umkehr Effect

In order to relate the NO_2 absorption measured in a sky spectrum to the concentration of the gas in the atmosphere it is necessary to understand the basic scattering and absorption properties of the atmosphere.

Much work has been done in this field, more recently with the aid of computers. An early stimulus to the understanding of atmospheric scattering was the possibility of measuring the vertical ozone distribution using the ground-based Götz Umkehr (Götz, Meetham & Dobson, 1934). It was found that the effective ozone absorption in sky spectra initially increased steadily towards sunset, reached a maximum at around 85° zenith angle, and then decreased again at still greater zenith angles. The instrument used was a Dobson spectrophotometer, measuring the relative intensities of two wavelengths which are absorbed to very different extents by ozone. Götz realised, from a simple consideration of scattering geometry, that an appropriate analysis of such twilight sky data could yield information on the vertical profile of ozone, especially in the stratosphere. A simple explanation of the behaviour of twilight sky ozone absorption may be given with reference to Fig 3. Crucial to this understanding is the concept of modal scattering height. Considering light that is only scattered once, first of all, it is clear that the scattered light received at the ground from any particular level in the zenith sky will vary with (1) the molecular number density of air at that level and (2) the atmospheric attenuation experienced by the light before and after scattering. The latter effect is naturally wavelength dependent. The effect of (1) is to decrease the scattered light received from greater heights. During the twilight period, when the oblique path of the solar beam through the atmosphere is in general optically denser than the vertical path down to the ground, the effect of (2) will be to increase the scattered light from greater heights. The combined effects of (1) and (2) give rise to a limited altitude range from which most of the light actually received at the ground is scattered; the modal scattering height (M.S.H) is defined as the height, within the above range, from which the scattering to the ground is greatest. The solar beam scattered at this height is known as the twilight beam. More radiation is received from greater altitudes at more strongly attenuated wavelengths and at larger solar zenith angles. In the region of the spectrum where Dobson measurements are made, the difference in the atmospheric attenuation experienced by the two wavelengths used (eg the 'C' wavelength pair 311 nm and 332 nm) leads to widely differing M.S.H's at zenith angles of 80° or more. Consider the expected relative intensities of the two wavelengths during the pre-sunset period. When the zenith angle is less than about 85° both M.S.H's will be below the stratospheric ozone maximum (see Fig 3(a)) and the wavelength more absorbed by ozone (311 nm) will be more strongly affected by increasing obliquity of the light path through the ozone layer.

The ratio of the intensities of 311 nm to 323 nm measured by the Dobson should therefore initially decrease. By about 85° the 311 nm M.S.H will be above most of the ozone while the 332 nm M.S.H will be below it (Fig 3(b)). At greater angles still, the intensity of 311 nm will change but slowly as the sun sets while 332 nm is still rapidly decreasing in intensity. In the limiting case when all the light is scattered so high in the atmosphere that there is negligible absorption before scattering takes place, all the absorption will occur in the vertical part of the path (Fig 3(c)), and the ratio of the two wave-lengths will be approximately the same as that when the sun is nearly overhead. Hence the ratio of 311 nm to 332 nm should decrease at first as the zenith angle increases, reach a minimum at about 85° and increase again for still larger angles, approaching a limiting value. This is the sort of behaviour that is observed prior to sunset (see Fig 4) and is understandable from the simplified flat-Earth single scattering geometry assumed above. The change from decreasing to increasing values of the above ratio is known as an 'Umkehr', and the position and shape of the Umkehr curve will depend on the vertical ozone profile, paticularly in the stratosphere. The inverse of this ratio may be considered a measure of the total ozone in the light path; thus the inverse of the curve in Fig 4 represents the variation in ozone absorption with zenith angle. The variations in ozone absorption which have been reported at greater angles than those considered above cannot be understood from flat-Earth considerations alone (Ramanathan, Angreji & Shah 1968). Particularly good instrumental sensitivity is required to measure ozone absorption reliably at very large zenith angles because of the extremely low sky intensities at such times. Various approaches to deducing the vertical ozone profile from Umkehr data have been tried, including a synthetic technique in which an initially assumed profile is altered by the method of successive approximations until satisfactory agreement between calculated and observed Umkehr data is obtained. (Mateer & Dütsch, 1964). Ramanathan and Dave (1957) have shown that a correction for the effect of secondary scattering is necessary in interpreting the data, particular at large zenith angles when optical paths become so great that it is no longer sufficient to assume primary scattering alone. Obviously, such a correction is unnecessary if the ozone absorption due to secondary light alone does not differ from the primary absorption, but this is not the case at large zenith angles.

At the wavelengths used to measure twilight NO_2 absorption, the scattering and absorption properties of the atmosphere are such that the M.S.H has a different dependence on zenith angle. The implications for twilight NO_2

absorption are discussed in section 5.

3(ii) Published Calculations of Atmospheric Scattering

The earliest calculations of atmospheric scattering and absorption assumed several simplifications, such as negligible multiple scattering, a flat, isothermal atmosphere and very coarse density layering. Without the aid of computers it was necessary to make further mathematical approximations to some of the terms which arise in the scattering equations. In some instances these simplifications are not serious, but when the phenomena under theoretical study are sensitive to atmospheric curvature, the temperature profile and higher orders of scattering, problems arise. Rozenberg (1966) has reviewed the work up to then on calculating sky brightness. Most workers have only treated the single scattering. However, as will be demonstrated later, at NO_2 absorption wavelengths the contribution of the multiply scattered light is significant beyond about 94^{o}. Hulburt (1938) estimated the contribution of multiply scattered light but arrived at too low a value for its relative intensity because he assumed an isothermal atmosphere with a temperature appropriate for the Earth's surface. Fesenkov (1966) calculated the polarization of doubly scattered light by approximating the contribution of the primary twilight to a uniformly bright arc along the horizon. The most recent work is by Collins et al (1972) and Blattner et al (1974) who have developed a Monte Carlo method that treats the full multiple scattering problem with allowance for the polarization of scattered light, atmospheric refraction and ozone absorption. Multiple scattering computer models, the simplest of which are secondary scattering models, require far more computer time than single scattering models because complex three-dimensional geometry is involved.

Atmospheric scattering models have been applied to twilight sky NO_2 absorption by Harrison (1979), Noxon (1979(a), (b), (c)), and Brewer, McElroy & Kerr (BMK, 1973). BMK assumed single scattering only while Noxon made Fesenkov's twilight arc approximation in order to allow for secondary scattering. Harrison assumed Noxon's model results in interpreting his observations of twilight sky NO_2 absorption. In the present study, the approach used is similar to that adopted by Dave (1956), whose aim was to understand the observed variations in the intensity and polarization of the multiply scattered light from the sky during twilight at around 435 nm. Details are given in the next section.

4. The Computer Scattering Model

4(i) Dave's Approach to Secondary Scattering

Dave's scattering calculations were performed without the aid of a computer, necessitating certain physical simplifications and mathematical approximations. He allowed for scattering up to second order, as well as atmospheric curvature and light polarization, and found that he could explain the known behaviour of the twilight sky intensity and polarization with reasonable accuracy. At the time there was no interest in measuring stratospheric NO_2 concentrations, but the model to be described in the present study permits in addition the prediction of how twilight sky NO_2 absorption should vary with solar zenith angle.

In Dave's calculations, the atmosphere was assumed isothermal with a scale height of 7 km, and was divided into 4 km-thick concentric layers for the purposes of calculating the intensities of primary and secondary scattered light. The vertical optical depth for Rayleigh scattering was taken to be 0.2, believed at the time to be the correct value at around 435 nm. The depolarization factor due to molecular anisotropy was taken to be 0.04. Primary scattered light from the zenith is easily calculated, but to arrive at the secondary scattered intensity it is necessary to integrate the primary contribution incident upon each zenith layer from the locally visible portion of the sunlit atmosphere. The downward (secondary) scattered intensity from each layer may then be calculated and summed for all the layers. Dave made tabulations of several quantities, such as the optical depth and physical distance between any specified two points in the atmosphere, and the intensity of primary and secondary scattered light emitted downwards from each layer. Summations were truncated whenever further contributions were judged to make a negligible difference to the total.

4(ii) Theory

The theory upon which Dave's and the present work is based may be understood with reference to Fig 5(a), in which the path of a typical doubly scattered light ray has been traced from the sun (S) to a ground-based observer (R_o). Atmospheric refraction, aerosol scattering, ground reflection and higher orders of scattering than secondary are not considered. ABC represents a section of the Earth with centre O and radius a. OR_o is the direction of the observer's zenith; Q is a point in the zenith sky. The Z - axis lies along the observer's zenith, the Y-axis is perpendicular to the plane of the paper passing through O and the X-axis lies in the plane of the paper such that the XOZ plane is parallel to the incident solar radiation. The polar coordinates (θ, ϕ) of a given direction are such that θ is the angle which the direction makes with the Z-axis, and ϕ is the azimuth with XOZ as the reference plane. Thus the polar coordinates of the incident

solar radiation SP are (Z_o, O) where Z_o is the solar zenith angle, and the zenith direction of observation is (0,0). PQ the direction of primary scattered radiation is given by $(\hat{\theta}, \hat{\phi})$. The unit vectors along SP, PQ and QR_o are denoted respectively by $\underline{s}$, $\hat{\underline{k}}$ and $\underline{k}$. In Fig 5(a) the primary scattering occurs at P, where the local zenith angle of the sun is Z, and the height R_1P is c_m. The primary scattered light travelling along PQ gets scattered again at Q (height b_n) along QR_o towards the observer.

Consider a beam of initial intensity I_∞ travelling along SP, where I_∞ denotes the intensity of solar radiation outside the Earth's atmosphere in a specified narrow wave band (being the energy received per unit area normal to the vector $\underline{s}$). Let σ denote the mass coefficient of Rayleigh scattering and ρ the air density at a distance s from P along PS. Then

$$\tau_{SP} = \int_\infty^P \sigma \rho \, ds \qquad (4)$$

is the optical path traversed by the solar radiation before reaching P. The intensity of solar radiation at P is then given by

$$I = I_\infty \exp(-\tau_{SP}) \qquad (5)$$

From the Rayleigh law of scattering the energy scattered from P in a cone of small solid angle $d\hat{k}$ with apex at P in the $\hat{\underline{k}}$ or PQ direction $(\hat{\theta}, \hat{\phi})$ is given by

$$E_1 d\hat{k} = \frac{3\sigma I_\infty}{(16\pi(1+\frac{1}{2}d)} \exp(-\tau_{SP})(1+\cos^2\hat{\psi} + d\sin^2\hat{\psi})\, d\hat{k} \qquad (6)$$

where d is the depolarization factor due to molecular anisotropy and $\hat{\psi}$ the angle between $\underline{s}$ and $\hat{\underline{k}}$ is given by

$$\cos\hat{\psi} = \cos Z_o \cos\hat{\theta} + \sin Z_o \sin\hat{\theta} \sin\hat{\phi} \qquad (7)$$

This scattered radiation is polarized and resolvable into two beams of plane polarized light at right angles to each other. Let $E_{1\hat{n}}$ represent the primary scattered emission from P in the direction PQ with its electric

vibration along the vector $\hat{n}$ perpendicular to the plane defined by $\underline{s}$ and $\hat{k}$ at P, and let $E_{\perp\hat{t}}$ be the intensity of the radiation with its electric vector along $\hat{t}$ perpendicular to $\hat{n}$. Then

$$E_{\perp\hat{n}} = \frac{3\sigma I_\infty}{16\pi(1+\frac{1}{2}d)} \exp(-\tau_{sp}) \tag{8}$$

and

$$E_{\perp\hat{t}} = K E_{\perp\hat{n}} \tag{9}$$

where

$$K = d + (1-d)\cos^2\hat{\psi} \tag{10}$$

Consider a small surface area dA at Q perpendicular to PQ. The amount of primary scattered radiation from P passing through dA per second is given by

$$E_{\perp\hat{n}}(1+K)\exp(-\tau_{PQ})\frac{dA}{\ell^2} \tag{11}$$

where dA/ℓ^2 is the solid angle subtended by dA at P, ℓ is the distance from P to Q and τ_{PQ} the optical path from P to Q, defined similarly to τ_{sp} (see equation 4). If dV is a small volume element surrounding P and subtending a small solid angle $d\hat{k}$ at dA, and if ρ_P is the air density at P, then the amount of primary scattered light passing through dA per second from a mass element $\rho_P dV$ surrounding P is given by

$$E_{\perp\hat{n}}(1+K)\exp(-\tau_{PQ})\frac{dA}{\ell^2}\rho_P\, dV \tag{12}$$

and the intensities $R_{\perp n'}$ and $R_{\perp\hat{t}}$ of the normal and transverse components of primary scattered radiation passing normally through unit area at Q through unit solid angle along the $\hat{k}$ direction is given by .

$$R_{\perp\hat{n}} = \int_Q^\infty E_{\perp\hat{n}} \exp(-\tau_{PQ}) \frac{\rho_P\, dV}{dA\, d\hat{k}} \frac{dA}{\ell^2} \tag{13}$$

and $$R_{\perp\hat{t}} = K R_{\perp\hat{n}} \tag{14}$$

The integration must extend from ∞ to Q when the whole path is illuminated by solar rays or up to the shadow limit when a part of PQ lies in the Earth's shadow (as in Fig 5(a)). Substituting for $E_{\perp\hat{n}}$ and $dV = \ell^2 ds\, d\hat{k}$, we have

$$R_{1\hat{n}} = \frac{3\sigma I_\infty}{16\pi(1+\frac{1}{2}d)} \int_Q^\infty \exp(-\tau_{sp}) \exp(-\tau_{PQ}) \rho_P \, ds \qquad (15)$$

$$R_{1\hat{t}} = K R_{1\hat{n}} \qquad (16)$$

Thus the primary scattered radiation incident upon any point in the atmosphere from any direction is given by the above theory. This information is required to calculate the secondary scattered radiation received from a given direction at the ground. Only the secondary radiation received from the zenith direction will be considered here. In the special case where the direction PQ is the zenith direction (0,0) and Q is on the Earth's surface, the above equations give the single scattered intensity received at the ground.

Having obtained the values of $R_{1\hat{n}}$ and $R_{1\hat{t}}$ for different values of $\hat{\theta}$ and $\hat{\phi}$ at Q, the next problem is to find the effective contribution by the volume element at Q towards the secondary scattered radiation travelling along QR_o . Let $\underline{n}$ be the unit vector perpendicular to the $\underline{\hat{k}}$ $\underline{k}$ plane at Q. If E_{2n} and E_{2t} are defined as the energy of the secondary emission for normal and transverse components emitted at Q respectively, then as shown by Hammad (1948)

$$E_{2n} = \frac{3\sigma}{16\pi(1+\frac{1}{2}d)} \int \{A_1 + KA_2\} R_{1\hat{n}} \, d\hat{k} \qquad (17)$$

and

$$E_{2t} = \frac{3\sigma}{16\pi(1+\frac{1}{2}d)} \int \{B_1 + KB_2\} R_{1\hat{n}} \, d\hat{k} \qquad (18)$$

where

$$\begin{aligned} A_1 &= d + 2(1-d)\cos^2 \chi_{n\hat{n}} \\ A_2 &= d + 2(1-d)\cos^2 \chi_{n\hat{t}} \\ B_1 &= d + 2(1-d)\cos^2 \chi_{t\hat{n}} \\ B_2 &= d + 2(1-d)\cos^2 \chi_{t\hat{t}} \end{aligned} \qquad (19)$$

$\chi_{n\hat{n}}$, $\chi_{n\hat{t}}$, $\chi_{t\hat{n}}$ and $\chi_{t\hat{t}}$ are respectively the angles between the vectors $\underline{n}$ and $\hat{\underline{n}}$, $\underline{n}$ and $\hat{\underline{t}}$, $\underline{t}$ and $\hat{\underline{n}}$ and $\underline{t}$ and $\hat{\underline{t}}$ and the formulae for obtaining their values are as given by Hammad.

$$\begin{aligned} \cos\chi_{n\hat{n}} &= \cos(\zeta - \hat{\zeta}) \\ \cos\chi_{n\hat{t}} &= \cos\hat{\psi}\sin(\zeta - \hat{\zeta}) \\ \cos\chi_{t\hat{n}} &= \cos\psi\sin(\zeta - \hat{\zeta}) \\ \cos\chi_{t\hat{t}} &= \sin\psi\sin\hat{\psi} + \cos\psi\cos\hat{\psi}\cos(\zeta - \hat{\zeta}) \end{aligned} \qquad (20)$$

where $\psi, \hat{\psi}, \zeta$ and $\hat{\zeta}$ are defined by the equations

$$\cos\psi = \cos Z_o \cos\theta + \sin Z_o \sin\theta \tag{21}$$

$$\sin\zeta = \frac{\sin\theta \sin\phi}{\sin\psi} \tag{22}$$

and $\hat{\psi}$, $\hat{\zeta}$ are similarly defined.

Since only the zenith direction (0,0) is of concern for the calculation of secondary scattering, the above equations simplify. Substituting $\theta = \phi = 0$ into (21) and (22), it is apparent that $\zeta = 0$ and $\psi = Z_o$. Equations 19 and 20 may then be simplified considerably. Since $d\hat{k} = \sin\hat{\theta}\, d\hat{\theta}\, d\hat{\phi}$ the equations for E_{2n} and E_{2t} may be written

$$E_{2n} = \frac{3\sigma}{16\pi(1+\frac{1}{2}d)} \iint \{A_1 + KA_2\} R_{1\hat{n}} \sin\hat{\theta}\, d\hat{\theta}\, d\hat{\phi} \tag{23}$$

and

$$E_{2t} = \frac{3\sigma}{16\pi(1+\frac{1}{2}d)} \iint \{B_1 + KB_2\} R_{1\hat{n}} \sin\hat{\theta}\, d\hat{\theta}\, d\hat{\phi} \tag{24}$$

The normal and transverse components of the total secondary scattered radiation received at R_o along QR_o , obtained by integrating all contributions from the zenith, are given by

$$R_{2n} = \int_{R_o}^{\infty} E_{2n} \exp(-\tau_{QR_o}) \rho_Q\, dy \tag{25}$$

$$R_{2t} = \int_{R_o}^{\infty} E_{2t} \exp(-\tau_{QR_o}) \rho_Q\, dy \tag{26}$$

where ρ_Q is the density of air at Q, τ_{QR_o} is the optical path from Q to R_o , and y the distance from Q to R_o .

4(iii) Methods of Calculation

Dave's major simplifying assumption was that of an isothermal atmosphere, which enabled him to derive an analytic approximation to the Rayleigh optical path between any two points in the atmosphere. The quantities τ_{SP}, τ_{PQ} and τ_{QR_o} could then be found. Fig 5(b) illustrates the situation where the optical depth from the sun to a point P (height c_m) within the atmosphere is required, and the incident solar radiation makes an acute angle Z with the local vertical at P. With reference to Fig 5(b) it is apparent that

$$(a+h)^2 = s^2 + (a+c_m)^2 + 2s(a+c_m)\cos Z \tag{27}$$

where a is the Earth's radius.

Now, from equation 4 , substituting $\rho = \rho_0 \exp(-\frac{h}{H})$, where ρ_0 is the surface air density and H the scale height

$$\tau_{sp} = \sigma \rho_0 \int_{\infty}^{P} \exp(-h/H) \qquad (28)$$

If the c_m^2 and h^2 terms may be neglected in (27), we have

$$h = \frac{s^2}{2a} + \frac{(a+c_m)\cos Z}{a} s + c_m \qquad (29)$$

Substituting for h into (28) gives

$$\tau_{sp} = \sigma \rho_0 \sqrt{\frac{\pi a H}{2}} \exp(-\frac{c_m}{H}) \exp\left(\frac{(a+c_m)^2 \cos^2 Z}{2aH}\right)\left\{1 - \mathrm{erf}\left(\frac{(a+c_m)\cos Z}{\sqrt{2aH}}\right)\right\} \qquad (30)$$

Similar equations were derived by Dave for other geometrical possibilities, details of which are given in his paper, together with details of the many tabulations of scattering quantities made. It can be shown that the vertical optical depth is equal to $\sigma \rho_0 H$; all optical paths may be related to the assumed value of the vertical optical depth. Dave replaced all of the integrals shown in the previous sub-section by summations, where points P and Q (see Fig 5(a)) were assumed respectively to be at the centres and bases of 4 km-thick layers. Angular integrations (equations 23 and 24) were also replaced by summations with an increment in ϕ of 15° and a varying increment in θ to take account of (1) the greater angular accuracy required in the calculation of optical paths at very oblique angles and (2) the greater gradient of sky intensity in the zenith direction than in the azimuth direction (particularly at large solar zenith angles) Dave's θ values were 0°,15°,30°,45°,60°,75°,80°,85° and 90°, for instance, when the position of Q was at ground level. In the present study also, the above-mentioned integrals were replaced by summations, and the entire scattering calculation was executed by a computer program run on the IBM 360/195 computer, which is more efficient for this purpose than the 370/158 machine. About one minute of CPU time was required, at most, to calculate the quantities of interest at a given solar zenith angle. At large solar depressions, fewer scattering calculations were necessary and therefore less CPU time needed.

Dave's values for the depolarization factor (d), scale height (H) and vertical Rayleigh optical depth were 0.04, 7 km and 0.2 respectively. The

following assumptions were made in the scattering computer program or model:

(1) The atmosphere was considered to consist of 25 concentric 4 km - thick layers for the purposes of carrying out the scattering calculations at points P and Q (assumed respectively to be at layer centres and bases), and the Earth considered spherical with 6370 km radius.

(2) The azimuthal and altitudinal angular increments used were 5° and 2° respectively, for all geometrical situations.

(3) NO_2 absorption was included by assigning a constant NO_2 number density to each of 50 1 km-thick layers from the surface up to 50 km. The total NO_2 in any path was found by summing the contributions from the appropriate layers.

(4) The incident solar beam was assumed to be unpolarized.

(5) The effect of the assumed NO_2 profile on the sky radiation received at the ground was found by calculating all quantities both with and without NO_2 absorption.

(6) Two different approaches to calculating optical paths were used. In the first approach, Dave's analytic approximations to optical paths were utilised (see 4(ii)). With this approach, an isothermal atmosphere had to be assumed, having a fixed scale height. However, in the second approach, any temperature profile could be specified from the surface up to 100 km at 1 km resolution. This was used, assuming a value for the surface pressure, to calculate the atmospheric density profile, represented by 100 1 km-thick constant density layers. Atmospheric optical paths were then calculated in an analogous manner to the NO_2 absorption, using an appropriate value for the Rayleigh mass scattering coefficient. The first approach will subsequently be referred to as Method 1 and the second approach as Method 2.

No truncations of summations were necessary in the model for the calculation of scattered intensities. Summations over angle and distance were always carried out in full. A study of the effect of assuming different layer thicknesses and angular increments showed that those given in (1) and (2) above gave the best results consistent with reasonably fast program execution. CPU time is quadrupled when the layer thickness is halved and doubled when either of the angular increments is halved. The model was used to predict the variation of twilight sky NO_2 absorption with zenith angle and to test the sensitivity of this absorption to the assumed atmospheric properties. Noxon, on the basis of twilight sky NO_2 absorption measurements, has reported the existence of strong horizontal stratospheric NO_2 gradients in the region of strong horizontal

stratospheric temperature gradients (Noxon 1979 (b), (c)). Consideration is given to the possibility that Noxon's results may have at least partially been due to a dependence of the apparent twilight sky NO_2 absorption on atmospheric temperature. The next section deals with the results of the above studies.

5. Model Results

5(i) The Variation with Solar Zenith Angle of Twilight Sky Intensity and Polarization

A check on model performance was necessary before proceeding to study the sensitivity of twilight sky NO_2 absorption to solar zenith angle or the atmospheric temperature profile. Dave's published values of intensity and polarization were compared with model values calculated assuming the same atmospheric properties as in Dave's case. Both methods of calculating optical depths (see previous section) were tested. Method 1 was tested using Dave's values for the scale height, vertical Rayleigh optical depth and depolarization factor. Method 2 was applied to an isothermal atmosphere at 239.2 K (giving Dave's scale height), using Dave's depolarization factor again and choosing the mass scattering coefficient to give Dave's assumed vertical Rayleigh optical depth for a surface pressure of 1013 mbar. Thus, making the above assumptions, the performance of the scattering model could be assessed by comparing the calculated values of intensity and polarization with Dave's values. Model performance test results obtained using Method 1 and Method 2 will subsequently be referred to as PT1 and PT2 results, respectively.

Two radically different temperature profiles were employed, using Method 2, to test the temperature sensitivity of scattering (and hence NO_2 sky absorption): the 60°N Winter Cold and Winter Warm temperature profiles (Handbook of Geophysics and Space Environments, 1965). These will subsequently be referred to as the cold and warm atmospheres, respectively. At 30 km the temperatures of the two atmospheres differ by nearly 30°C (see Fig 6). In the temperature sensitivity tests, the presently accepted values of the depolarization factor (.0279) and the Rayleigh mass scattering coefficient at Noxon's differential NO_2 absorption wavelength of 439.5 nm (2.349×10^{-11} $Kg^{-1}km^2$) were used (Penndorf, 1957 and Young, 1980). The two atmospheres were assumed to have a 1013 mbar surface pressure, giving in both cases a vertical Rayleigh optical depth of .2426. Fig 7 shows the density profiles which were calculated from the different temperature profiles used. In all the model runs the solar zenith angle (Z_o) was varied from 84° to 102°. The results of the model performance and temperature sensitivity tests are presented in Figs 8-17. All intensities

have been normalized with respect to the extra terrestrial solar intensity and are therefore dimensionless. NO_2 is omitted from the model at this stage.

1. Fig 8 illustrates the rapid decrease in the single scattered twilight sky intensity with increasing Z_o . PT1 and PT2 results agree almost exactly with Dave's results, but small differences are apparent between the warm and cold atmosphere results, particularly at larger Z_o values when a greater sensitivity to optical path lengths might be expected for the more oblique light paths involved. The PT1 and PT2 results were sufficiently close for only a single representative curve to be shown.

2. Fig 9 shows the corresponding variation with Z_o of the normal and transverse components of secondary scattered light intensity at twilight. Again a marked decrease with increasing Z_o may be seen, with the biggest deviations from Dave's values occurring in the warm and cold atmosphere cases. This plot is a much more sensitive test of model performance than the previous one because it is the result of a complex fully three dimensional scattering calculation involving many more light paths. Some minor differences are apparent between Dave's results, PT1 results and PT2 results. These are explainable by

   (i) Greater model angular resolution than in Dave's case.

   (ii) Approximations made in the derivation of an analytic expression for optical paths in an exponential atmosphere (see eqns 28, 29).

   (iii) The inevitable small errors introduced when assuming the atmosphere to consist of constant-density layers .

   (iv) Better model evaluation of summations than in Dave's case (see section 4(iii).

3. Fig 10 is a comparison of Noxon's, Dave's and various model calculations of the variation with Z_o of the proportion of twilight sky intensity due to secondary scattering (assuming no higher orders of scattering). All the curves show that secondary scattering plays a relatively small role until Z_o exceeds about 94^o, when the proportion of secondary scattered light rises fairly steeply, reaching 100% by 100^o. No single scattered contribution to the zenith intensity is expected beyond 100^o, since at greater angles the terminator is above the 100 km model atmosphere in the zenith direction. Even if the model atmosphere were deeper, the single scattered contribution at such large Z_o values would be negligible. Note the very close agreement between the PT1/PT2 values and Dave's values, while the warm and cold atmosphere curves show differences from each other and from Dave's values. Noxon's curve

indicates a higher degree of secondary scattering than any of the others.

4. Fig 11 shows the calculated variation with Z_o of the degree of polarization of the primary, secondary and net radiation reaching the surface from the zenith sky. The differences between the PT1 and PT2 polarization values were very small; these values are therefore represented by a single set of polarization curves. The biggest departures from Dave's values are exhibited by the warm and cold atmosphere curves. At lower Z_o values the net polarization curve follows the single scattering curve while at higher values it follows the secondary scattering curve, since secondary scattering becomes of greater relative importance at high Z_o (see Fig 10).

5. The concept of modal scattering height (M.S.H) was discussed in section 3. Figs 12 and 13 illustrate how the single scattered M.S.H ascends with increasing Z_o. Fig 12 is a PT1 result. It shows the contribution from different heights in the zenith to the single scattered radiation received at the surface, for several different values of Z_o. The M.S.H is at the level from which the greatest contribution is received; its variation with Z_o is given in Fig 13. The differences between the PT1 and PT2 values of M.S.H were negligibly small, as were the differences between the cold and warm atmosphere values of M.S.H. Representative curves are therefore given for the above in Fig 13. It may be seen that there is excellent agreement between the PT1 / PT2 results and Dave's results, and that the M.S.H's obtained using the warm and cold atmospheric profiles are consistently higher than in Dave's case. This is probably due to the slightly greater optical depth of these atmospheres than Dave's isothermal atmosphere. No such curves are available from Noxon's publications, but BMK's (1974) M.S.H versus Z_o curve is shown in Fig 13. The influence of their high values of M.S.H on their model calculations of NO_2 absorption is discussed in section 5(iii).

6. Figs 14-17 show the contribution from different heights in the zenith to the secondary scattered radiation received at the surface, for different values of Z_o, and for the different model assumptions. A secondary scattering M.S.H could obviously be defined as before, but this concept is less useful to the understanding of twilight NO_2 absorption than in the single scattering case. There are only slight differences between the PT1 and PT2 vertical distributions, but bigger differences are apparent in the warm and cold atmosphere cases, which are almost certainly real manifestations of the more sensitive dependence of secondary scattered

intensity on the density profile. The single and secondary scattering vertical distributions shown in Fig 12 and Figs 14-17 may be compared with Fig 18, which is after Dave. Good agreement between the PT1 and PT2 results and Dave's results is apparent, with slight departures from these values in the warm and cold atmosphere cases.

7. In Figs 19-22, contours of equal primary scattered light intensity (normal component) received at the surface are plotted using polar coordinates, with zero azimuth vertical. Comparison is made between Dave's published intensity distributions and the corresponding PT1 results. Symmetry about the sun's meridional plane is exploited, and the zenith angles 90°, 94°, 98° and 102° are considered. Fesenkov's (1966) approximation of the primary twilight to a uniformly bright arc along the horizon (adopted by Noxon), in which the length and intensity of the arc were varied with solar zenith angle, may be compared with the more realistic distributions shown here. In the scattering model these primary scattered intensity distributions are calculated at every model level before the secondary scattered intensity is found. Extremely good agreement with Dave's results is apparent in Figs 19-22. The PT2 results (not shown) differed negligibly from the PT1 results. These distributions provide particularly strong evidence for the correct treatment by the model of the angular dependence of scattering.

In summary, Figs 8 -22 demonstrate very close agreement between the scattering-related quantities published by Dave and those calculated by the model using the same atmospheric parameters. This not only inspires confidence in the model treatment of scattering, but also implies that remarkable accuracy was achieved by Dave, whose calculations had to be performed manually. The good agreement between the PT1 results and the PT2 results strongly suggests that the layer method of calculating optical paths (Method 2) works satisfactorily and that the warm and cold atmosphere results are therefore valid. Some sensitivity of scattering to the temperature profile is indicated.

5(ii) Model Predictions of Twilight Sky NO_2 Absorption

In section 3(i), the ozone Umkehr effect was related to the variation of M.S.H with Z_o . The M.S.H of the more attenuated of the two wavelengths used in Dobson Umkehr studies reaches the ozone maximum by about $Z_o = 85^{\circ}$ typically, and the first Umkehr may be explained qualitatively without recourse to spherical Earth geometry. In the 435-450 nm wavelength range used to measure

NO_2 absorption the atmospheric attenuation is far less and therefore the M.S.H much lower. Estimates obtained to date for the altitude of the stratospheric NO_2 maximum range from 15 to 45 kilometres (Noxon 1979(a)). Fig 13 shows that the M.S.H does not approach the maximum until after sunset. Thus curved atmosphere considerations are needed to understand the expected variation with Z_o of NO_2 sky absorption, in which the primary twilight beam may or may not traverse the NO_2 maximum twice before scattering (depending on the precise values of M.S.H and Z_o as well as the altitude of the maximum). It is not obvious therefore that NO_2 sky absorption should vary with Z_o in a similar fashion to the ozone Umkehr curve (Fig 3) . Simple geometrical considerations show that post-sunset NO_2 sky spectra should exhibit a variation of absorption with Z_o dependent primarily on the stratospheric NO_2 distribution. When there is not excessive tropospheric pollution the degree of absorption due to stratospheric NO_2 should also be greater. For such zenith angles the tangent height of the primary twilight beam will always be above the tropospheric NO_2, which will consequently only absorb sky radiation in the fixed vertical path through the troposphere down to the surface. However, changes in the obliquity of the path of the twilight beam through the stratospheric NO_2 during the twilight period will give rise to changes in the twilight sky NO_2 absorption observable from the surface. The method of interpreting twilight sky NO_2 absorption adopted in the present study follows that of Noxon and B.M.K. Synthetic curves of the variation of NO_2 differential absorption, ZN, with Z_o were generated for different assumed simple stratospheric NO_2 distributions, using the scattering model. A 5 km-thick layer of NO_2 containing 9×10^{15} molecules cm^{-2} of the gas was introduced into the model atmosphere at a fixed altitude and the variation of ZN with Z_o was calculated over the Z_o range from 84^o to 102^o. This was repeated for several layer altitudes. Tests showed that when thicker layers centred on the same altitude were used, the variation of ZN with Z_o was virtually unchanged; this was Noxon's finding also.

There is little point in calculating ZN at greater zenith angles than 102^o since higher orders of scattering than those modelled probably become important around 100^o and, in any case, the sky intensity is too weak to measure reliably at such large zenith angles, using ordinary methods (see Figs 8 and 9). The exact definition of ZN is given in section 2, and was calculated by the model using the relationship between ZN and absolute absorption given in equation 3 , assuming the same value Noxon used for the absolute and differential NO_2

absorption cross-sections at 439.5 nm. Absolute NO_2 absorption is of course the ratio of the zenith sky intensity including atmospheric NO_2 to the value excluding atmospheric NO_2. There is no need to consider the effect of differing M.S.H's over the relatively narrow 435-450 nm NO_2 measurement range. In the ozone Umkehr effect a consideration of the separation in MSH's at the two measurement wavelengths is necessary, because of the widely differing Rayleigh optical path lengths. For NO_2 the M.S.H at 439.5 nm may beconsidered representative of the 435-450 nm range, since the variation in Rayleigh optical path length across this range is relatively small. Noxon's differential absorption measurements were made at 439.5 nm anyway; entire spectra were obtained in his case only in order to unambiguously identify the presence of NO_2 absorption by its characteristic spectral structure, and to allow the straight line method of defining differential absorption to be used. In his paper Noxon admits that full use could have been made of the entire spectrum, as was done in the present study (see section 2).

Synthetic NO_2 absorption curves were calculated by the model under the same conditions that were assumed in 5(i), namely the warm and cold atmosphere conditions and the model performance test conditions. However, the PT2 absorption curves will not be considered, since the PT1 and PT2 curves were found to agree almost exactly (the latter requiring more computer time). In principle, from the shape and magnitude of the experimentally determined variation of ZN with Z_o during twilight it is possible, by comparison with the model synthetic curves, to estimate the concentration and approximate 'centre of mass' altitude of stratospheric NO_2. Results of a test of this synthetic method on a known model distribution of NO_2 are given in section 6.

A subject of concern here is the dependence of the synthetic curves on the temperature profile, since different curves could lead to different interpretations of actual twilight measurements. Mention was made earlier of Noxon's reports of strong horizontal gradients in stratospheric NO_2. Perhaps his most surprising measurements, based on the twilight sky method, were of an apparent rapid poleward decline or 'cliff' in the stratospheric NO_2 concentration at the outer edge of the northern winter circum polar vortex, where there is also a strong poleward gradient in stratospheric temperature (see Figs 23(a), (b)). Noxon's photochemical and dynamical interpretations of the 'cliff' are given in his paper. Coffey, Mankin and Goldman (1981) have made aircraft-based stratospheric NO_2 measurements using the principle of high resolution Fourier transform absorption spectroscopy with the sun as a source. They found no evidence for the presence of the pronounced winter 'cliff' reported by Noxon,

though a more gradual poleward decrease was observed. Mankin has suggested (private communication) that the abruptness of Noxon's 'cliff' may have been due to changing amounts of stratospheric NO_2, possibly because of advection, during the relatively long period that Noxon required to transport his spectrometer northwards, by road. Another possibility , which is considered here, is that changes in stratospheric temperature across the 'cliff' may have influenced scattering in such a way as to affect the twilight sky NO_2 absorption. Noxon's model studies simply assumed an isothermal atmosphere with a typically stratospheric temperature.

The synthetic ZN versus Z_o curves obtained from the model are compared in this section with those of Noxon and BMK, and their temperature sensitivity is examined.

It should perhaps be emphasized at this stage that implicit in all the model calculations is the assumption of spherically homogeneous atmospheric NO_2. Noxon pointed out that the oblique light paths (typically several hundred km long) important to this technique will generally be in an east-west direction, for obvious reasons, and that less variability in stratospheric NO_2 is expected on photochemical and dynamical grounds in this direction than in the latitudinal direction. Another important assumption is that of unchanging NO_2 with time over the twilight period. The fact that rapid changes in stratospheric NO_2 are expected just at this time complicates the interpretation of the measurements. The effect of this and other complications due to the presence of cloud (avoided when possible) and high levels of tropospheric NO_2 (quite common at Beaufort Park) will be discussed in section 6. Fig 24 shows how the PT1 values of NO_2 absorption seen separately in singly and doubly scattered light are predicted to vary with Z_o . In this example a uniform distribution of NO_2 between 15 and 45 km is assumed and the results are compared with those published by Noxon (1979(a)) who assumed the same NO_2 distribution. It may be seen from both sets of results that there is in general more secondary absorption than primary absorption, particularly beyond about 96^o when absorption of singly scattered light reaches a limiting value but the secondary absorption continues to increase because it involves a longer path through volume containing NO_2. The effective absorption will of course depend on the relative intensities of primary and secondary scattered radiation. Fig 25 shows the complete PT1 set of synthetic absorption curves obtained for all the considered NO_2 layer positions, together with the curve obtained for a 15-45 km NO_2 distribution. Each curve has a characteristic shape, with an inflection that occurs at greater zenith angles for higher altitude NO_2 layers. The inflection is most marked in the case

of the 20-25 km curve. Differences between curves are more apparent at larger zenith angles. Note that an inflection is present in the 15-45 km curve, although it is rather broader and less well defined than the others. Figs 26 (a) and 26(b) are the synthetic absorption curves generated by the scattering models of Noxon and BMK respectively. BMK's chosen layer thicknesses and positions differ slightly from those assumed here, and by Noxon. There are clearly differences between BMK's and Noxon's results, which must be related to differing model assumptions. In contrast to the absorption curves of Fig 25 (for an isothermal atmosphere), Fig 27 shows the corresponding curves for the warm model atmosphere. Here the behaviour is different, with well defined maxima in the 15-20 km and 20-25 km curves; the other curves more closely resemble those of Fig 25. Figs 28-32 provide an indication of the sensitivity to the temperature profile of the behaviour of the absorption curves. They show, for each layer altitude, the PT1 curve (which is for an isothermal atmosphere) and the 'warm' and 'cold' curves. There is never more than about a 10% difference between the 'warm' and 'cold' values of ZN at any given Z_o for any of the assumed NO_2 layer altitudes. The overall difference for a given curve is much smaller than 10%. Greater temperature sensitivity is apparent for the lower NO_2 layers, with slightly more NO_2 absorption occurring in the cold atmosphere in these cases. For higher NO_2 layers there is in general less temperature sensitivity, with more NO_2 absorption occurring this time in the warm atmosphere. Since the warm and cold profiles represent extremes that may occur in Winter, it may be concluded that the temperature sensitivity of NO_2 absorption in the twilight sky is small, despite somewhat greater sensitivity of the radiation intensities to the assumed profile (see 5(i)). Thus Noxon's 'cliff' can not be explained by changes in the apparent twilight sky NO_2 absorption due to changes in the temperature profile. Further model experiments were confined to the warm model atmosphere.

5(iii) A Qualitative Understanding of the Predicted NO_2 Absorption Curves

The behaviour of the synthetic curves described in 5(ii) may be understood qualitatively if single scattering alone is considered initially. Secondary scattering becomes important at relatively large zenith angles, when, as mentioned earlier, the longer light paths involved give rise to increased twilight sky NO_2 absorption. In the following simple argument, for angles less than about 96°, secondary scattering is ignored.

The obvious differences between the different sets of synthetic absorption curves derived by Noxon, BMK and in the present study need explaining. It is argued here that the behaviour of the curves is determined primarily by the

assumed value of vertical Rayleigh optical depth. Consider the spherical geometry shown in Fig 33 in which the path of the primary twilight beam is shown for differing values of zenith angle. In this example, a 20-25 km NO_2 layer is assumed, and the twilight beam scattering geometry derived from PT1 calculations and BMK's values of M.S.H (Fig 13). Considering the BMK scattering geometry first, Fig 33(a) shows the M.S.H to be well below the NO_2 layer, which is traversed obliquely by the twilight beam. By $Z_o = 90^\circ$ the M.S.H reaches the bottom of the layer (Fig 33(b)). After surface sunset, at 92°, the M.S.H is above the layer while the tangent height is within the layer. There are therefore oblique and vertical traversals of the twilight beam through the NO_2 layer (Fig 33(c)). At larger angles still, the M.S.H is even further above the layer, the vertical component of NO_2 absorption remaining constant. However the tangent height is in this case above the layer, leading to no oblique component of NO_2 absorption (Fig 33(d)). By $Z_o = 96^\circ$ (Fig 33(e)), the M.S.H is still higher but the tangent height has descended to the upper part of the NO_2 layer. Clearly, at the relatively small zenith angles which occur around midday, far less NO_2 sky aborption is to be expected than during the sunrise or sunset period, when the twilight beam passes very obliquely through volume containing NO_2. Since the twilight beam has a finite vertical extent, the changes in NO_2 absorption expected from Fig 33(a)-(e) will be considerably smoothed. From the above considerations, a steady increase in NO_2 sky absorption might be expected for increasing Z_o values up to around 92° due to increasing obliquity of the twilight beam through the NO_2 layer, together with the additional effect of vertical traversal through the layer. A reduction in sky absorption should then be expected during the period (around 94°) when the tangent height remains above the layer and there is no oblique traversal of the twilight beam through the layer. Finally, a resumed increase in NO_2 sky absorption beyond about 96° would be expected as the twilight beam traverses the top of the layer again. Inspection of BMK's 19.2-24.8 km curve in Fig 26(b) shows that there is broad agreement with the type of behaviour expected from a consideration of simplified scattering geometries, using BMK's M.S.H values. Clearly, for a sufficiently low altitude NO_2 layer, the tangent height will not descend sufficiently to give rise to a resumed increase in NO_2 sky absorption (see BMK's 13.6-19.2 km curve). Also, if the layer is sufficiently high in the atmosphere no maximum in the absorption would be expected at all over the above range in Z_o, assuming BMK's M.S.H values to be valid.

Different behaviour of twilight sky NO_2 absorption is expected from a consideration of the PT1 scattering geometry, also shown in Fig 33(a)-(e). The tangent height of the twilight beam does not in this case reach the altitude of the NO_2 layer. Beyond about 93° zenith angle the twilight beam passes twice through the NO_2 layer, the tangent height remaining about constant. A steady increase in twilight NO_2 absorption is thus expected up to Z_o=94°, followed by a levelling off at larger angles. Fig 25 shows that this generally agrees with the model synthetic curve for 20-25 km, although at zenith angles greater than 95° the synthetic curve is seen to rise again due to the increased importance of secondary scattering at these angles. Secondary scattering is of course neglected in Fig 33. Fig 13 shows that the M.S.H's calculated for the warm and cold atmospheres are intermediate between the BMK values and the PT1 values (the latter being based upon Dave's atmospheric parameters). These differing values of M.S.H are primarily due to the differing values of vertical Rayleigh optical depth assumed, greater optical depths giving rise to greater M.S.H's. Noxon (1979(a)) states that this depth was assumed to be about 0.23. As mentioned earlier, the value adopted in the warm and cold atmosphere studies was .2426, based on the best available data, while Dave assumed that in the 435 nm spectral region a reasonable value to take would be 0.2. It appears that BMK must have assumed the vertical optical depth to be relatively large in order to get such high values of MSH; they do not state what their assumed optical depth was. BMK expressed concern that they did not detect any NO_2 'Umkehrs' from their measurements of twilight sky absorption. They concluded that this meant either all the NO_2 was above 30 km (see BMK synthetic curves in Fig 26(b)) or that the NO_2 was approximately uniformly distributed throughout the atmosphere (ie: there was no layer). Noxon's synthetic NO_2 absorption curves do not predict an Umkehr even for the 15-20 km NO_2 layer; no Umkehrs are predicted by the scattering model under Dave's conditions either. However, as pointed out in 5(ii), the 15-20 km and 20-25 km warm atmosphere curves in Fig 27 do exhibit broad maxima, followed by increasing absorption with solar zenith angle.

These differences in behaviour may be understood in the light of the above simplified description of scattering geometry. In the warm atmosphere model calculations, the M.S.H's were just high enough to give rise to weak Umkehrs in the synthetic NO_2 curves for the two lowest NO_2 layers considered. Adopting Dave's value of .2 for the optical depth, on the other hand, led to lower M.S.H's and an absence of any Umkehr effect. In the case of ozone the M.S.H's are so high, due to greater atmospheric attenuation at the shorter wavelengths

concerned, that Umkehrs are expected even prior to sunset (see section 3(i)). BMK's M.S.H values are probably unrealistically high, while Noxon's are more reasonable. The warm atmosphere absorption curves more closely resemble Noxon's curves than those of BMK; however, unlike Noxon, absorption maxima are predicted for the 15-20 km and 20-25 km NO_2 layers. Beyond about 95° there is growing divergence between Noxon's curves and the warm atmosphere curves, the former rising more steeply than the latter. This may be due to the different approaches to scattering adopted (see 3(ii)). No closer agreement with Noxon was obtained (at large Z_o) when a trial vertical optical depth of 0.23 (Noxon's value) was assumed using the warm model atmosphere. Comparison with BMK's curves is not possible beyond $Z_o = 96°$, since BMK did not model scattering at larger zenith angles (probably because of their omission of secondary scattering).

6. Experimental and Theoretical Difficulties

6(i) Crepuscular Changes in NO_2

Several problems arose in the measurement and interpretation of twilight sky NO_2 absorption. Besides the difficulty of measuring light intensities at zenith angles great er than 96° or 97°, complicating effects were introduced by occasional cloud passages and high tropospheric amounts of NO_2. The usefulness of the twilight sky method is probably limited most of all by changes in the NO_2 concentration which occur at sunrise and sunset. NO_2 is known to decrease at sunrise due to photo-dissociation while at sunset a reaction occurs which increases the NO_2. Both of these reactions are important and rapid in the stratosphere, with a time constant typically of around 20 minutes. Fig 34 shows the diurnal cycle in the total vertical NO_2 column abundance predicted by a one dimensional photochemical model used in Met O 15. Fig 35 shows the vertical NO_2 profile at noon obtained from the same model. There is relatively little tropospheric NO_2, and the large total column changes shown in Fig 34 are stratospheric in origin. The problem of taking these changes into account afflicts all attempts to measure NO_2 during the crepuscular period, such as the balloon-based absorption measurements reported by Ackerman et al (1975) who used the sun as a source at sunset. Kerr, Evans & McConnell (1977) chemically modelled the twilight transition in NO_2 and Ackerman et al found experimental evidence consistent with KEM's conclusion that at 20 km the day to night transition is nearly complete by $Z_o = 90°$ whereas above 30 km the concentration is close to the daytime value. Since twilight sky NO_2 absorption is heavily weighted towards NO_2 near 90° (the tangent height of the twilight beam), it may be concluded that when the twilight sky method indicates a relatively low altitude the inferred NO_2 abundance should be

considered a 'night' value. Conversely, an indicated high altitude should be associated with a 'day' value. Noxon decided that altitudes below 20 km should be associated with night values while altitudes above 25 km should be associated with day values. Whenever the method gave intermediate altitudes, the abundance was not assumed to be representative of either a day or night-time value. A wider region of uncertainty than this seems sensible in the light of Ackerman et al's and KEM's work, and in the present study this region was assumed to extend from 20 km to 30 km. Thus it was considered that implied NO_2 centre of mass altitudes below 20 km should be associated with night-time and altitudes above 30 km with daytime.

6(ii) The Effect of Cloud

Measurements of twilight sky NO_2 absorption were made under clear sky conditions whenever possible, but on occasions cumulus clouds passed over the observing site and across the region of zenith sky being monitored by the spectrometer system. The theoretical treatment of scattering given earlier made no allowance for cloud scattering. It was found that the received light intensity often rose dramatically when clouds passed overhead and the sun was still above, or just below the horizon. Light intensity more than doubled in many cases. It seems likely that the cause of this was simply that clouds still in view of the sun scattered more sunlight down to the spectrometer than skylight. Sufficiently high clouds would have this property after surface sunset, for example. The effect of a continuous cloud sheet on light intensity is probably rather different from that of isolated clouds, depending on the extent and thickness of the sheet. It was not possible to measure the absorption in sky spectra reliably during isolated cloud passages using the Beaufort Park spectrometer system. This was because of unacceptably rapid variations in intensity during scanning caused by cloud structure. Thus it was not possible to compare the NO_2 absorption seen in cloud light with the neighbouring clear sky light, but the observation of increased intensity strongly suggests that a major contribution to the absorption measured would have been due to the total NO_2 in the light path from the cloud to the sun, and therefore inappropriate to the twilight sky technique. Uniform featureless cloud sheets did not present measurement problems, but it was not then possible to determine whether different absorption values would have been obtained in their absence. Noxon (1979(a)) attempted to show that only negligible differences from clear sky absorption values would occur in overcast conditions. His modelling calculations indicated that the effect on NO_2 absorption of viewing the sky in directions other than the zenith is small except near the horizon. He concluded that since clouds act as diffusers of light from the whole sky, absorption measurements made under cloudy conditions should be equally as useful to the twilight sky technique as clear sky measurements. To test this hypothesis, he measured twilight sky absorption

alternately with and without a translucent diffuser placed horizontally in front of the clear zenith sky, and found no anomalous behaviour in the resulting ZN versus Z_o curve. It is not stated whether the diffuser was in full view of the sun while the sun was above the horizon. If this was the case, then it seems probable that the diffuser would have acted more like an isolated cloud than a uniform cloud sheet. In the present study, observations made during isolated cloud passages were rejected, but when uniform cloud sheets passed overhead during twilight, observations were accepted. Absorption measurements commenced only when twilight sky conditions were clear, though on a few occasions cloud interference did occur subsequently.

6(iii) The Effect of High Tropospheric NO_2 Levels

An investigation was carried out into the influence of relatively large tropospheric NO_2 concentrations on twilight absorption, using the scattering model. High levels of boundary layer NO_2 were detected at Beaufort Park during previous work carried out there in which NO_2 absorption in the direct solar beam was measured (McMahon & Simmons, 1980(a), (b)). The additional model studies included a test of whether the synthetic method satisfactorily gave the centre of mass altitude and stratospheric column abundance of a known vertical NO_2 distribution. By adding a fixed quantity of tropospheric NO_2 'pollution' to this vertical distribution it was possible to calculate the theoretical effect on the ZN versus Z_o curve, and whether a determination of the stratospheric NO_2 abundance and altitude was still possible. Fig 36 shows the results of a set of pollution tests carried out using the warm model atmosphere. Several different NO_2 profiles were used, three of which only had NO_2 in the troposphere. It may be seen from Fig 36 that there are differences in the variation of ZN with Z_o for the two purely tropospheric profiles in which the total NO_2 is 10^{16} molecules cm^{-2}; in one case the gas was taken to be uniformly distributed throughout the lowest 1 km and in the other case, the lowest 5 km. These differences in behaviour may be partially understood in terms of the variation with Z_o of single scattering M.S.H. In the 'lowest 1 km' case, the M.S.H and twilight beam tangent height are well above the NO_2 over the range in Z_o shown. Secondary scattering of course begins to predominate around $Z_o = 95°$ or $96°$, when the single scattering M.S.H concept becomes less useful. Some enhancement of absorption occurs in the 'lowest 5 km' case due to oblique traversal of the upper part of the NO_2 distribution by the primary twilight beam. When both M.S.H and tangent height are above the NO_2, then, as mentioned in section 5(iii) in connection with the stratospheric absorption curves, the only absorption

which occurs is in the downward vertical path to the surface. As expected, this occurs at larger Z_o values for the 'lowest 5 km' case. Fig 36 shows that the effect of increasing the total NO_2 by a factor of five in the case of a 1 km high layer is to increase ZN by about the same factor for all Z_o . A ZN curve is given for a simple 25-30 km stratospheric NO_2 distribution, with a total column amount of 2×10^{16} molecules cm^{-2}. This curve may be compared with that obtained when 10^{16} molecules cm^{-2} of NO_2 were added to the distribution in the lowest 1 km. The effect on ZN of including tropospheric 'pollution' is seen to be purely additive. In this particular case, ZN values are increased by about the same amount for all Z_o . Thus the shape of the ZN versus Z_o curve is virtually unaltered, despite the presence of five times more tropospheric NO_2 than stratospheric NO_2. Note also that the smaller stratospheric amount gives rise to more zenith sky absorption than the tropospheric amount, particularly at larger zenith angles when there is more oblique traversal of the twilight beam through the stratospheric layer and secondary scattering also becomes important. This demonstrates the sensitivity of the twilight sky technique to stratospheric NO_2. A deeper surface layer of NO_2, if added to the above purely stratospheric distribution, would increase ZN by varying amounts, depending on the value of Z_o , as the 5 km surface layer curve shows. Also, the more heavily polluted the layer, the greater the magnitude of the effect would be. Fortunately, the direct solar absorption measurements made earlier at Beaufort Park showed that the total vertical NO_2 column rarely exceeded 2×10^{16} molecules cm^{-2} , and that most of this was probably located in the lowest kilometre. It was therefore assumed, in interpreting the absorption measurements presented in the next section, that tropospheric pollution had the effect of increasing ZN equally for all zenith angles. The results of one further test of the effect of tropospheric pollution, which also provide a test of the usefulness of the synthetic method, are presented in Fig 37. The photochemical model profile (Fig 35) was assumed initially, and then 1×10^{16} molecules cm^{-2} of NO_2 added to the lowest 1 km. Again, ZN values are increased by a roughly equal amount for all zenith angles when the tropospheric pollution is added. With the aid of Fig 27, which shows the full set of synthetic curves generated by the scattering model for the warm atmosphere, it is possible to estimate the NO_2 stratospheric column and altitude for the photochemical model profile of Fig 35. The position of the inflection, which is independant of the assumed pollution, is seen to be intermediate between that of the 30-35 km and

35-40 km synthetic curves. The increase in ZN in Fig 37 from 84° to 96° is 1.8%, which is also independent of the assumed pollution, whereas the mean corresponding increase for the 30-35 km and 35-40 km curves is 5.8%. Since these latter curves are for a 9×10^{15} molecules cm^{-2} layer, the stratospheric NO_2 column implied by Fig 37 is $\frac{1.3}{5.8} \times 9 \times 10^{15}$ molecules cm^{-2} ('daytime'), or 2.02×10^{15} molecules cm^{-2}, at an approximate altitude of 35 km. The correct values should be 1.85×10^{15} molecules cm^{-2} and 32 km, respectively. Thus reasonable agreement is obtained, part of the discrepancy arising from errors of judgement when comparing with the synthetic set of curves and part due to the fact that the 'real' distribution is not a simple uniform 5 km-thick layer. Noxon suggested that errors of up to 10 km in altitude are possible with the twilight sky technique, and that there is a 20% uncertainty in the stratospheric column. The above test of the synthetic method of course does not take into account the possibility that the real atmosphere may have slightly different scattering properties from those assumed in the model. Horizontal inhomogeneity and crepuscular changes in NO_2 will also contribute to the uncertainties in the stratospheric NO_2 altitudes and concentrations inferred from experimental data. The assumed spectrum of NO_2 absorption coefficients, and measurement error are additional sources of uncertainty.

7. Experimental Absorption Measurements

Twilight sky NO_2 absorption has been measured at Beaufort Park since May 1980. The resulting ZN versus Z_o curves were analysed using the synthetic method discussed in sections 5(ii) and 6, employing warm model atmosphere synthetic curves. Early measurements suffered from inadequate photomultiplier sensitivity at large zenith angles; it was not possible to obtain reliable data beyond about $Z_o = 92°$. Changes were made to the system which enabled measurements to be made up to 97°. Difficulties with light leaks were overcome, and improved dynamic range achieved using the broad band normalization method described in section 2. A source of the wavelength drifts encountered in an earlier programme of total column NO_2 measurements was identified and removed. Those drifts which did occur were compensated for using the technique employed then (McMahon & Simmons, 1980(a)). Spectra were recorded in the evening beginning at zenith angles of around 80° and continuing until signal to noise became intolerable. Adjacent up/down scans in wavelength were averaged, the resulting spectrum corresponding to a total observing time of 40 seconds. Noxon appears to have scanned less frequently from the absorption plots he published, although in his case, spectra took less time to obtain. Ratio spectra were calculated using a midday spectrum

as reference. It was rarely possible to record a suitable midday spectrum on the same day as the twilight spectra, because of greater convective activity during the day. Percentage differential absorption at 439.5 nm was derived from the ratio spectra using equation 1. All of the above data processing was performed by a computer program.

An example of a set of ratio spectra obtained on a particular evening (5 November 1981) is given in Fig 38. Successive spectra are shifted obliquely in proportion to the time of measurement. The bottom spectrum is the NO_2 cross-section spectrum (suitably scaled for comparison purposes) derived from Wilkerson et al data (1974). Despite the noisy appearance of the later spectra, which was always found, reasonably consistent values of differential absorption were calculated from them (Fig 39). Only at greater zenith angles than those shown did absorption values become excessively noisy. Figs 40-46 are the ZN versus Z_o curves measured during evening twilight on various occasions from 2 June 1981 to 14 January 1982. The very restricted data obtained early in the measurement programme is not included. All of the curves exhibit scatter which is undoubtedly related to advection of tropospheric NO_2 as well as instrumental noise. All show an overall increase in absorption with zenith angle, as scattering theory predicts. However there is only one obvious example of a curve with an inflection (Fig 39). The other curves most of all resemble the 30-35 and 35-40 km model synthetic curves for the range in Z_o covered (Fig 27). Applying the synthetic method to each of the curves gives the values for the stratospheric NO_2 column shown in Table 2. These can be compared with the values reported by other workers (Table 1). The higher altitude 'daytime' curves imply stratospheric columns in the range 2.7-10.8 x 10^{15} molecules cm^{-2}. Around 6 x 10^{15} molecules cm^{-2} is obtained for the curve of Fig 39. The position of the inflection in this latter curve implies an anomalously low 15-20 km centre of mass altitude (associated with night-time). It is possible that unusually large advective changes in tropospheric NO_2, neglected in the determination of the stratospheric abundance and height, may have led to this result. Interestingly, Noxon (1979(a),(b)) reported occasional very low altitude NO_2 centre of masses.

8. Conclusion

This report has demonstrated the usefulness of a multiple scattering model in the interpretation of twilight sky NO_2 absorption. The model has been shown to give sensible values of scattered intensity and polarization, and was used with some confidence to demonstrate the insensitivity of sky NO_2 absorption

to the temperature profile. Noxon's observations of steep NO_2 gradients are concluded not to have been due to temperature effects.

Preliminary experimental measurements imply stratospheric abundances in the range 2.7-10.8 x 10^{15} molecules cm^{-2}, at mean altitudes (with one exception) of at least 30 km. Further measurements, using model synthetic curves as an interpretive tool, may shed more light on this apparently strong variability.

Acknowledgements

This work has benefitted from the advice and experimental assistance of Dr E.L.Simmons. A.J. Thomas helped to maintain the system's electronics.

References

Ackerman, M., Fontanella, J.C., Frimout, D., Girard, A., Louisnard, N.& Muller, C. Simultaneous Measurements of NO and NO_2 in the Stratosphere. Planet. Space Sci., 23, 651 (1975).

Blattner, W.G., Horak, M.G., Collins, D.G.& Wells, M.B. Monte Carlo Studies of the Sky Radiation at Twilight. Appl. Opt., 13, 535 (1974).

Bloxam, R.M., Brewer, A.W & McElroy, C.T. NO_2 Measurements by Absorption Spectrophotometer: Observation from the Ground and High Altitude Balloon, Churchill, Manitoba, July 1974. Proc. IV Conference on C.I.A.P., U.S. Dept. of Transportation, Washington, D.C. (1976).

Brewer, A.W., McElroy, C.T & Kerr, J.B. Nitrogen Dioxide Concentrations in the Atmosphere. Nature, 246, 129 (1973).

Brewer, A.W., McElroy, C.T.& Kerr, J.B. Spectrophotometric Nitrogen Dioxide Measurements. Proc. III Conference on C.I.A.P., 257-263 (Feb 1974).

Coffey, M.T., Mankin, W G & Goldman, A. Simultaneous Spectroscopic Determination of the Latitudinal, Seasonal and Diurnal Variability of Stratospheric N_2O, NO, NO_2, and HNO_3. J. Geophys. Res. 86, 7331-7341 (1981).

Collins, D.G., Blattner, W.G., Wells, M.B.& Horak, H.G. Backward Monte Carlo Calculations of the Radiation Emerging from Spherical - Shell Atmospheres. Appl. Opt., 11, 2684 (1972).

Crutzen, P.J. The Influence of Nitrogen Oxides on the Atmospheric Ozone Content. Quart. J.R. Met. Soc. 96, 320 (1970).

Dave, J.V., On the Intensity and Polarization of the Light from the sky During Twilight, II. Proc. Indian Acad. Sci. 43, 336 (1956).

Drummond, J.R.& Jarnot, R.F. Infrared Measurements of Stratospheric Composition II. Simultaneous NO and NO_2 Measurements. Proc. Roy. Soc. Lond. A. 364, 237-254 (1978).

Dziewulska - Losiowa, A.& Rajewska - Wiech, B. The Results of the Three - Years Series of the Measurements of Total NO_2 Amount at Belsk. Publ. Inst. Geophys. Pol. Acad. Sci., D-11 (141), 1980.

Fesenkov, V.G. A Polarization Method for Twilight Research. Sov. Astron. AJ. 10, 156 (1966).

Götz, F.W.P., Meetham, A.R.& Dobson, G.M.B. The Vertical Distribution of Ozone in the Atmosphere. Proc. Roy. Soc. Lond. A. 145, 416-446 (1934).

Hall, T.C.& Blacet, F.E. Separation of the Absorption Spectra of NO_2 and N_2O_4 in the Range 2400-5000 A. J. Chem. Phys. 20, 1745 (1952).

Hammad, A. Scattered & Rescattered Sunlight. Astrophys. Journ. 108, 338 (1948).

Handbook of Geophysics and Space Environments. Pub: A.F.C.R.L., Office of Aerospace Research, U.S.A.F. (1965).

Harrison, A.W. Midsummer Stratospheric NO_2 at 45°S. Can. J. Phys. 57, 1110-1117 (1979).

Hulbert, E.O. The Brightness of the Twilight Sky and the Density and Temperature of the Atmosphere. J. Opt. Soc. Amer. 28, 227 (1938).

Kerr, J.B., Evans, F.J.& McConnell, J.C. The Effects of NO_2 Changes at Twilight on Tangent Ray NO_2 Measurements. Geophys. Res. Lett. 4, 577 (1977).

Kuznetsov, G.I.& Nigmatullina, K.S. Determination of Nitrogen Dioxide Content in the Atmosphere by an Optical Method. Moscow, Acad. Nauk USSR, Izv., Fiz. Atmos. Okean. 13, 886-889 (1977).

Mateer, C.L.& Dütsch, H.U. Uniform Evaluation of Umkehr Observations from the World Ozone Network Part 1. Proposed Standard Umkehr Evaluation Technique. N.C.A.R. Boulder, Colorado.

McMahon, B.B.& Simmons, E.L. Ground-Based Measurements of Atmospheric NO_2 by Differential Optical Absorption. Met O 19 Branch Memorandum No.59 (1980(a)).

McMahon, B.B.& Simmons, E.L. Ground-Based Measurements of Atmospheric NO_2 by Differential Optical Absorption. Nature 287, 710-711 (1980(b)).

Noxon, J.F. Nitrogen Dioxide in the Stratosphere and Troposphere Measured by Ground-Based Absorption Spectroscopy. Science 189, 547-549 (1975).

Noxon, J.F., Whipple, E C & Hyde, R S. Stratospheric NO_2 1. Observational Method and Behaviour at Mid-Latitude. J. Geophys. Res. 84, 5047-5065 (1979(a)).

Noxon, J.F. Stratospheric NO_2 2. Global Behaviour. J. Geophys. Res. 84, 5067-5076 (1979(b)).

Noxon, J.F., Marovich, E & Norton, R B. Effect of a Major Warming upon Stratosperic NO_2. J. Geophys. Res. 84, 7883-7888 (1979(c)).

Penndorf, R. Tables of the Refractive Index for Standard Air and the Rayleigh Scattering Coefficient for the Spectral Region between 0.2 and 20.0 and their Application to Atmospheric Optics. J. Opt. Soc. Amer. 47, 176-182 (1957).

Pommereau, J.P.& Hauchecorne A. Observations Spectroscopiques Depuis le Sol du Dioxyde d'Azote Atmospherique. C.R. Acad. Sci. Paris. B. 288, 135-138 (1979).

Ramanathan, K.R., Angreji, P.D.& Shah, G.M. The Second Umkehr Observed in Zenith Sky Twilight and its Interpretation. Symposium sur l'Ozone Atmosphèrique (Monaco), 129-134 (Sept 1968).

Ramanathan, D.R.& Dave, J.V. The Calculation of the Vertical Distribution of Ozone by the Götz Umkehr Effect (Method B). Int. Counc. Sci. Un., Spec. C.I.G.Y., A. I.G.Y., 1957-1958,5,1957, Pt 1, 23-45.
Rozenberg, G.V. Twilight. Plenum, New York (1966).

Wilkerson, T.D.et al. Absorption Spectra of Atmospheric Gases. Tech. Note BN - 784, Inst. for Fluid Dynamics & Applied Mathematics, Univ. of Maryland, College Park, MD (1974).

Yelanskiy, N.F.& Truttse, Y.L. Certain Features of the Distribution of Total Ozone and Nitrogen Dioxide Contents in the Atmosphere from Airplane Observations. Acad. Sci. USSR, Izv., Fiz. Atmos. Okean 15, 79-81 (1979).

Young, A.T. Revised Depolarization Corrections for Atmospheric Extinction. Appl. Opt., 19, 3427 (1980).

Year	Worker(s)	Method Used (ground-based unless stated otherwise)	NO_2 column/molecules cm^{-2}
1973 1974	Brewer, McElroy & Kerr	Optical absorption. A 3 wavelength method was employed (at absorption peaks and troughs) using a modified Dobson spectrophotometer.	$2\text{-}3 \times 10^{16}$ (total column)
1976	Bloxam, Brewer & McElroy	As above	1.3×10^{16} (total column)
1975	Noxon	Optical absorption. Measured entire spectrum from 435-450 nm, but only calculated NO_2 absorption at 439.5 nm.	$.5 \times 10^{16}$ (total column)
1977	Kuznetsov & Nigmatullina	Optical absorption. 6 wavelength method.	$.3\text{-}5 \times 10^{16}$ but usually 1×10^{16} (total column)
1979	Pommereau & Hauchecorne	Optical absorption, using whole spectrum from 435-450 nm. A balloon platform was used also.	a few $\times 10^{17}$ (total column) " (stratospheric column)
1979	Harrison	Optical absorption. 5 wavelength method measured sky absorption.	$.1\text{-}.3 \times 10^{16}$ (stratospheric column)
1979	Yelanskiy & Truttse	Optical absorption. 4 wavelength method. Aircraft platform used.	$1.3\text{-}6.5 \times 10^{15}$ (total column above 3 km)
1979	Noxon	Same method as in Noxon 1975 above, but sky absorption measured.	$.1\text{-}.6 \times 10^{16}$ (stratospheric column)
1980	McMahon & Simmons	Optical absorption, using whole spectrum from 435-450 nm	$0.8\text{-}5.6 \times 10^{16}$ (total column)
1980	Dziewulska-Losiowa & Rajewska-Wiech	Optical absorption, using modified Dobson spectrophotometer, working with 1 wavelength pair.	$1.3\text{-}5 \times 10^{17}$ (total column)

TABLE 1. Some published column measurements of NO_2, to date

DATE	Estimated Stratospheric NO_2 amount / 10^{15} mol cm^{-2}	Estimated mean altitude of NO_2 distribution/km	Whether associated with day or night
2 June 1981	10.3	35-40	day
5 November 1981	7.5	15-20	night
9 November 1981	5.5	35-40	day
12 December 1981	2.7	30-35	day
18 December 1981	9.5	35-40	day
11 January 1982	6.4	35-40	day
13 January 1982	3.7	35-40	day
14 January 1982	10.8	35-40	day

TABLE 2. Estimates of the stratospheric NO_2 column total and mean altitude at Beaufort Park. Errors in the amount are probably $\pm$ 20%, and the altitude uncertainty could be as great as 10 km.

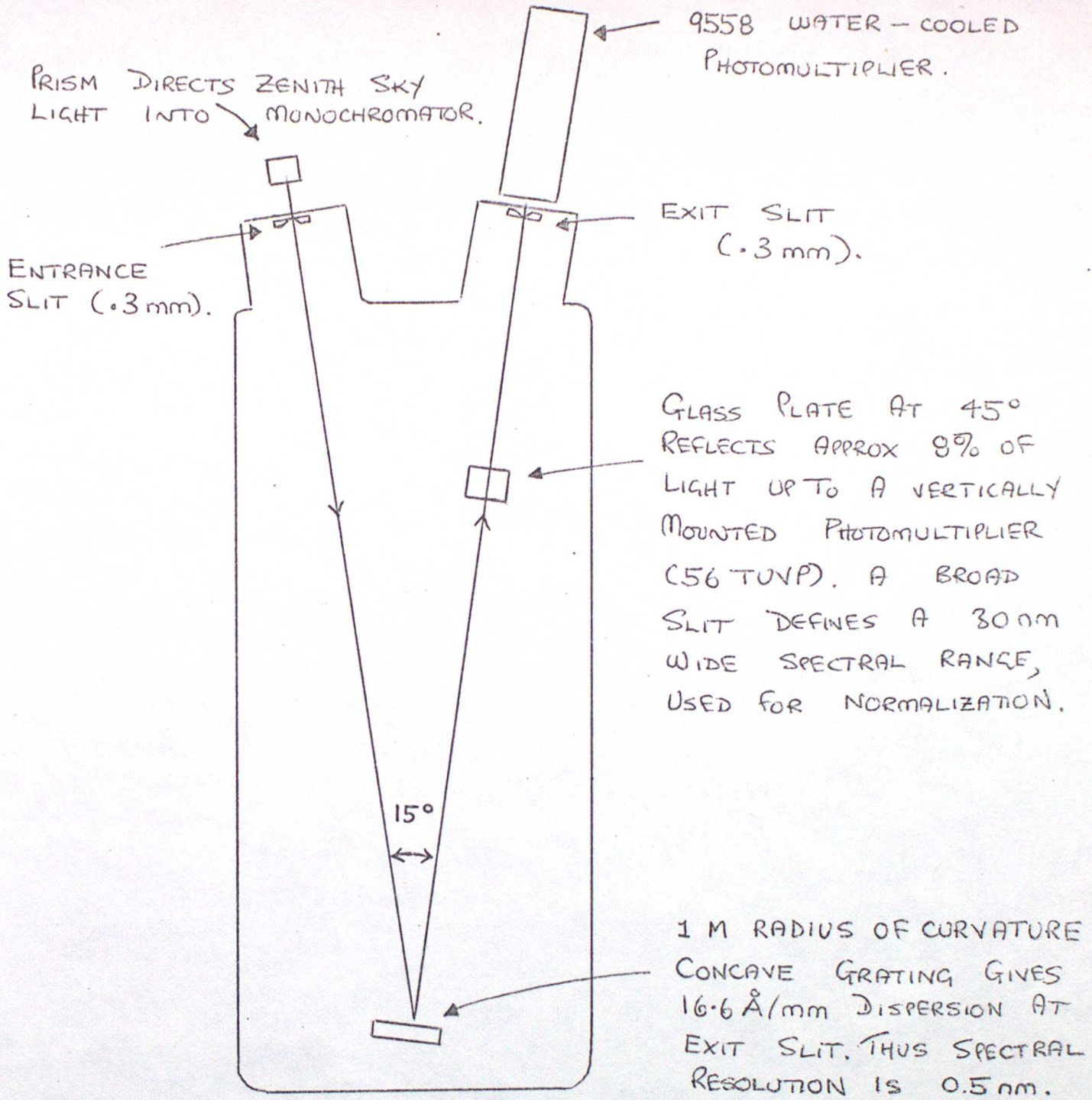

FIG 1 SIMPLIFIED OPTICAL ARRANGEMENT

(PLAN VIEW)

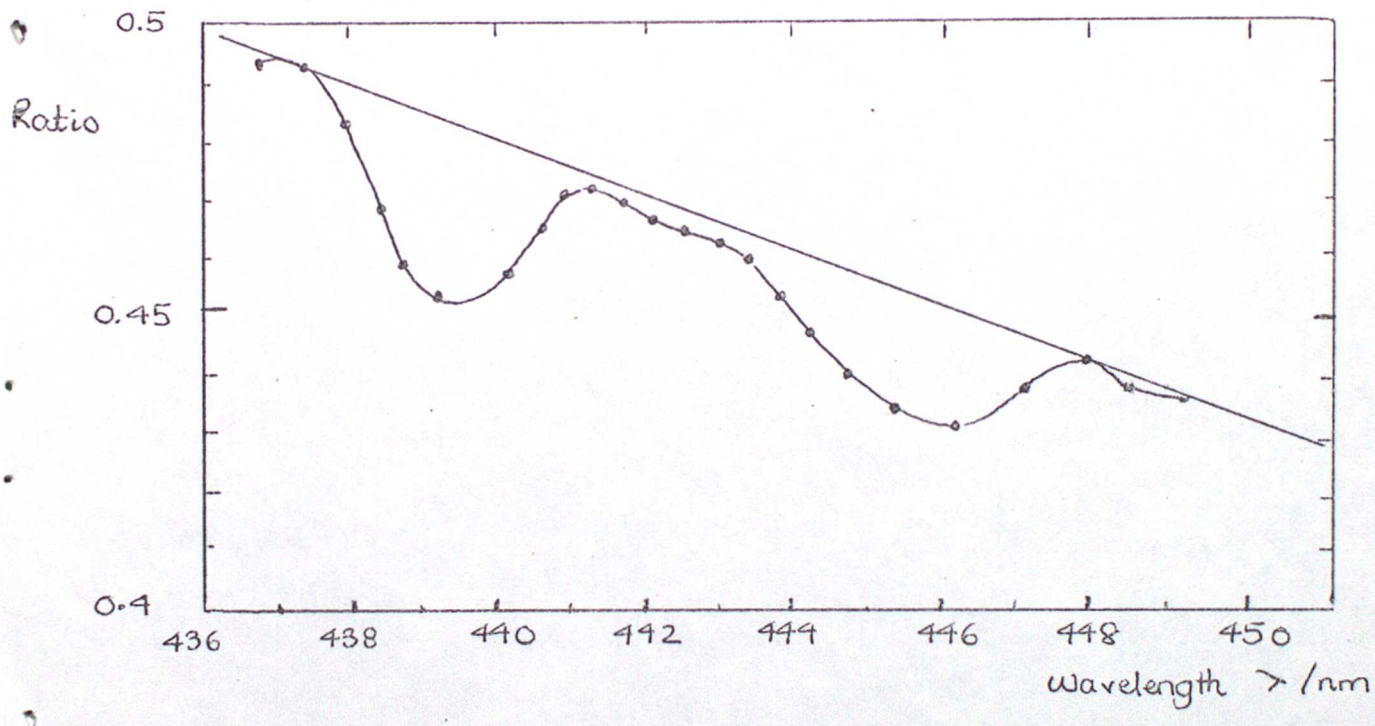

FIG 2 A ratio spectrum obtained by Noxon (1979) after dividing a twilight spectrum by a midday spectrum at the points shown (corresponding to Fraunhofer maxima and minima in the original spectra).

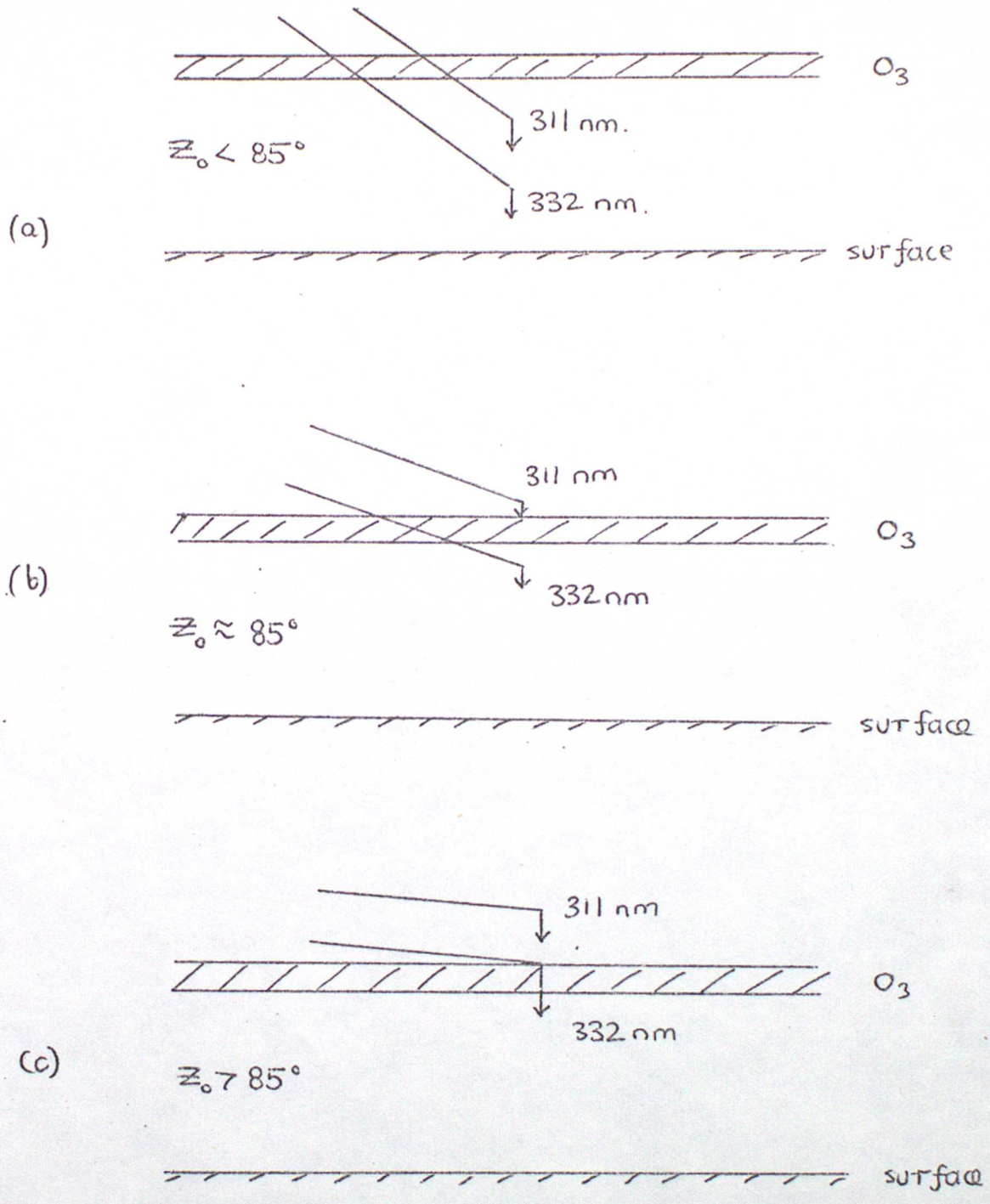

FIG 3 Flat Earth approximation to ozone scattering geometry at different solar zenith angles (Z_0). The rays scattered at the M.S.H. of the Dobson 'C' wavelength pair are shown. The ozone layer is at approx 22-26 km.

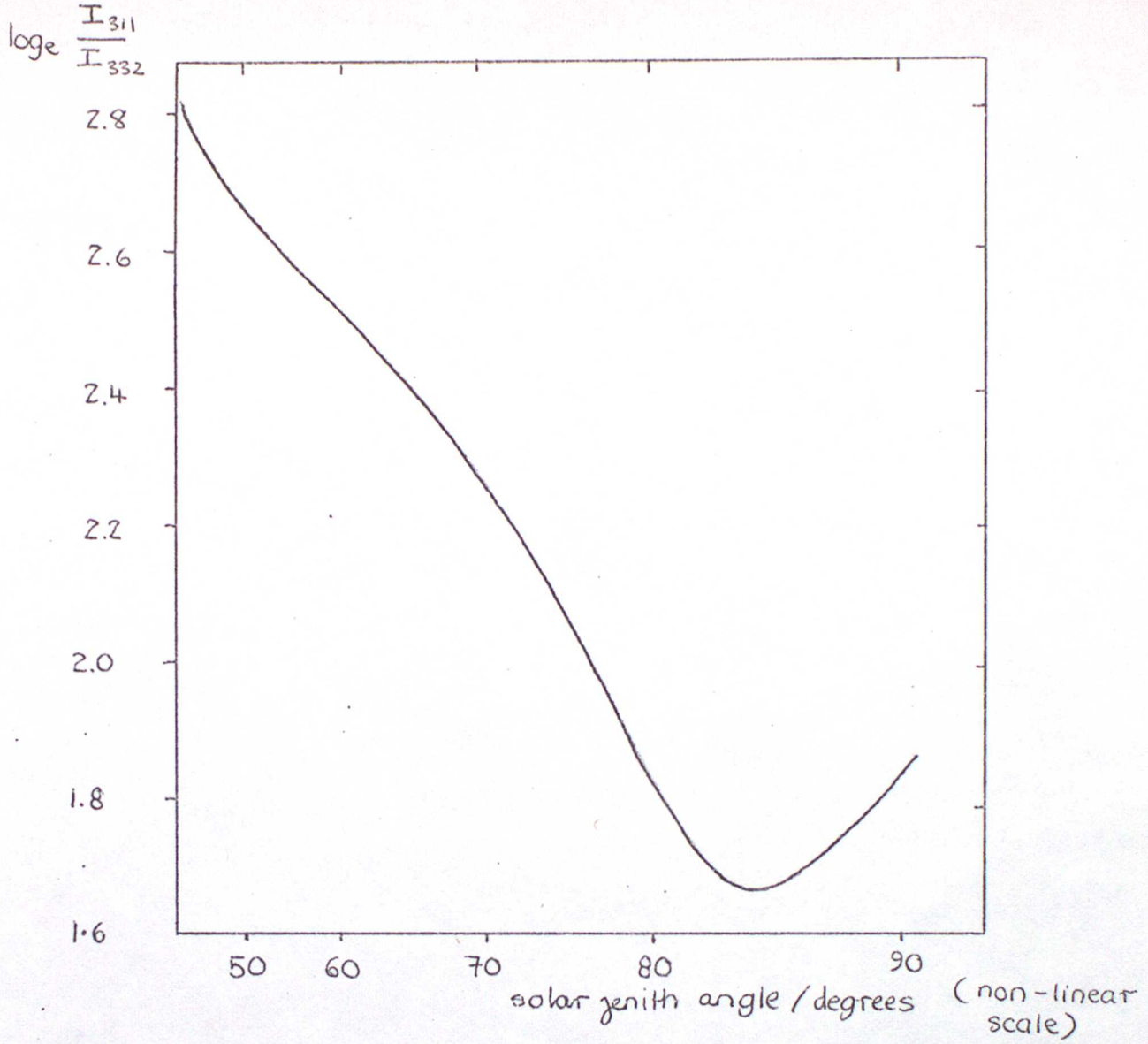

FIG 4 A typical ozone Umkehr curve

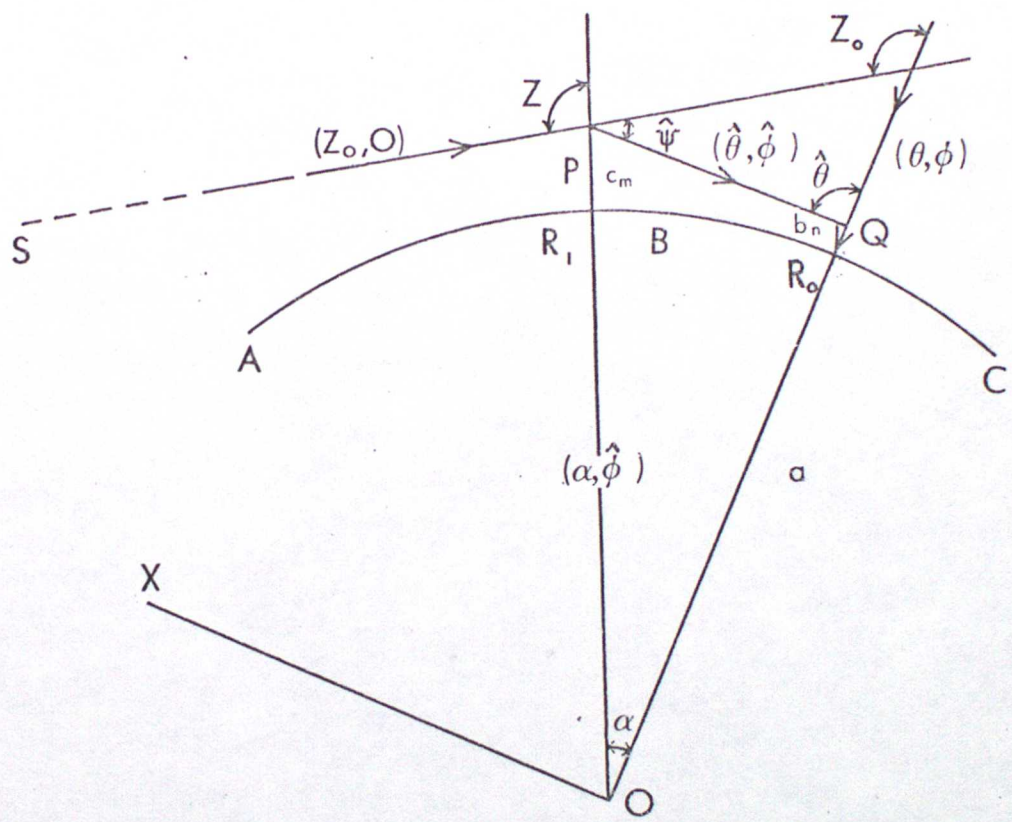

FIG 5 (a) MODEL SCATTERING GEOMETRY

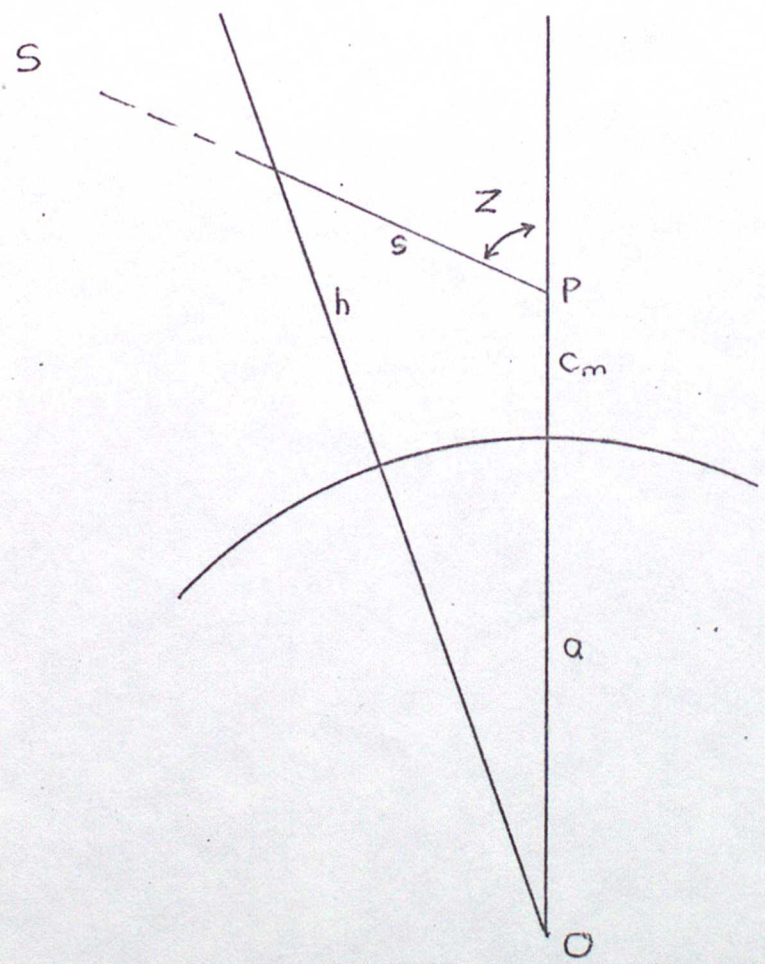

FIG 5(b) One of several possible light path geometries

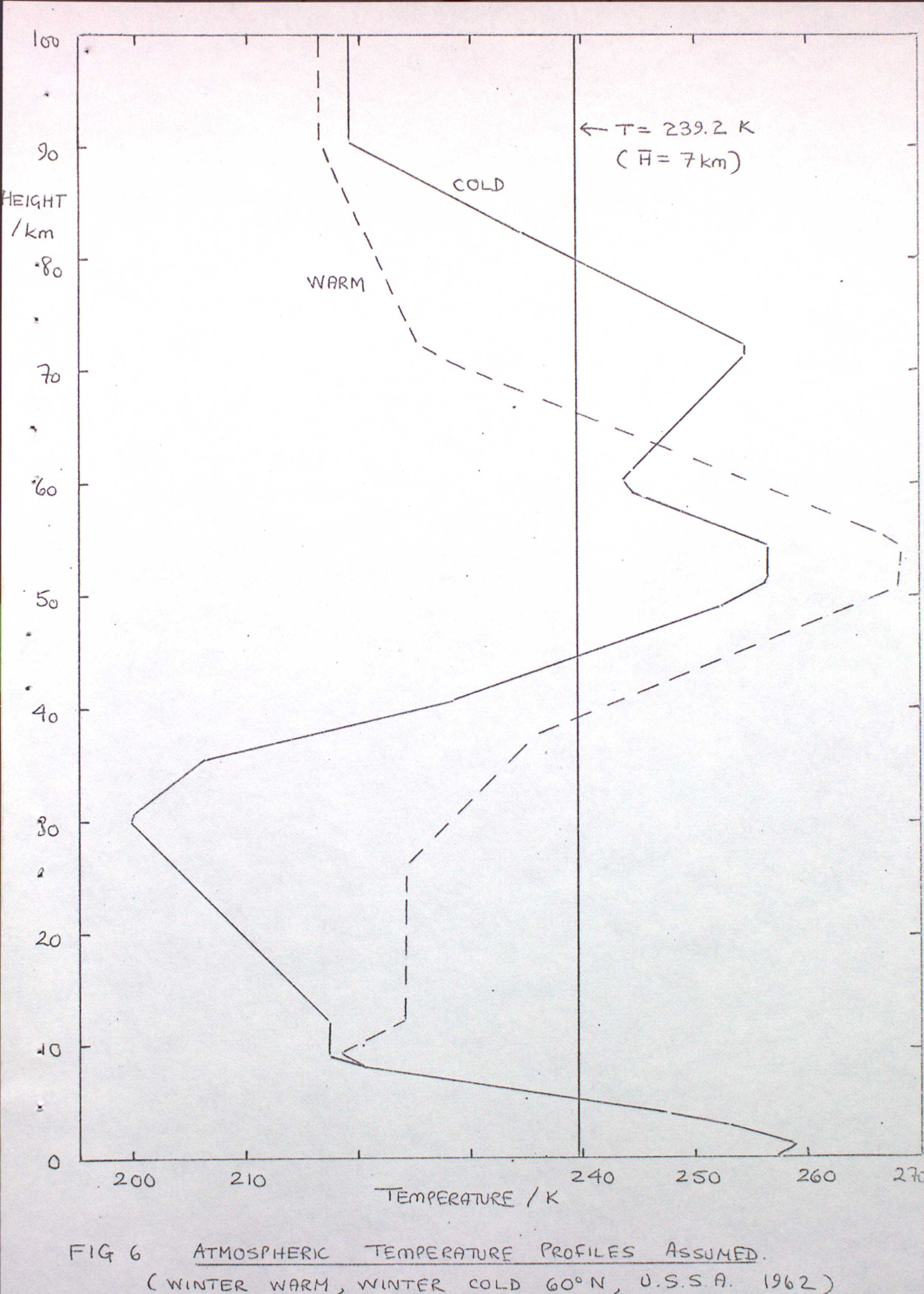

FIG 6 ATMOSPHERIC TEMPERATURE PROFILES ASSUMED.
(WINTER WARM, WINTER COLD 60° N, U.S.S.A. 1962)

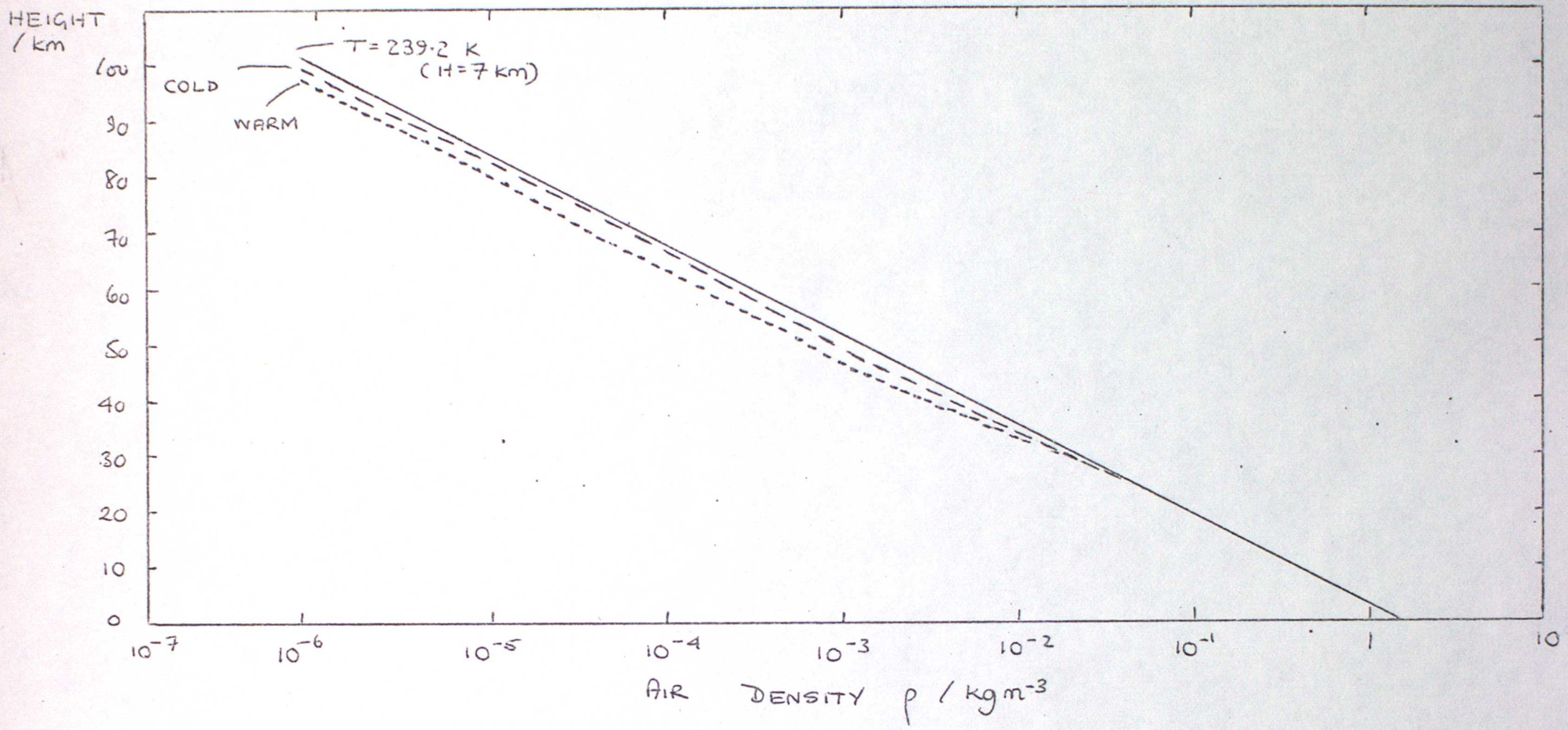

FIG 7 CALCULATED DENSITY PROFILES OF THE WARM & COLD ATMOSPHERES 60° N

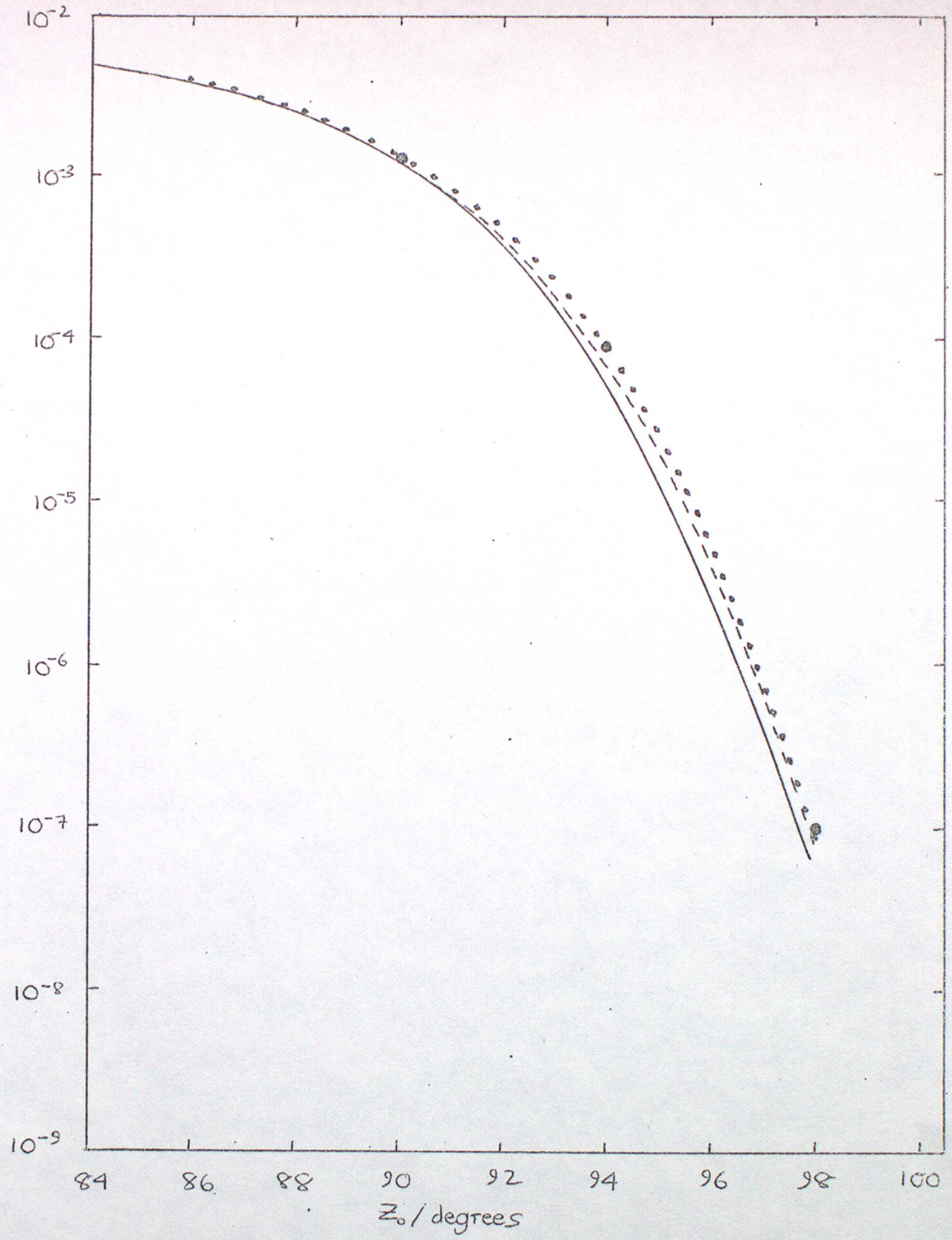

FIG 8 SINGLE SCATTERED RADIATION RECEIVED FROM ZENITH SKY AT THE GROUND

COLD ATMOSPHERE

WARM ATMOSPHERE

PT1 / PT2

FROM DAVE (1956)

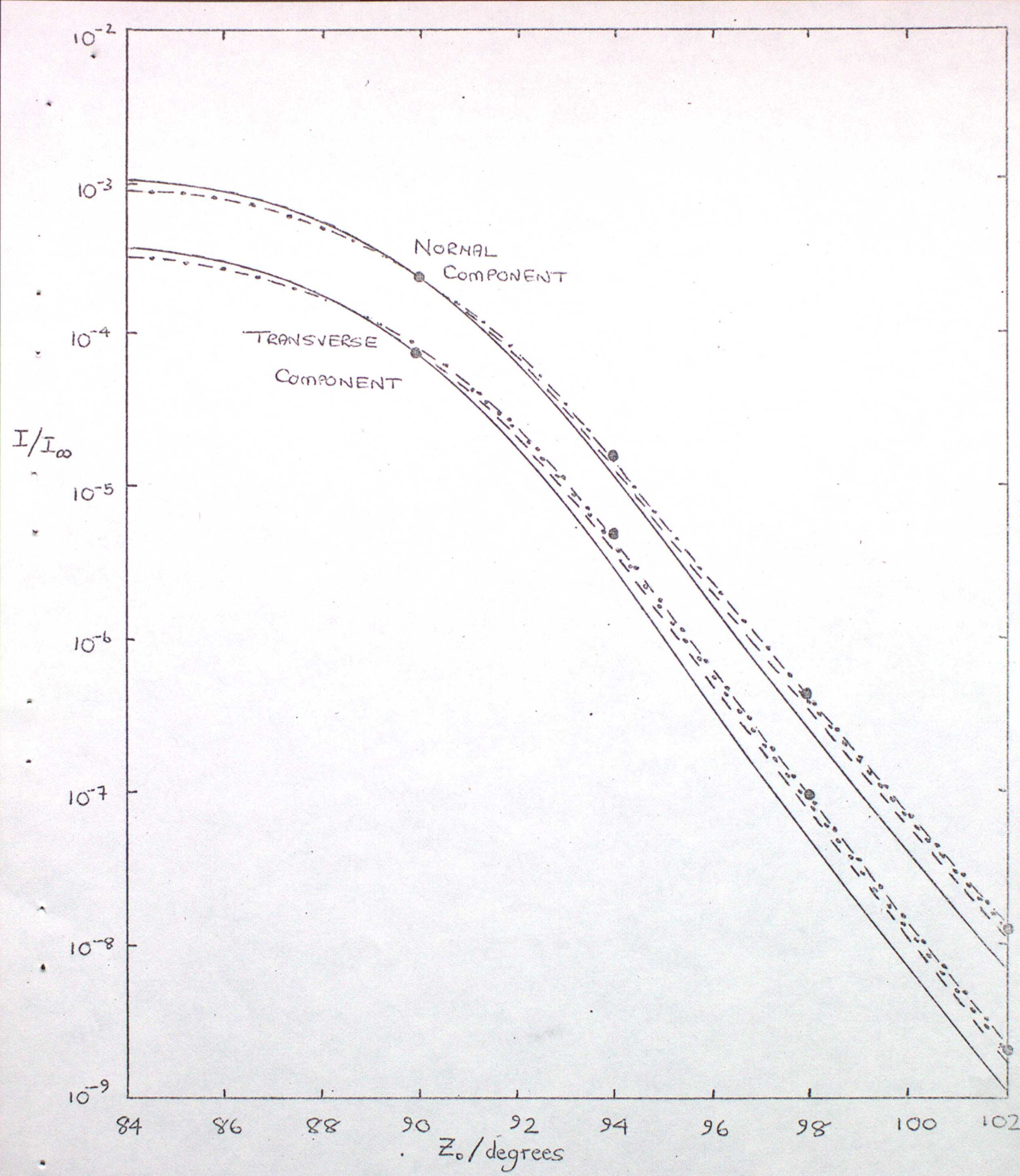

FIG 9 SECONDARY RADIATION RECEIVED FROM ZENITH SKY AT THE GROUND

COLD ATMOSPHERE

WARM ATMOSPHERE

PT 1

PT 2

● FROM DAVE (1956)

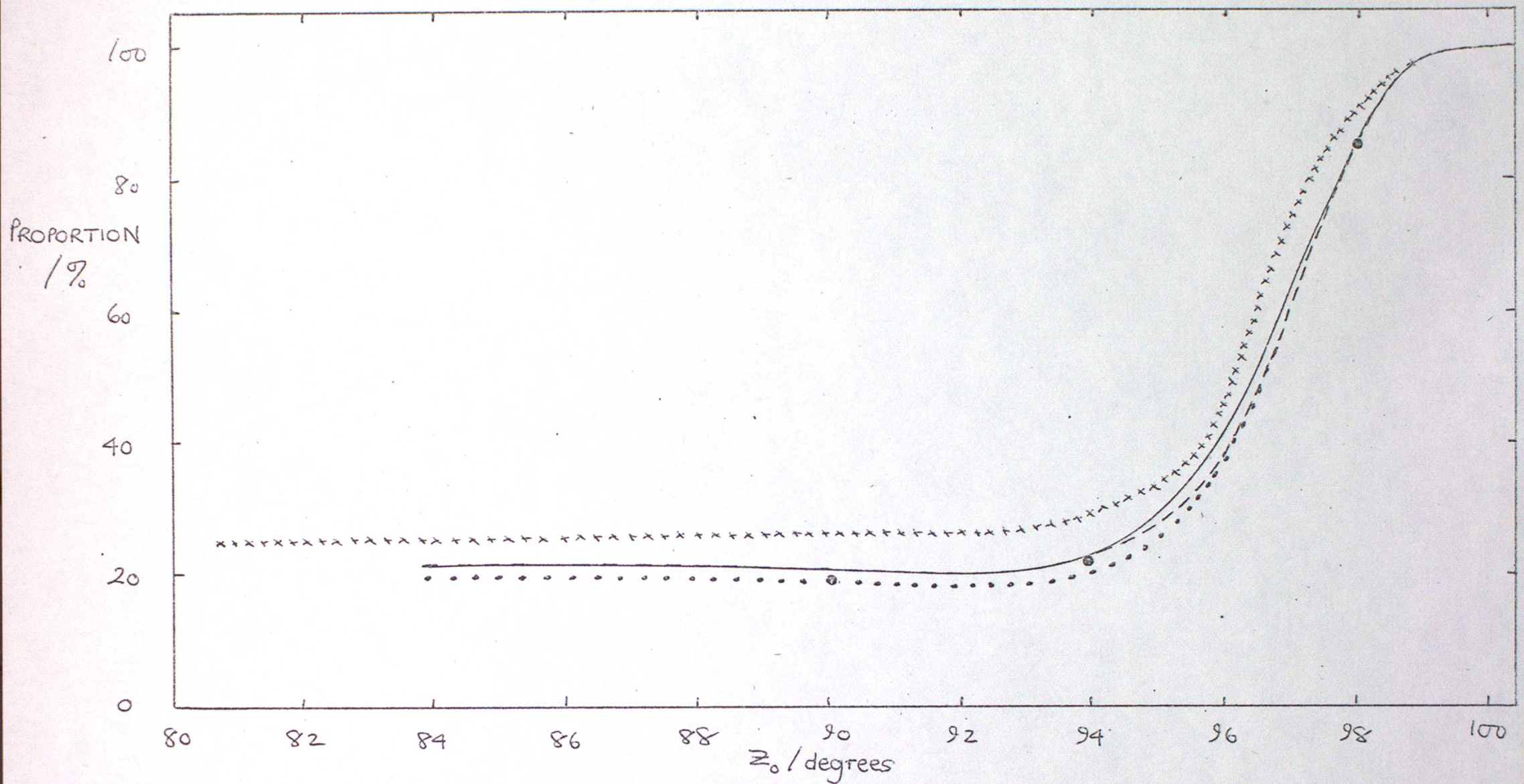

FIG 10 PROPORTION OF SECONDARY SCATTERED LIGHT AS A FUNCTION OF ZENITH ANGLE

xxxxxx AFTER NOXON (1979(a))

● FROM DAVE (1956),

—— COLD ATMOSPHERE

– – – WARM ATMOSPHERE

• • • • PT1 / PT2

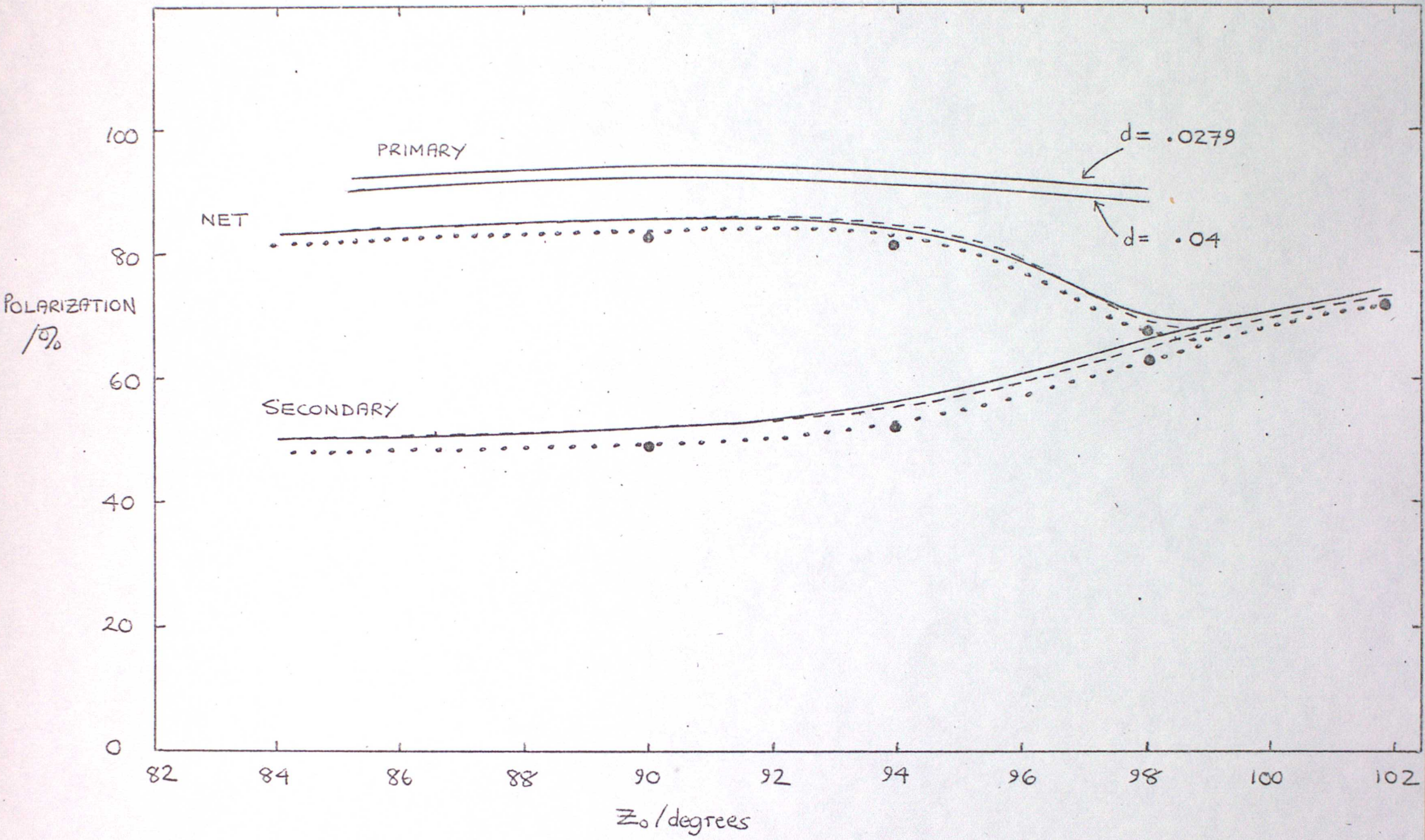

FIG 11 ZENITH SKY POLARIZATION VERSUS SOLAR ZENITH ANGLE

COLD ATMOSPHERE ... PT1/PT2

WARM ATMOSPHERE • FROM DAVE (1956)

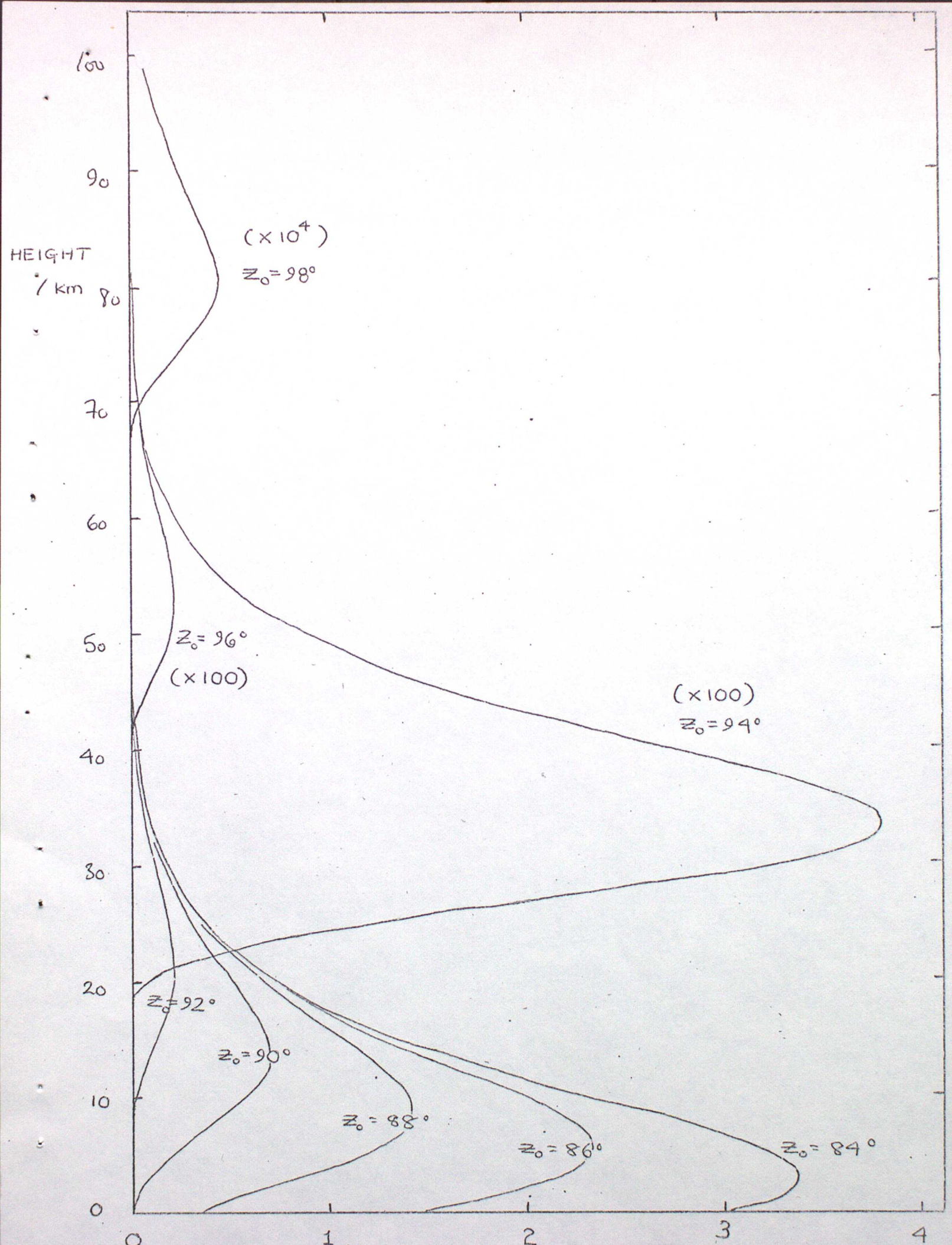

FIG 12 PTI RESULTS FOR THE SINGLE SCATTERED INTENSITY REACHING THE GROUND FROM VARIOUS HEIGHTS

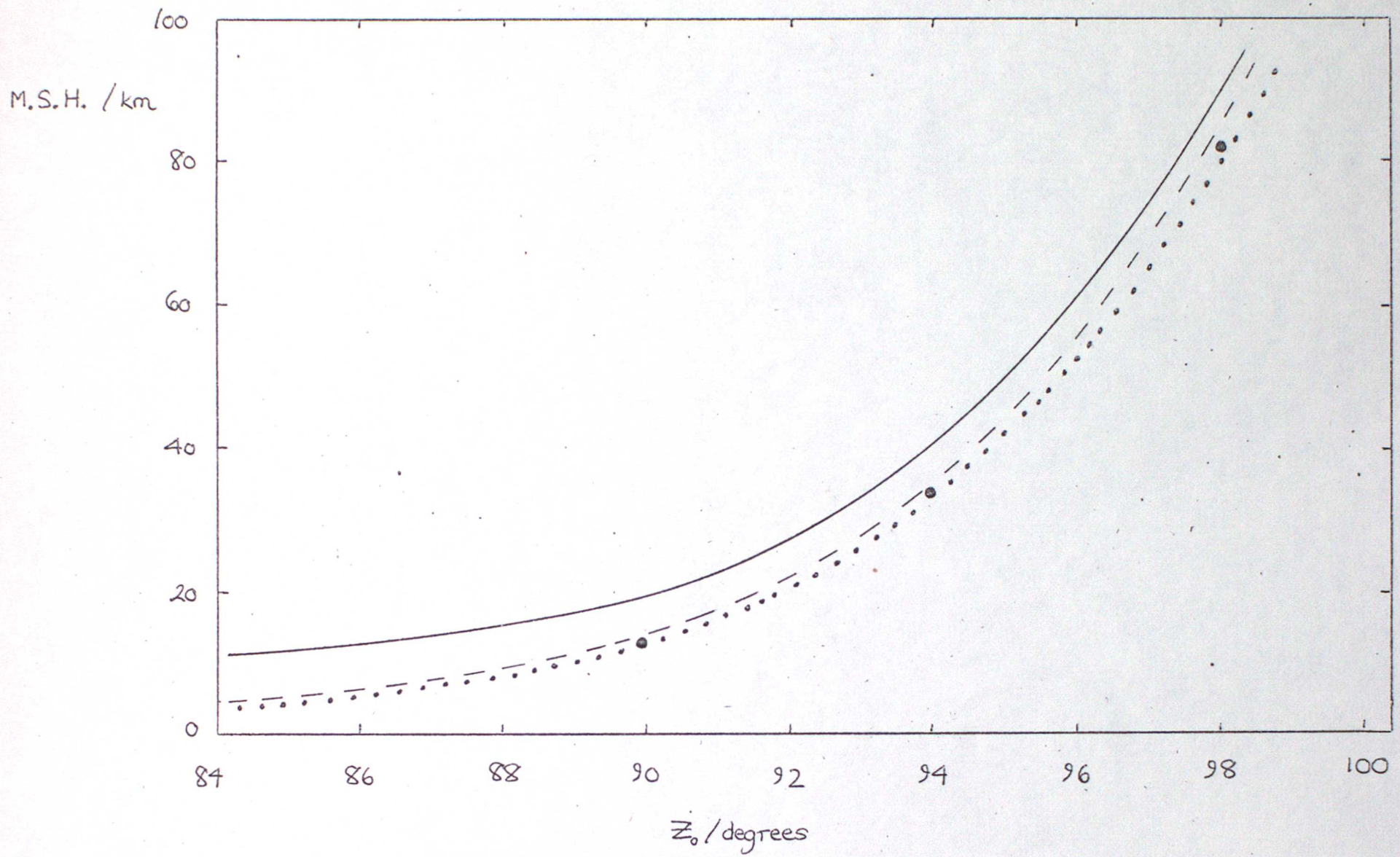

FIG 13 MODAL SCATTERING HEIGHT (M.S.H.) VERSUS SOLAR ZENITH ANGLE (Z_o)

FROM BMK (1974)

PT1 / PT2

WARM / COLD ATMOSPHERE

FROM DAVE (1956)

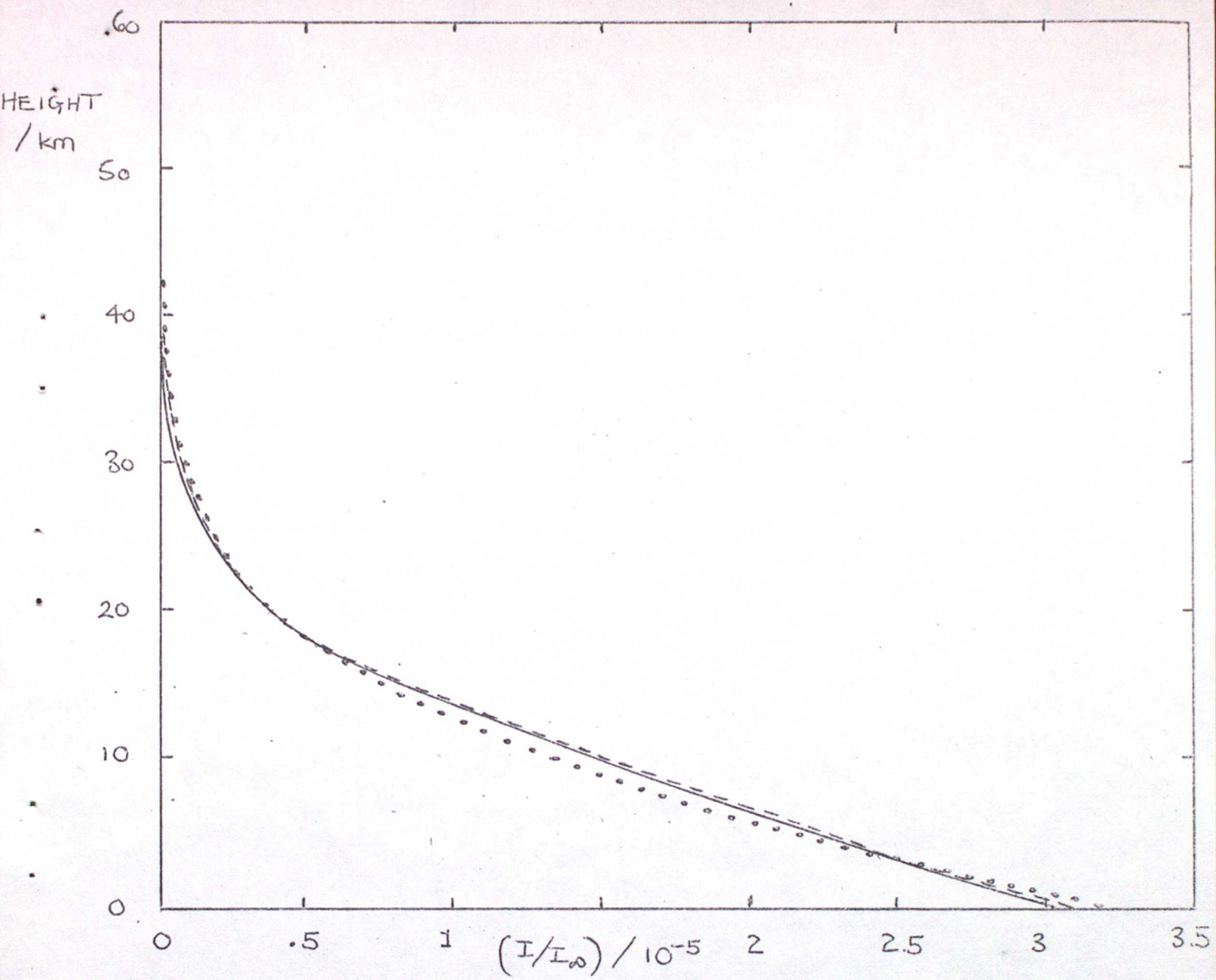

FIG 14 INTENSITY OF SECONDARY RADIATION TRANSMITTED TO GROUND FROM DIFFERENT HEIGHTS AT $Z_0 = 90°$

COLD ATMOSPHERE

WARM ATMOSPHERE

PT1 / PT2

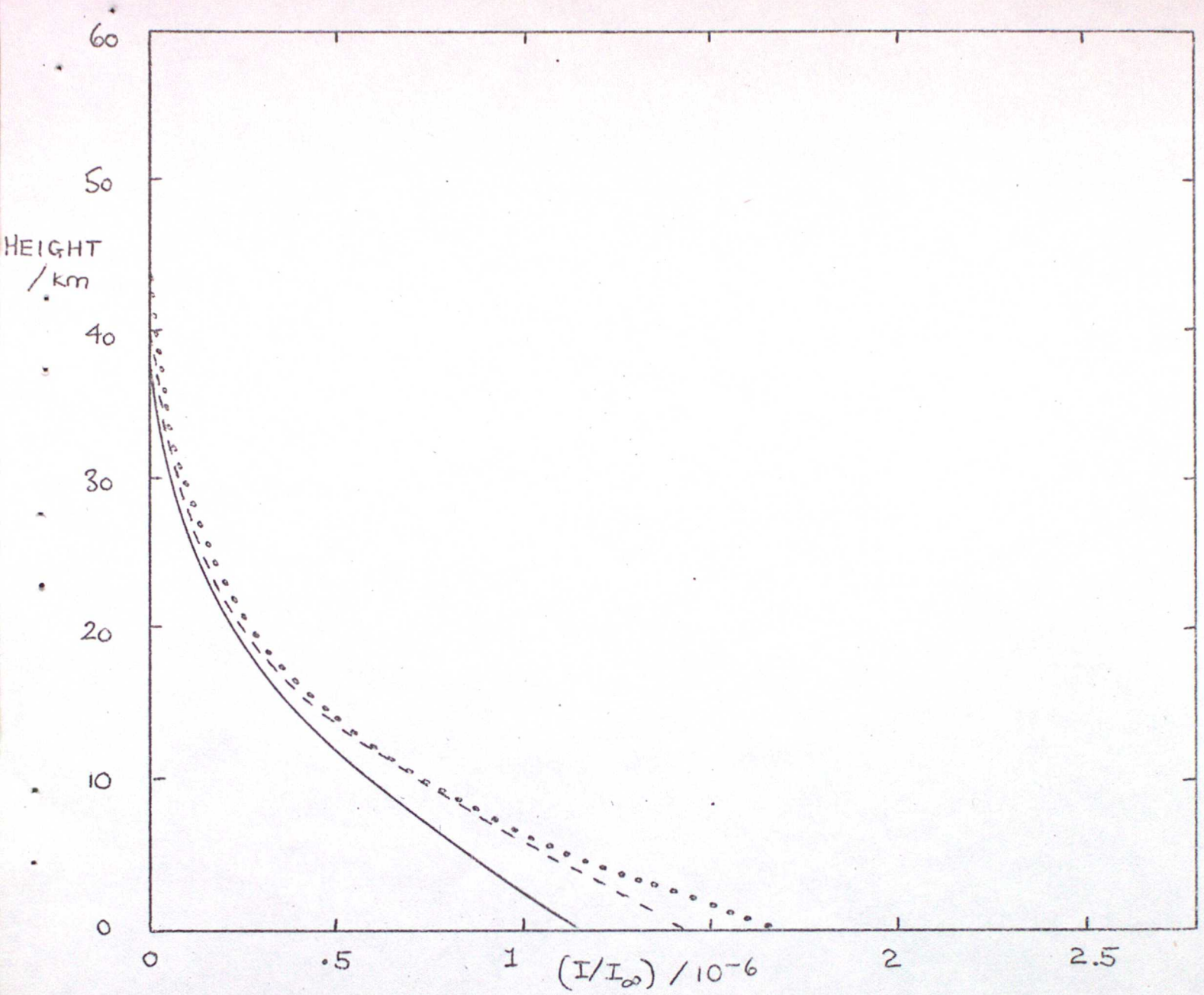

FIG 15 INTENSITY OF SECONDARY RADIATION TRANSMITTED TO GROUND FROM DIFFERENT HEIGHTS AT $Z_0 = 94°$

COLD ATMOSPHERE

WARM ATMOSPHERE

PT1/PT2

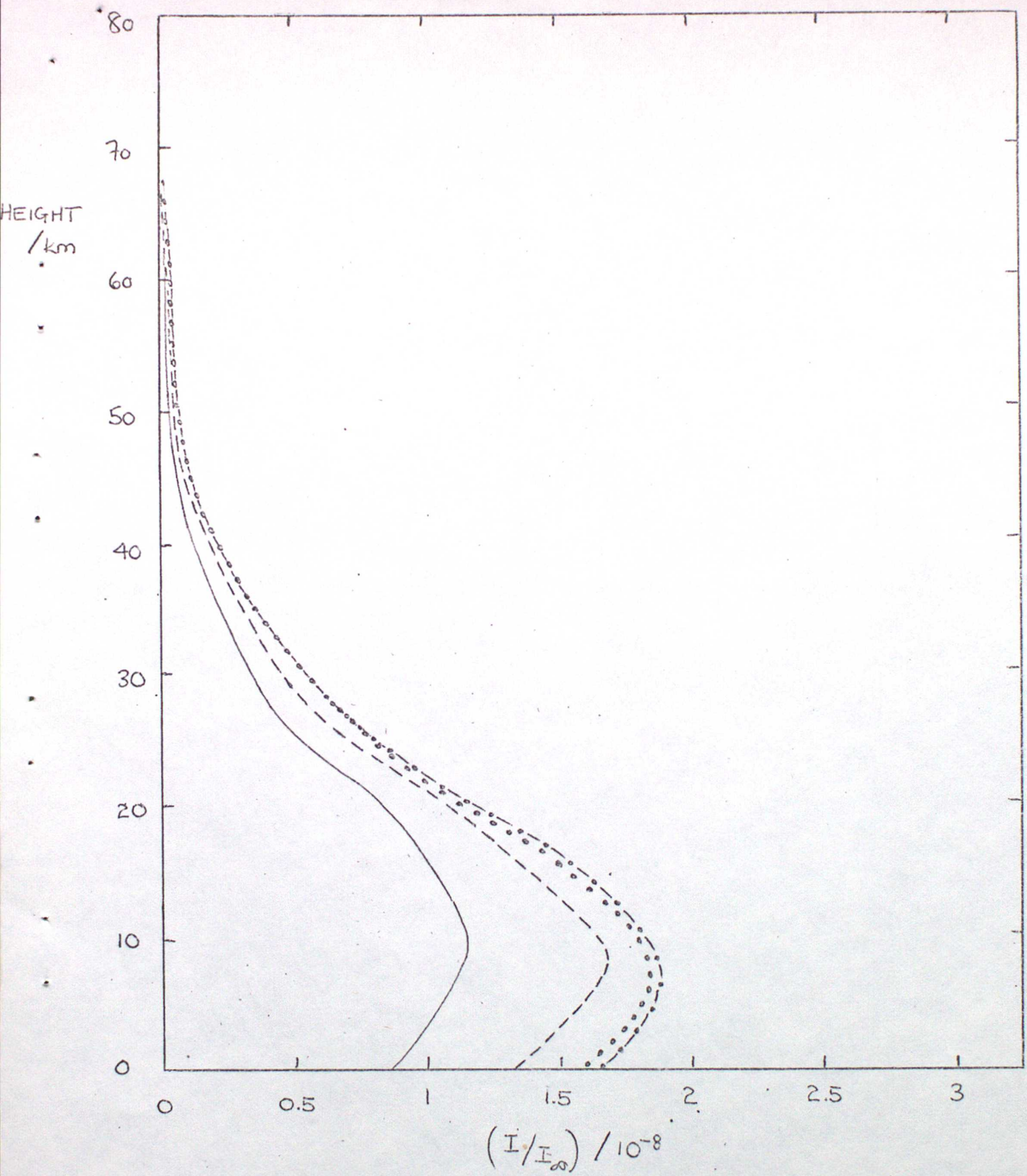

FIG 16 INTENSITY OF SECONDARY RADIATION TRANSMITTED TO GROUND FROM DIFFERENT HEIGHTS AT $Z_0 = 98°$

COLD ATMOSPHERE PT1

WARM ATMOSPHERE -.-.-.- PT2

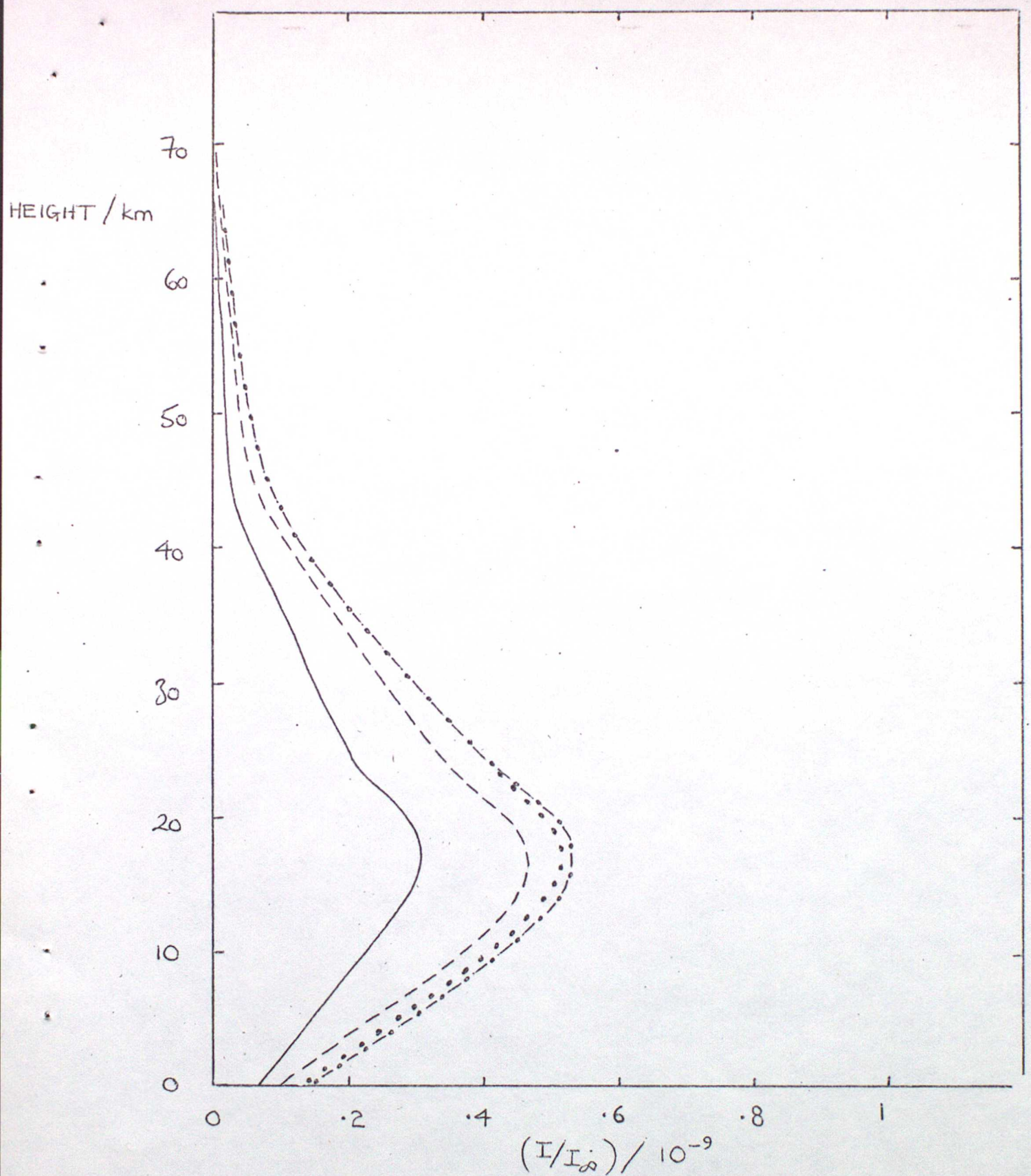

FIG 17 INTENSITY OF SECONDARY RADIATION TRANSMITTED TO GROUND FROM DIFFERENT HEIGHTS AT $Z_0 = 102°$

~ COLD ATMOSPHERE

-- WARM ATMOSPHERE

..· PT1

·-·-· PT2

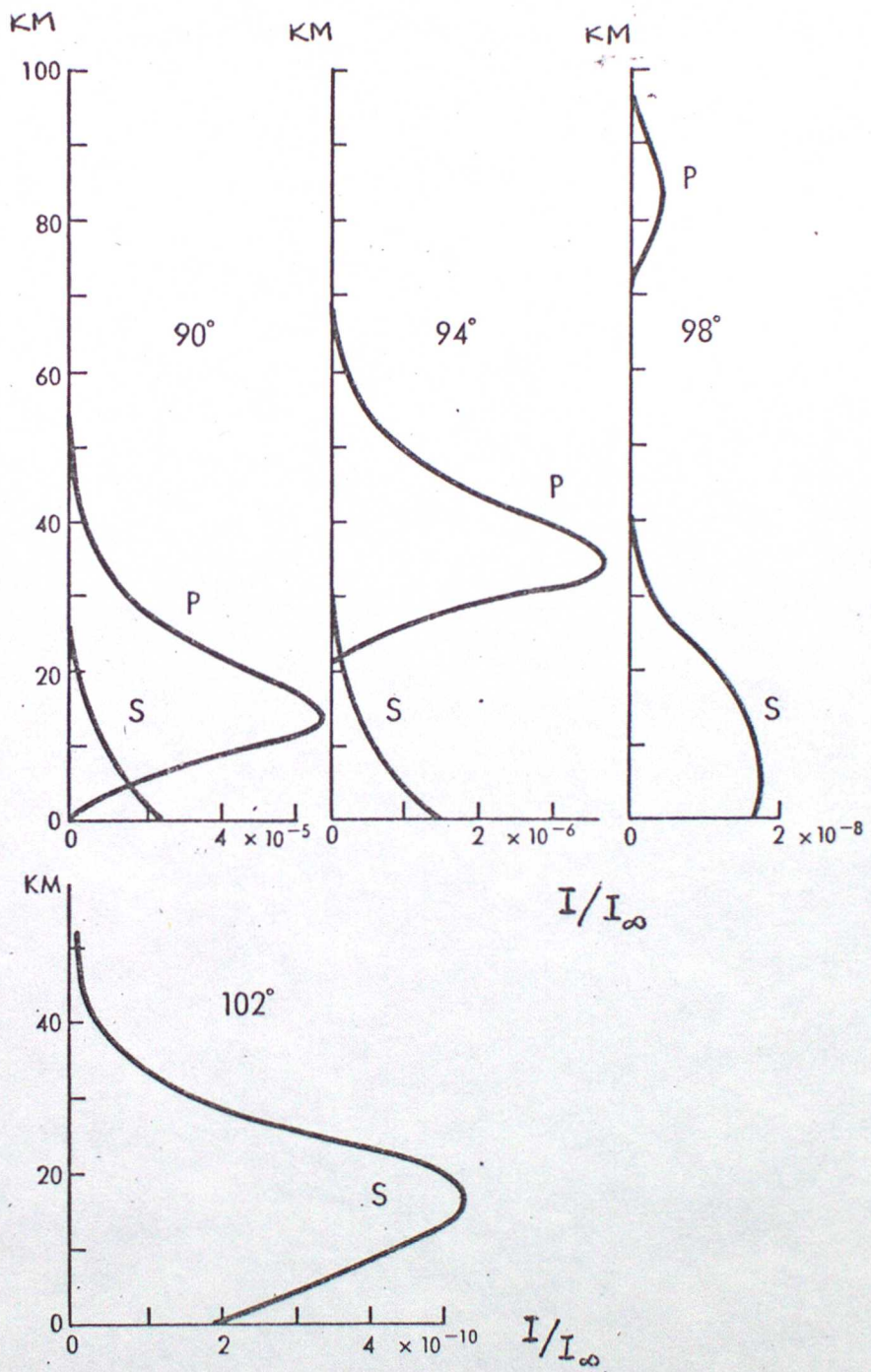

FIG 18 VERTICAL DISTRIBUTION PRIM. & SEC. SCATTERED RADIATION
(AFTER DAVE, 1956)

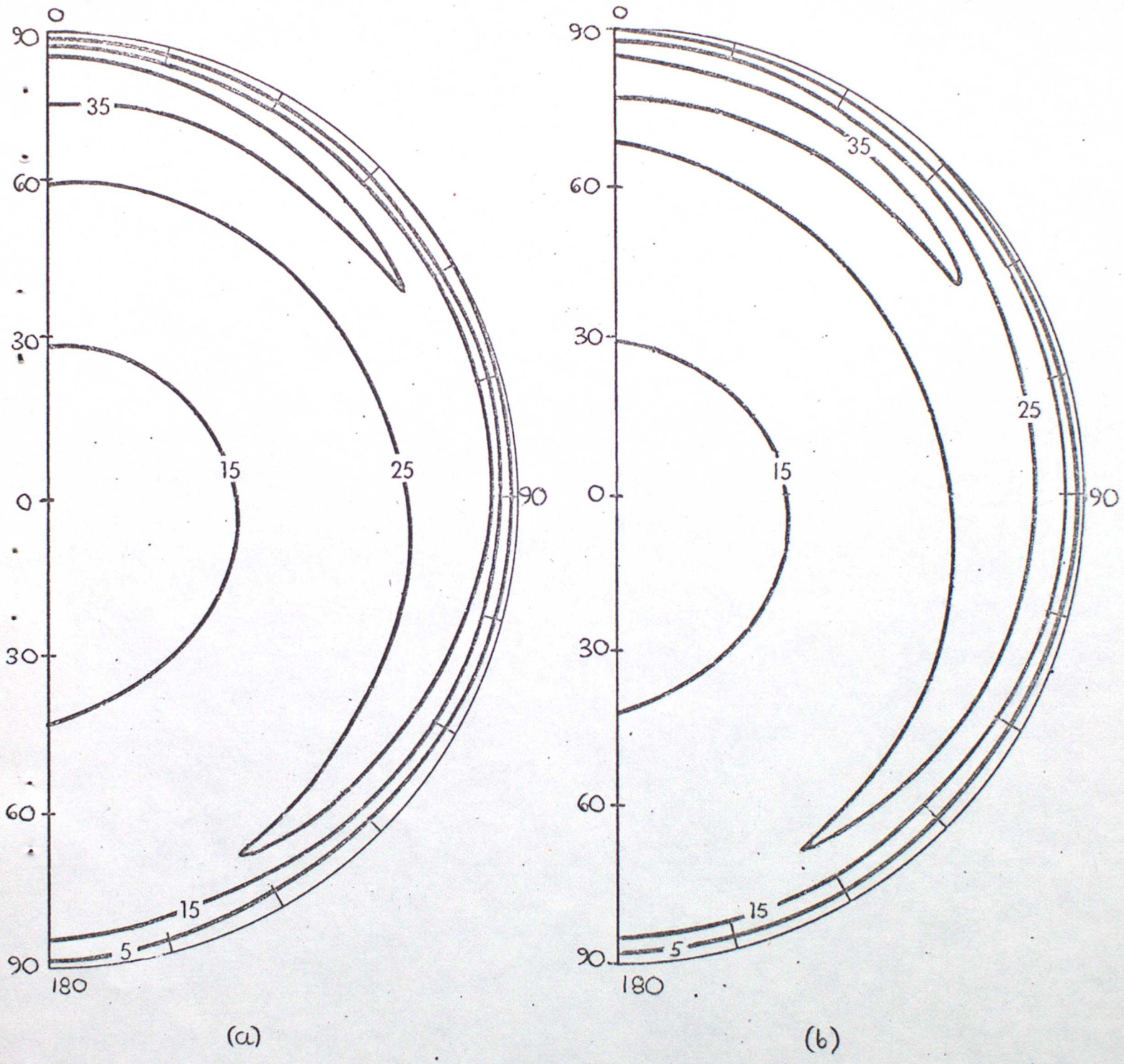

FIG 19 Isopleths of the normal component of primary scattered light received at the surface $(I/I_0)/10^{-4}$, $Z_0 = 90°$

(a) after Dave (1956) . (b) this work

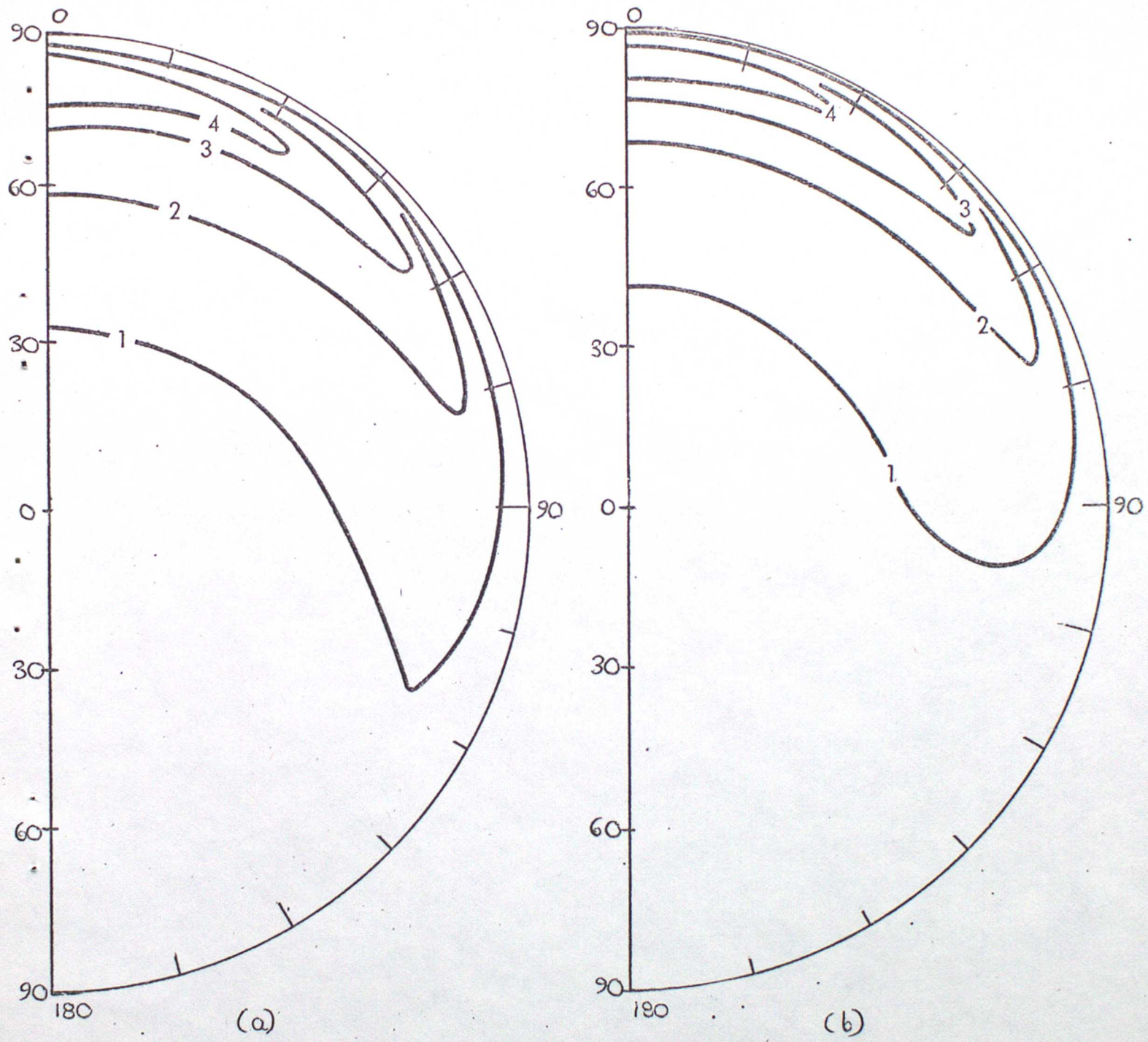

FIG 20 $\left(I/I_\infty\right)/10^{-4}$, $Z_0 = 94°$. (see FIG 19)

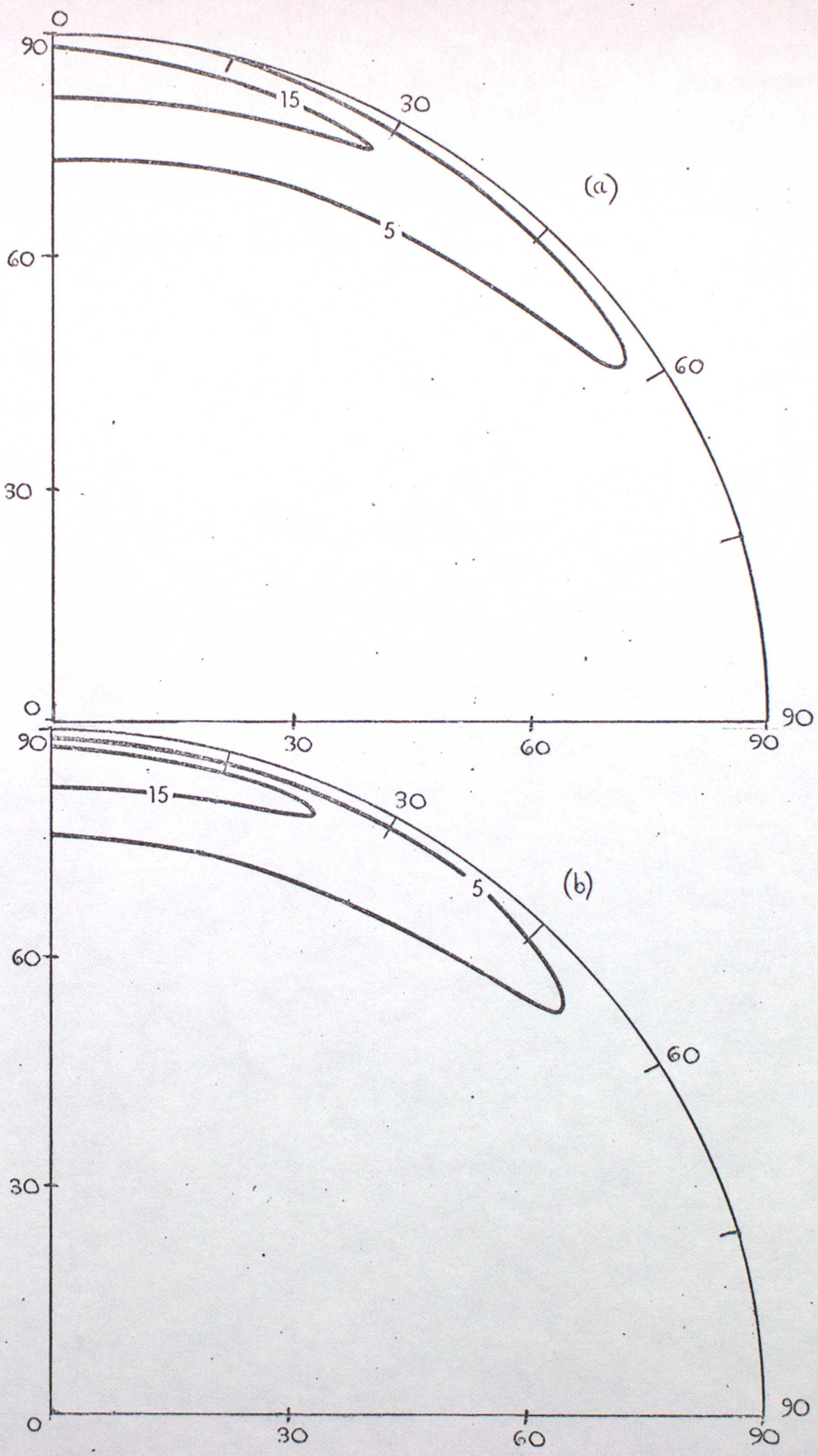

FIG 21 $(I/I_\infty)/10^{-6}$, $Z_0 = 98°$ (see FIG 19)

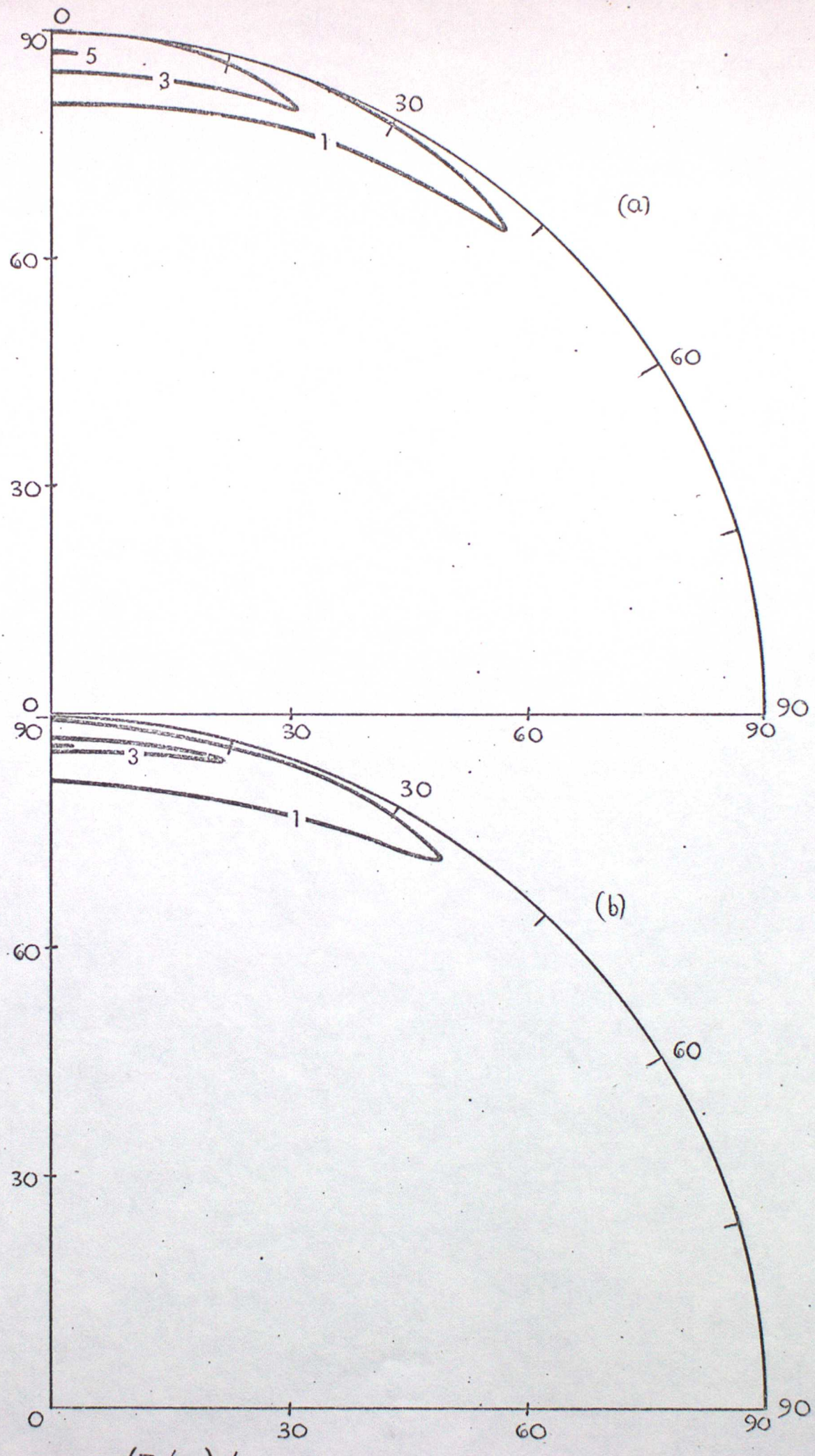

FIG 22 $(I/I_\infty)/10^{-7}$, $Z_0 = 102°$ (see FIG 19)

Fig. 23 Noxon's NO_2 'cliff'

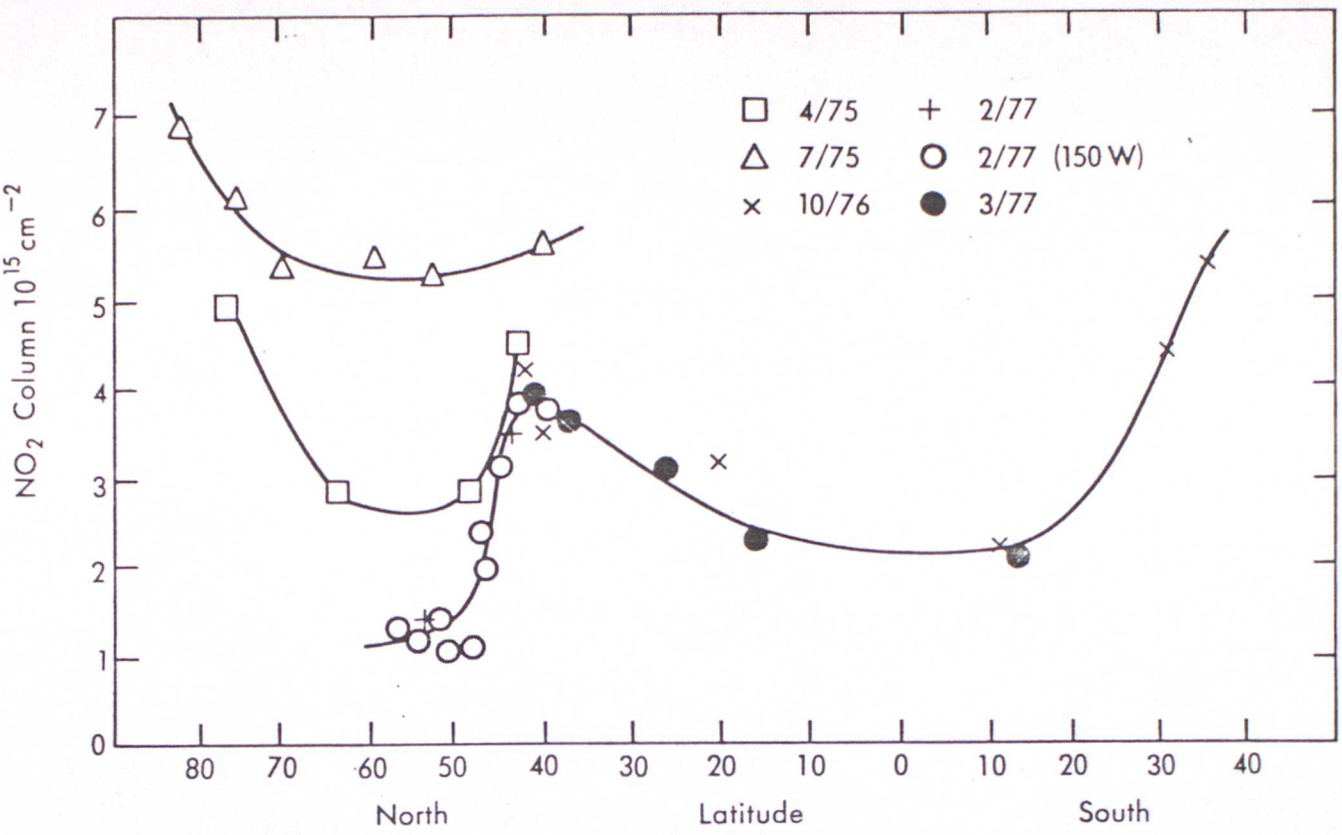

(a) Representative groups of measurements of the late afternoon total column abundance of stratospheric NO_2 to illustrate the dependence upon latitude and season. Except as noted, the measurements are all near 75°W

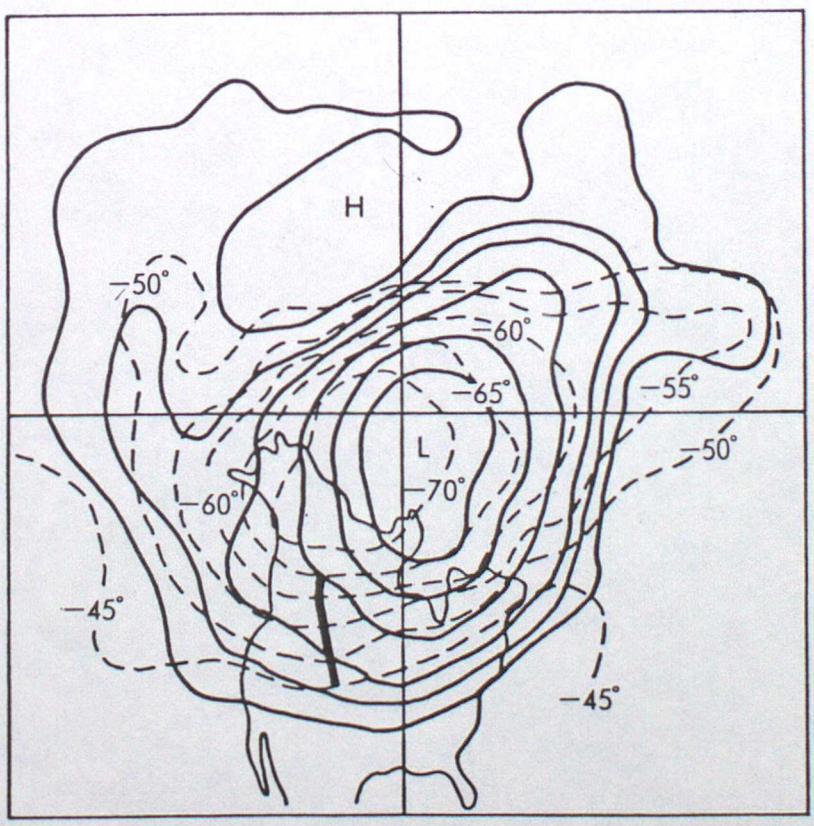

(b) Northern hemisphere at 10mbar during February 1977. Solid lines show streamlines of the polar vortex in which the circulation is counterclockwise. Dashed lines give temperature isotherms, and the thick line is the path driven by the van (containing a portable spectrometer).

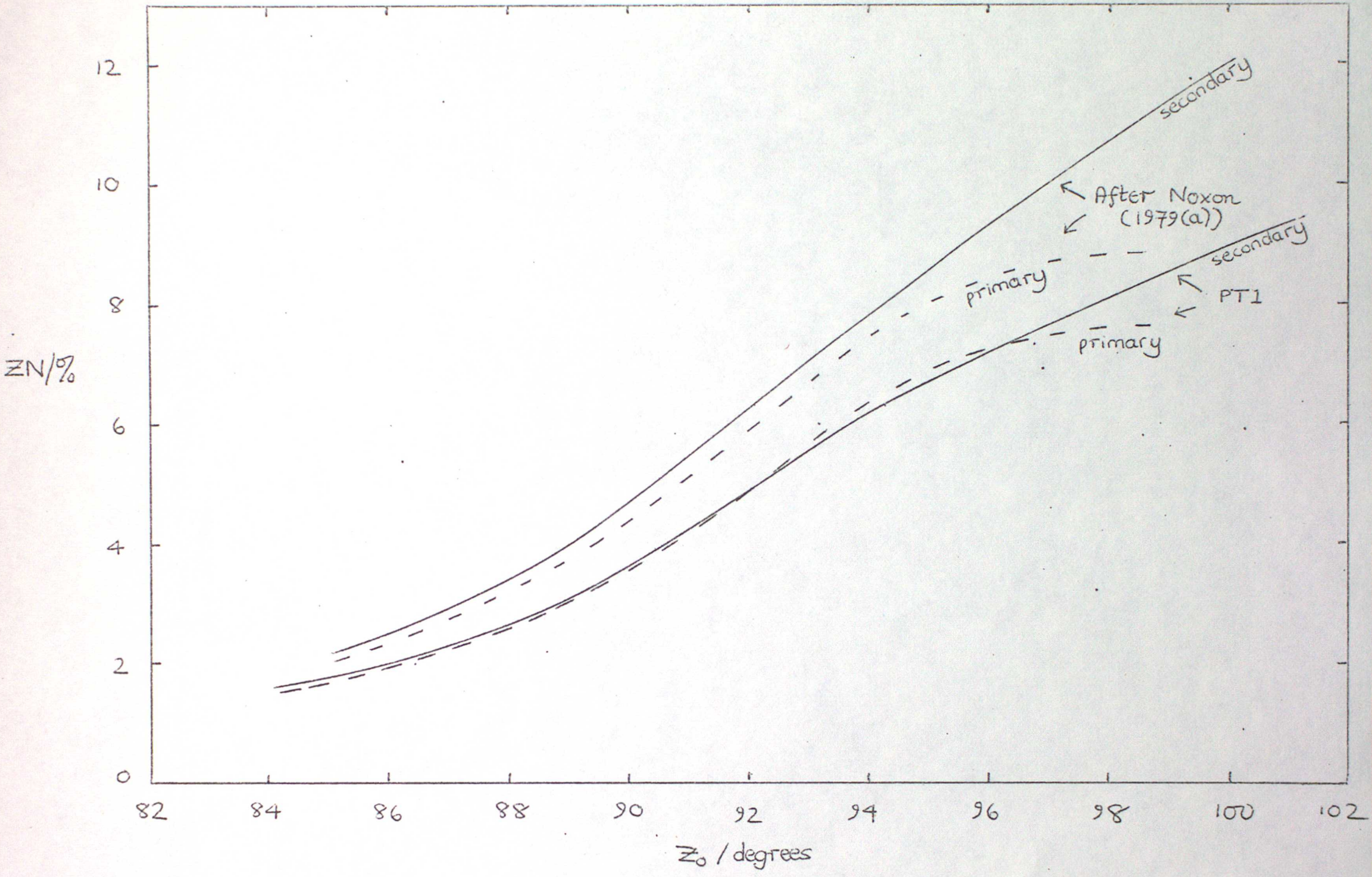

FIG 24 NO_2 ABSORPTION SEEN SEPARATELY IN SINGLY AND DOUBLY SCATTERED LIGHT FOR A UNIFORM (15–45 KM) NO_2 DISTRIBUTION.

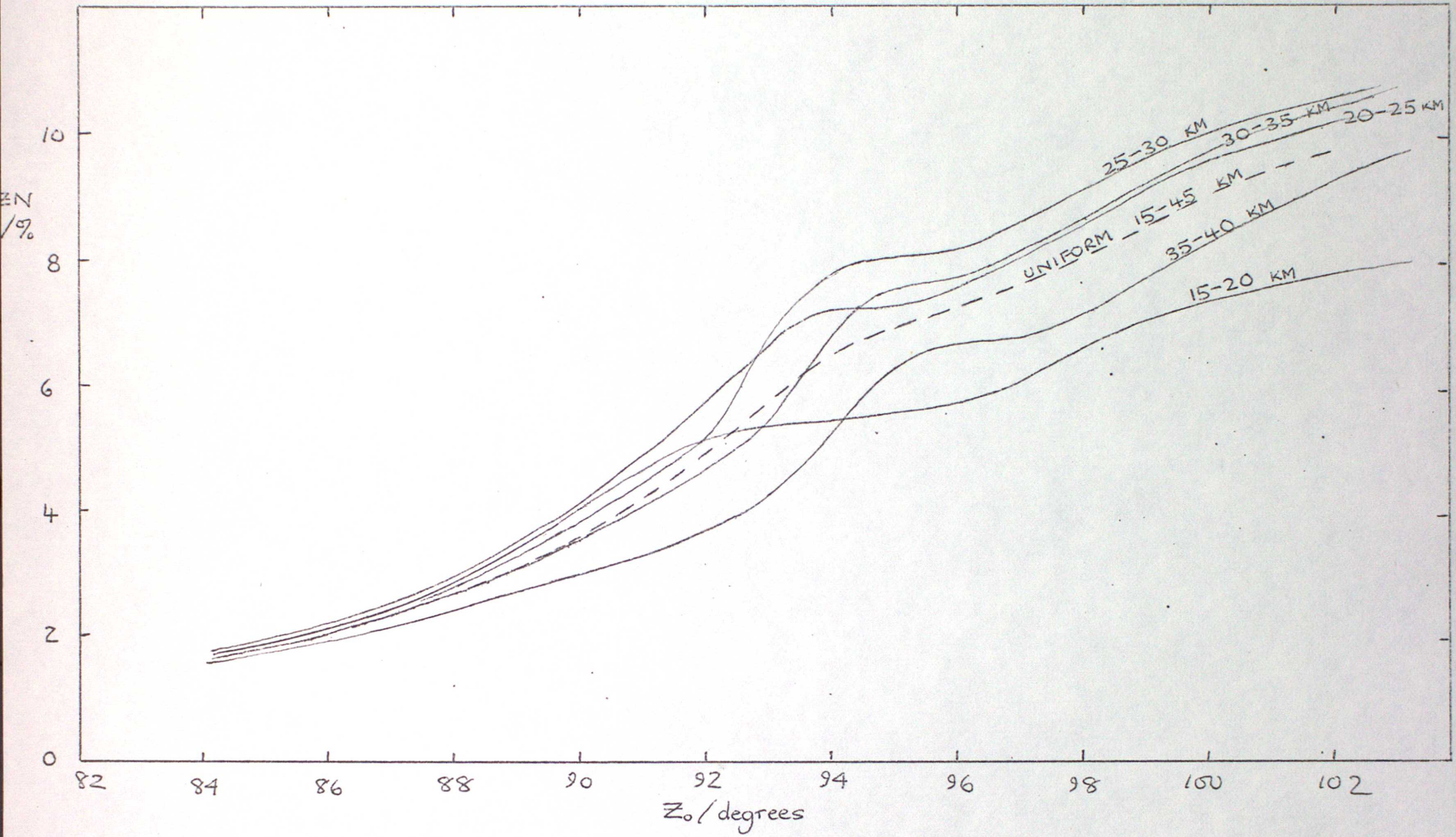

FIG 25 SYNTHETIC NO_2 ABSORPTION CURVES FROM PTI CALCULATIONS (ISOTHERMAL ATMOSPHERE)

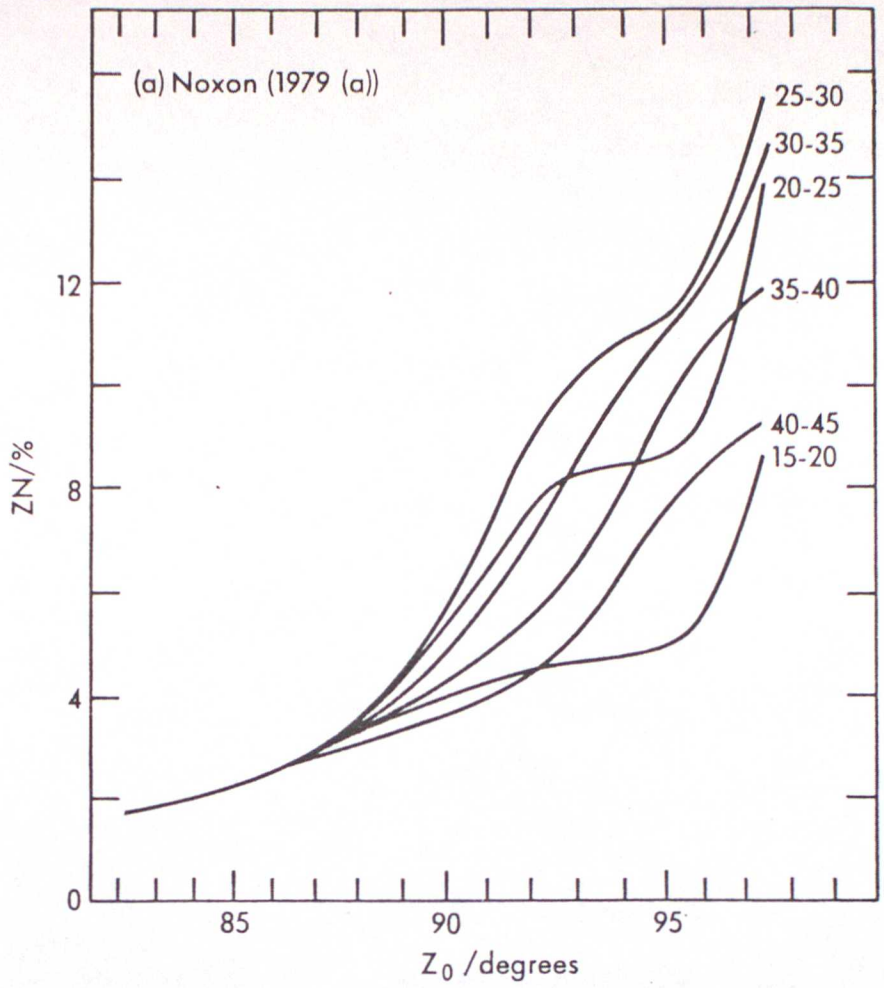

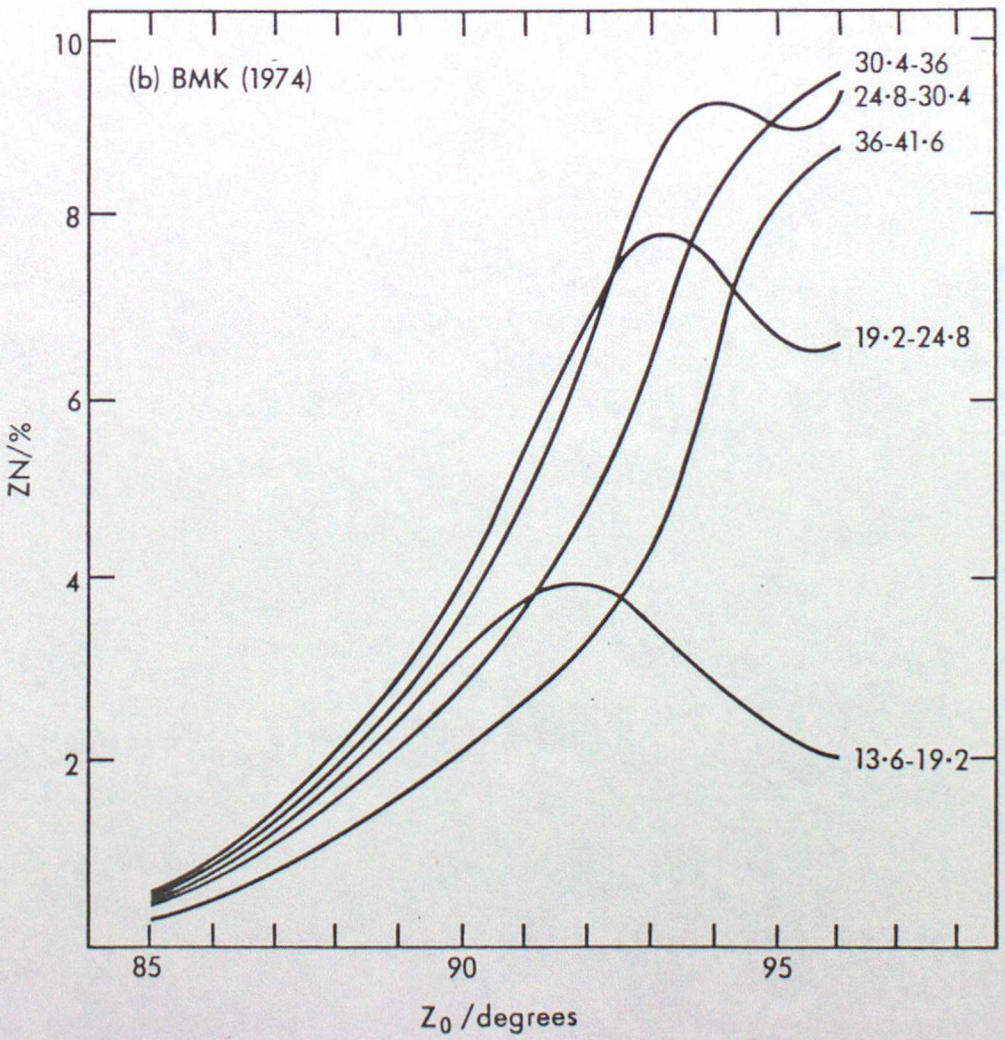

Fig. 26 Synthetic absorption curves calculated by Noxon and BMK.

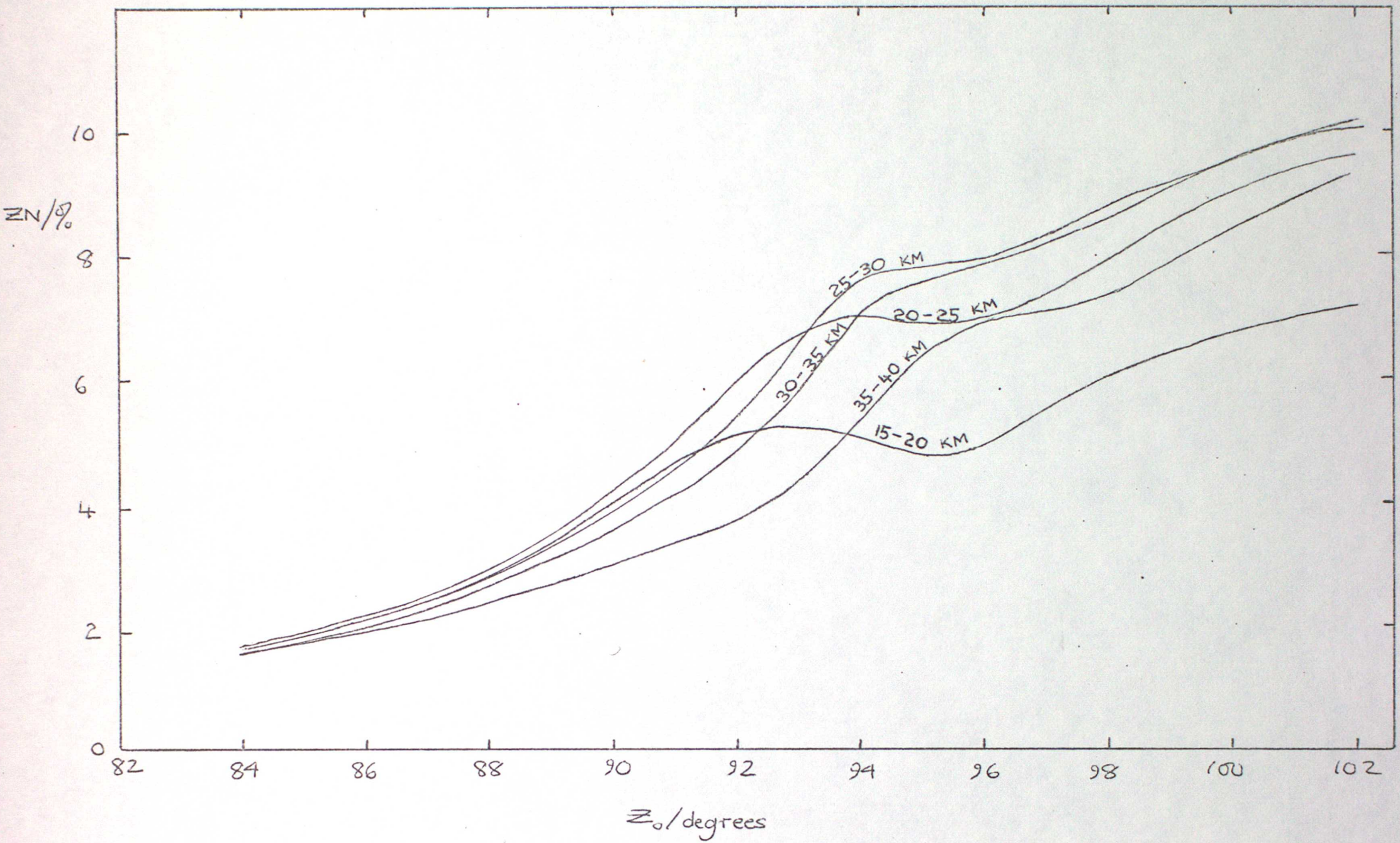

FIG 27 SYNTHETIC NO_2 ABSORPTION CURVES FOR WARM ATMOSPHERE.

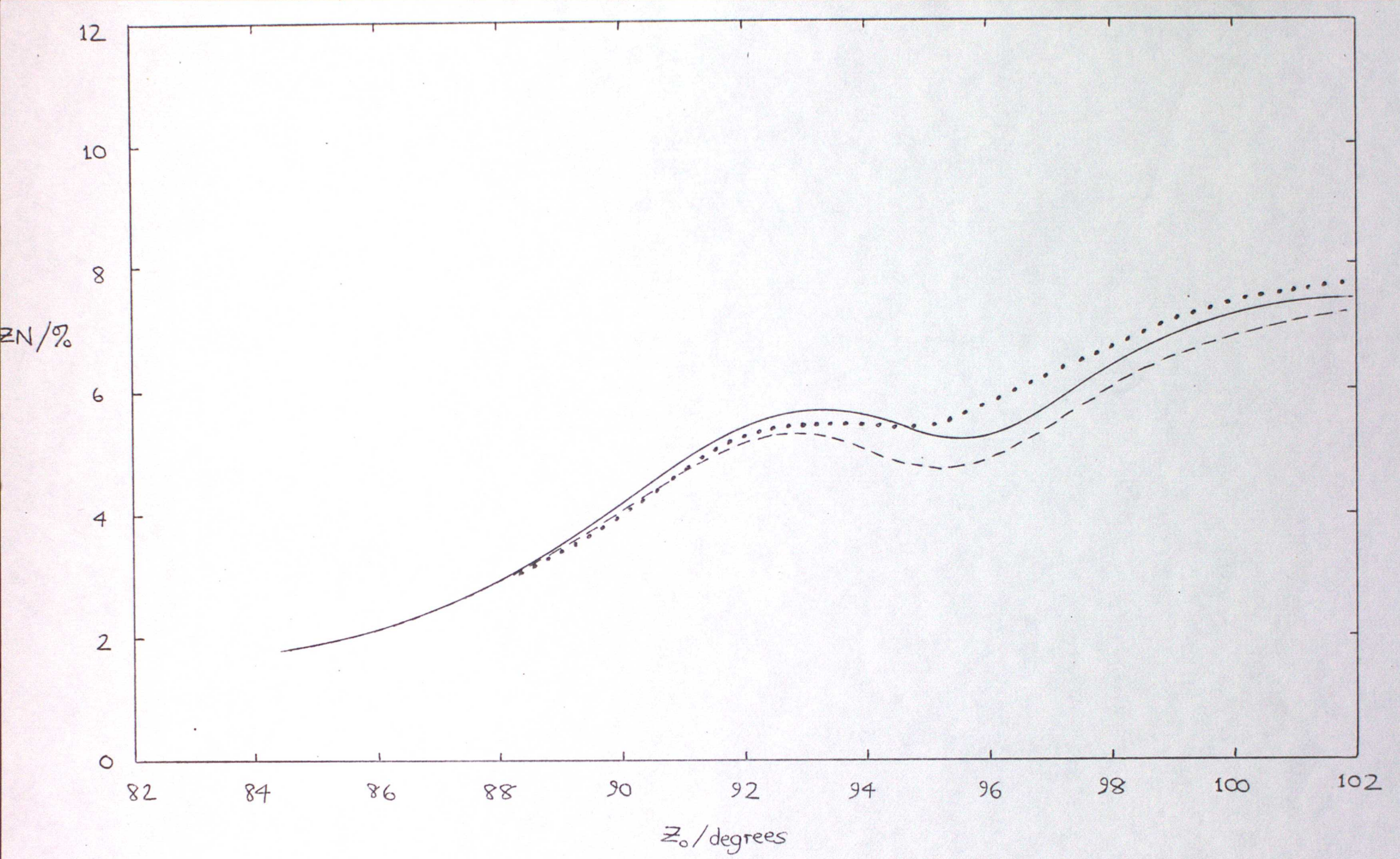

FIG 28 15–20 KM NO_2 ABSORPTION CURVES

COLD ATMOSPHERE

WARM ATMOSPHERE

PT1

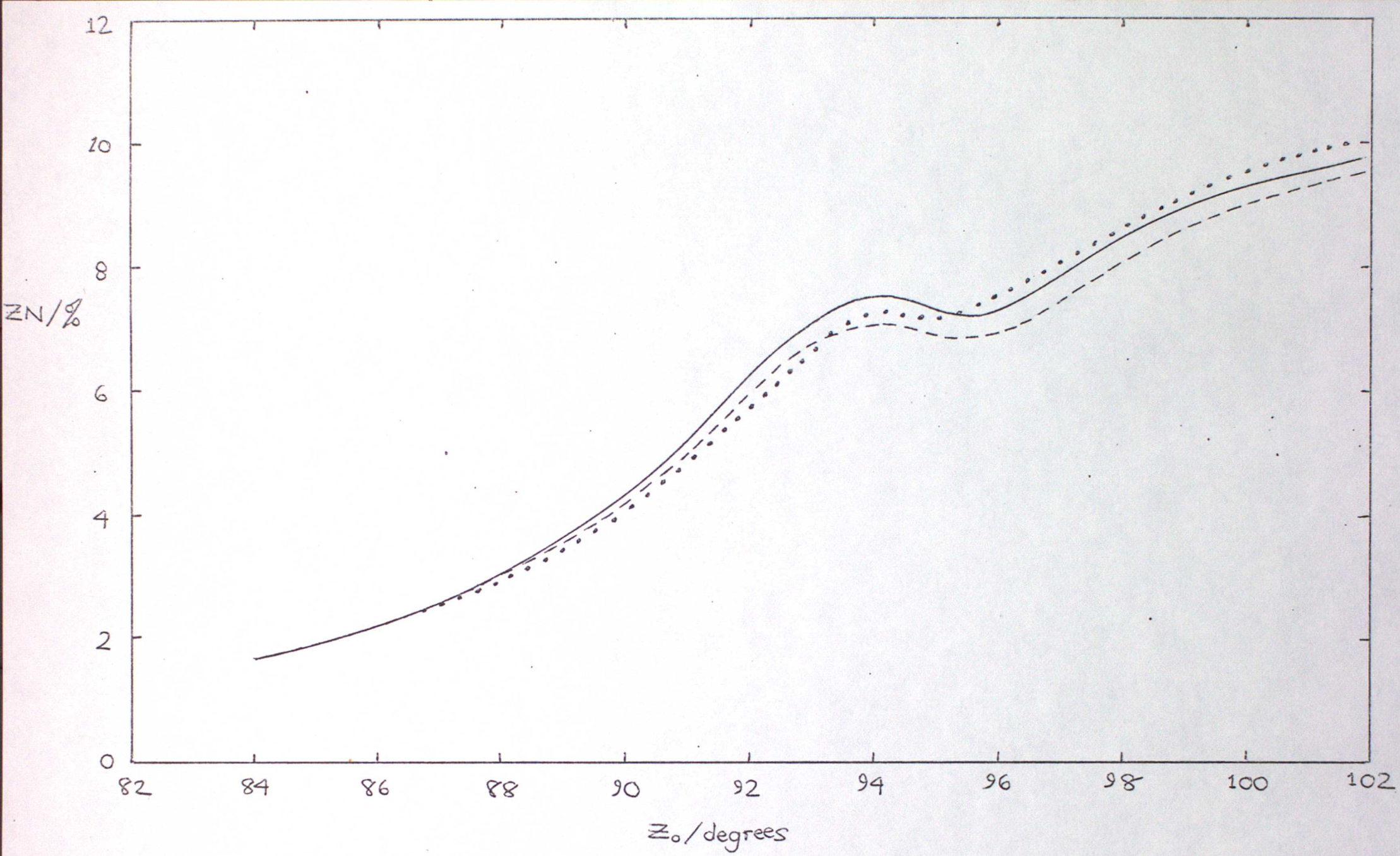

FIG 29 20-25 KM NO_2 ABSORPTION CURVES

COLD ATMOSPHERE

WARM ATMOSPHERE

PT1

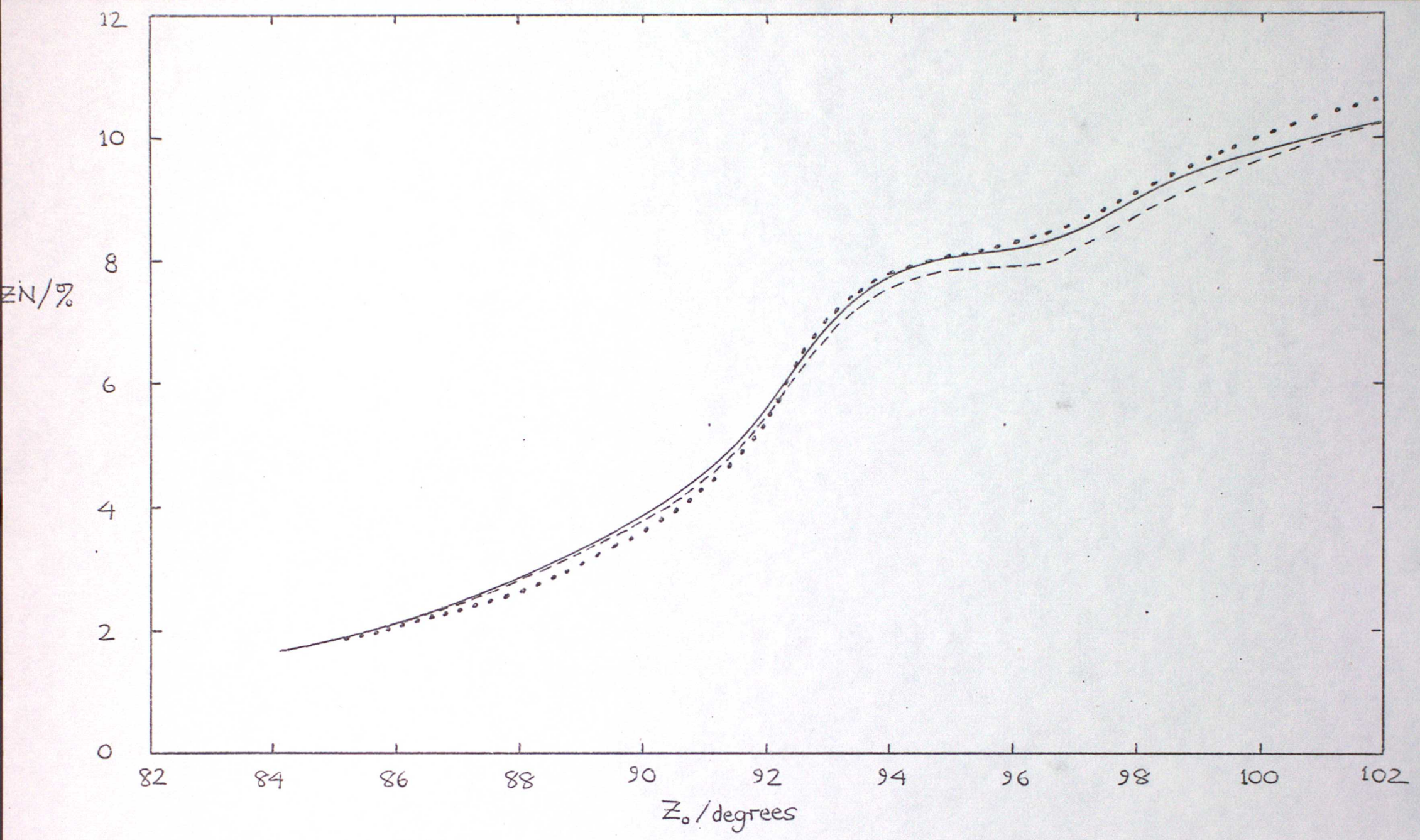

FIG 30 25 – 30 KM NO_2 ABSORPTION CURVES

COLD ATMOSPHERE

WARM ATMOSPHERE

PT1

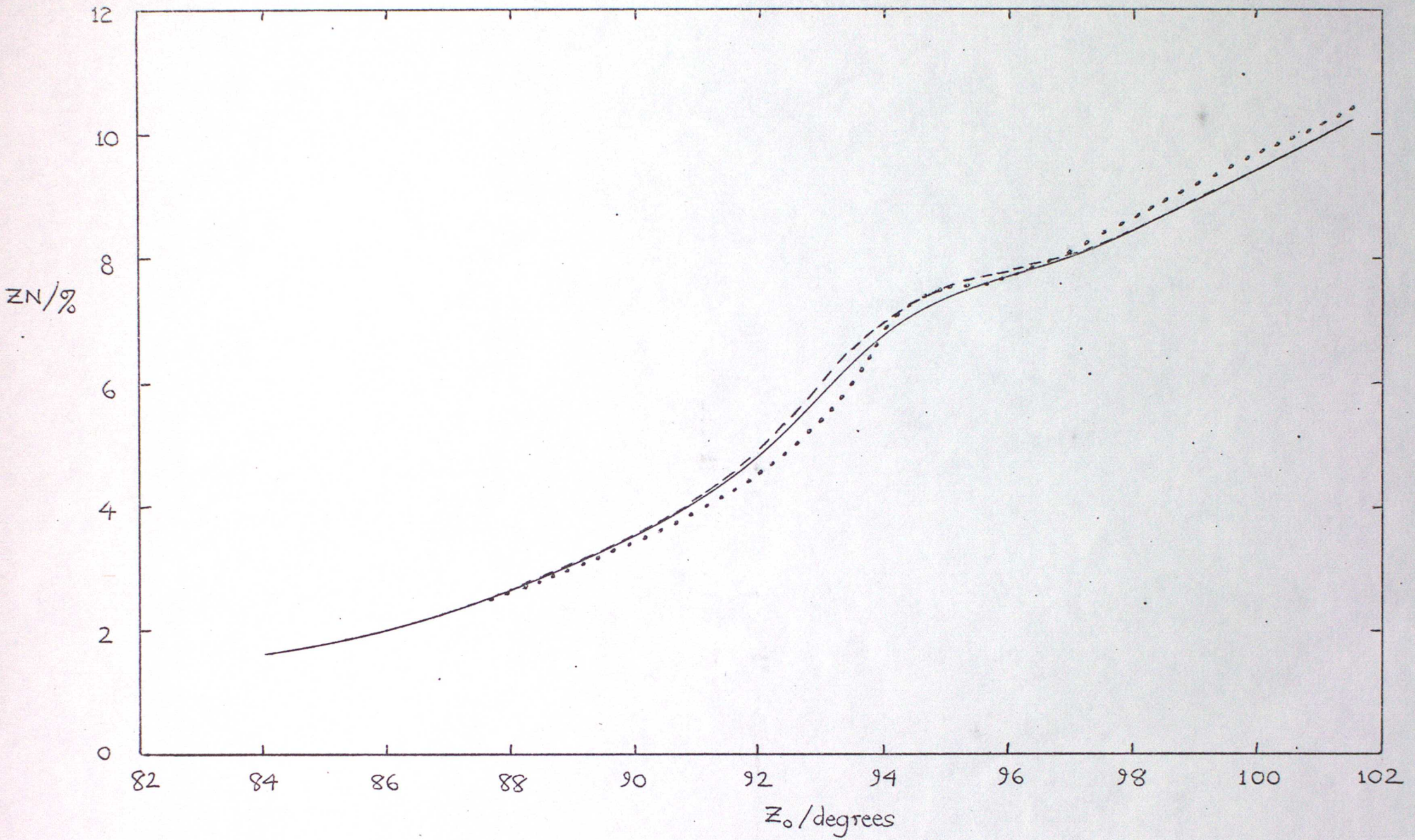

FIG 31 30-35 KM NO_2 ABSORPTION CURVES

COLD ATMOSPHERE

WARM. ATMOSPHERE

PT1

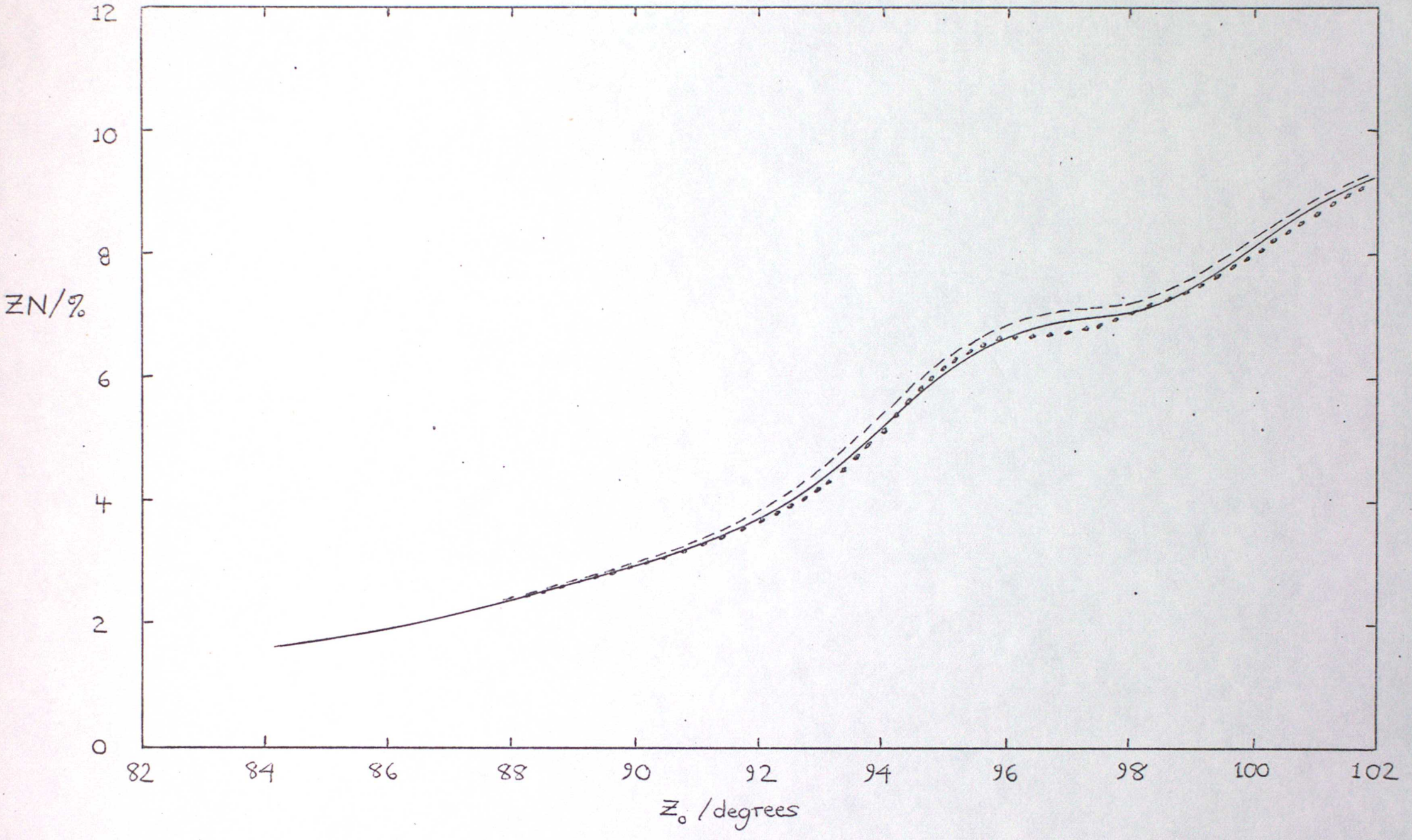

FIG 32 35–40 KM NO_2 ABSORPTION CURVES

COLD ATMOSPHERE

WARM ATMOSPHERE

PT1

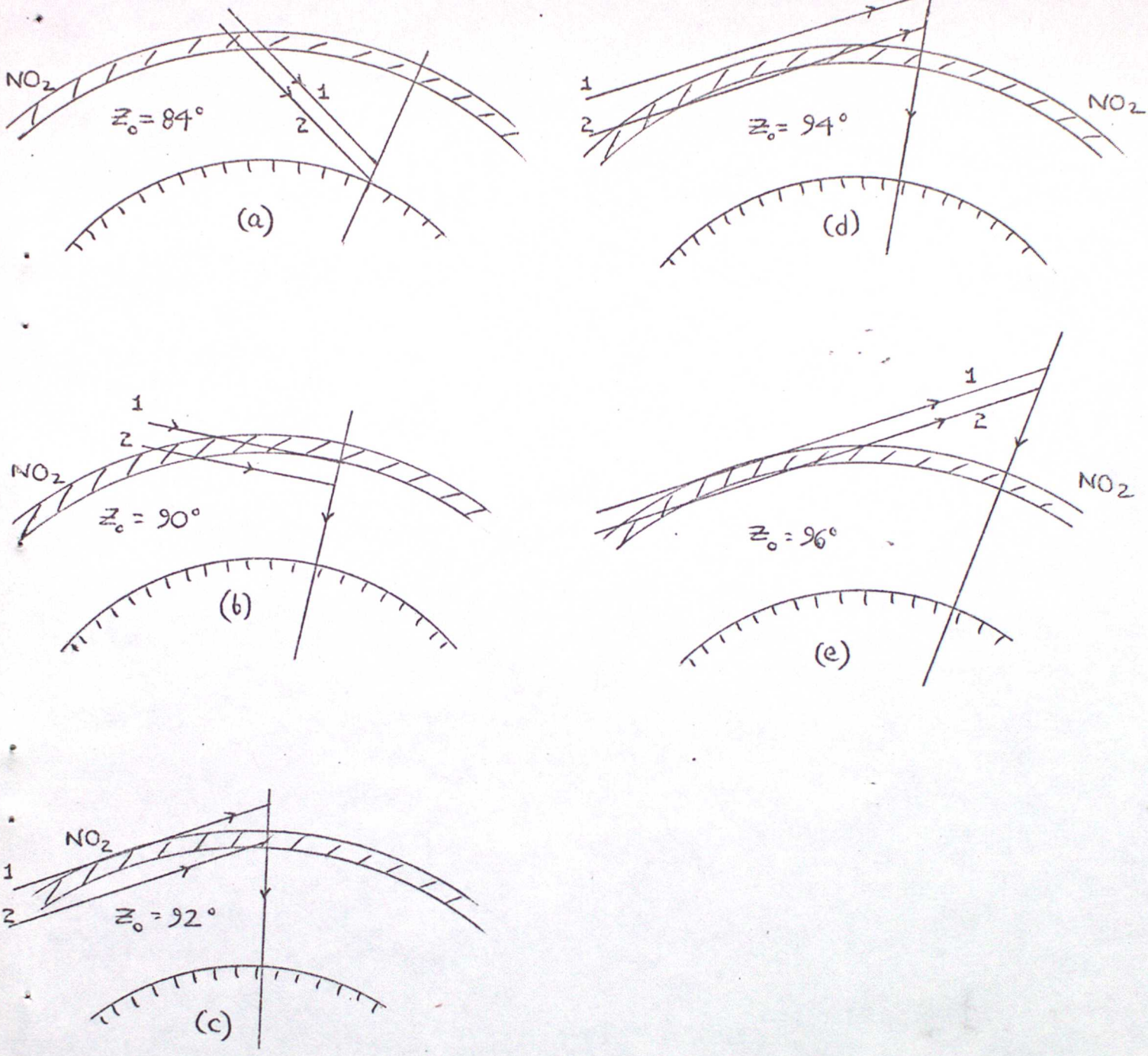

FIG 33 Spherical NO_2 twilight geometry. Rays scattered at the M.S.H. (in the NO_2 absorption range of wavelengths) are shown. The upper ray (1) is based on BMK (1974), while the lower ray (2) is from PTI calculations. The NO_2 layer is at 20-25 km.

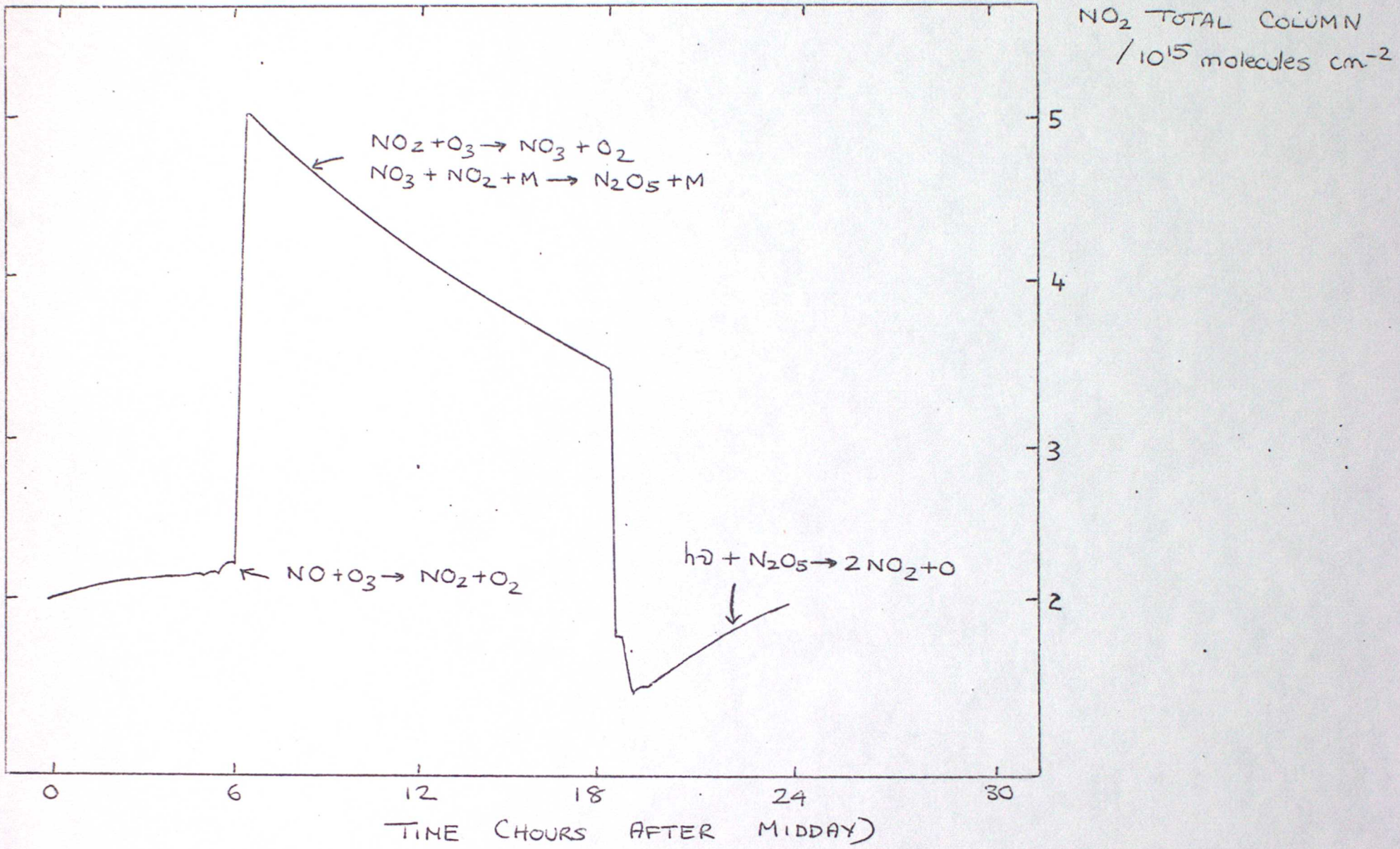

FIG 34 DIURNAL NO_2 FROM MET O 15 1 D PHOTOCHEMICAL MODEL

(NB: MODEL ASSUMES INSTANTANEOUS SUNRISE / SET THROUGHOUT THE VERTICAL COLUMN. EQUINOX CONDITIONS, 34.3° N)

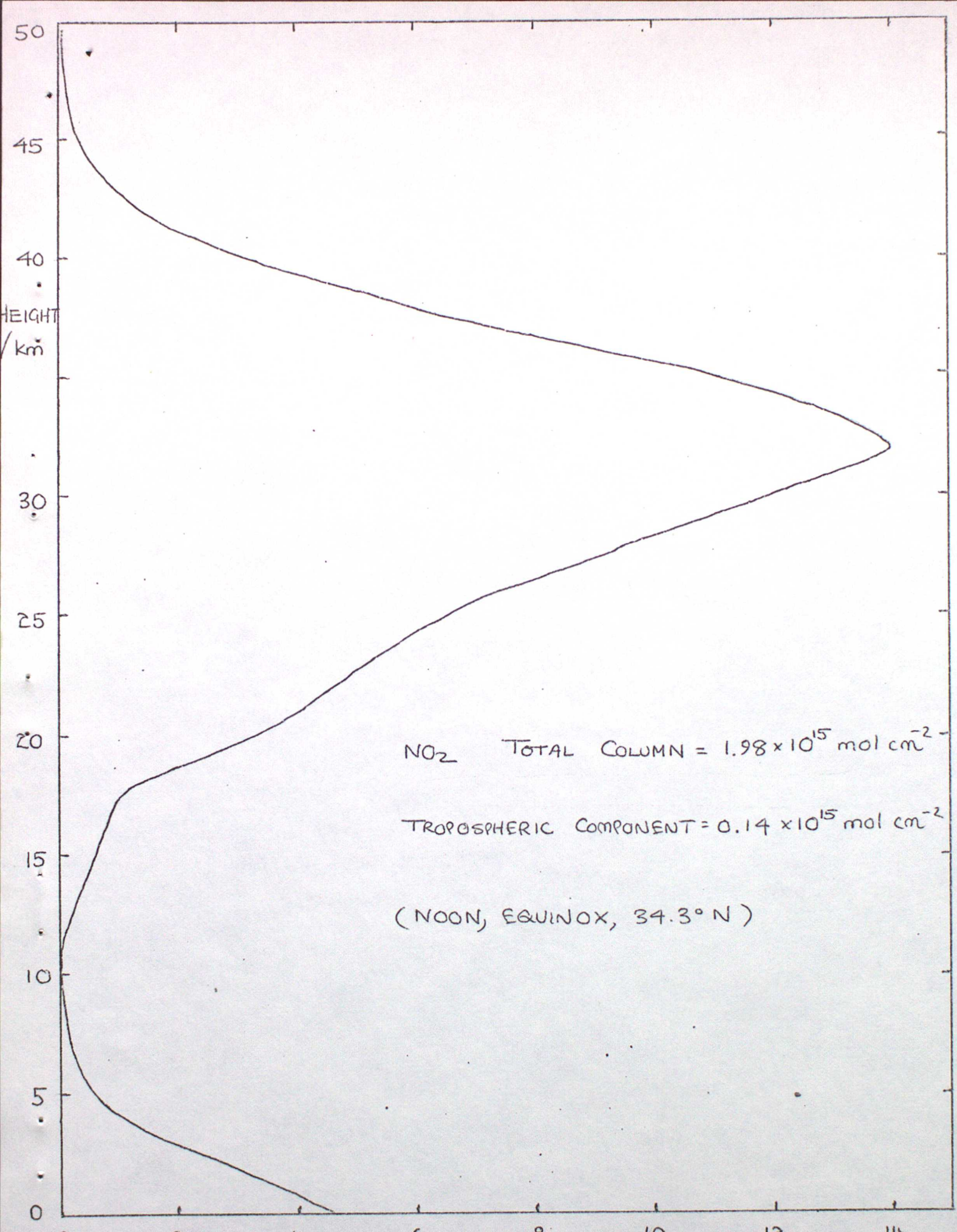

FIG 35 CHEMICAL MODEL VERTICAL NO_2 PROFILE

FIG 36 POLLUTION TEST RESULTS FOR WARM ATMOSPHERE

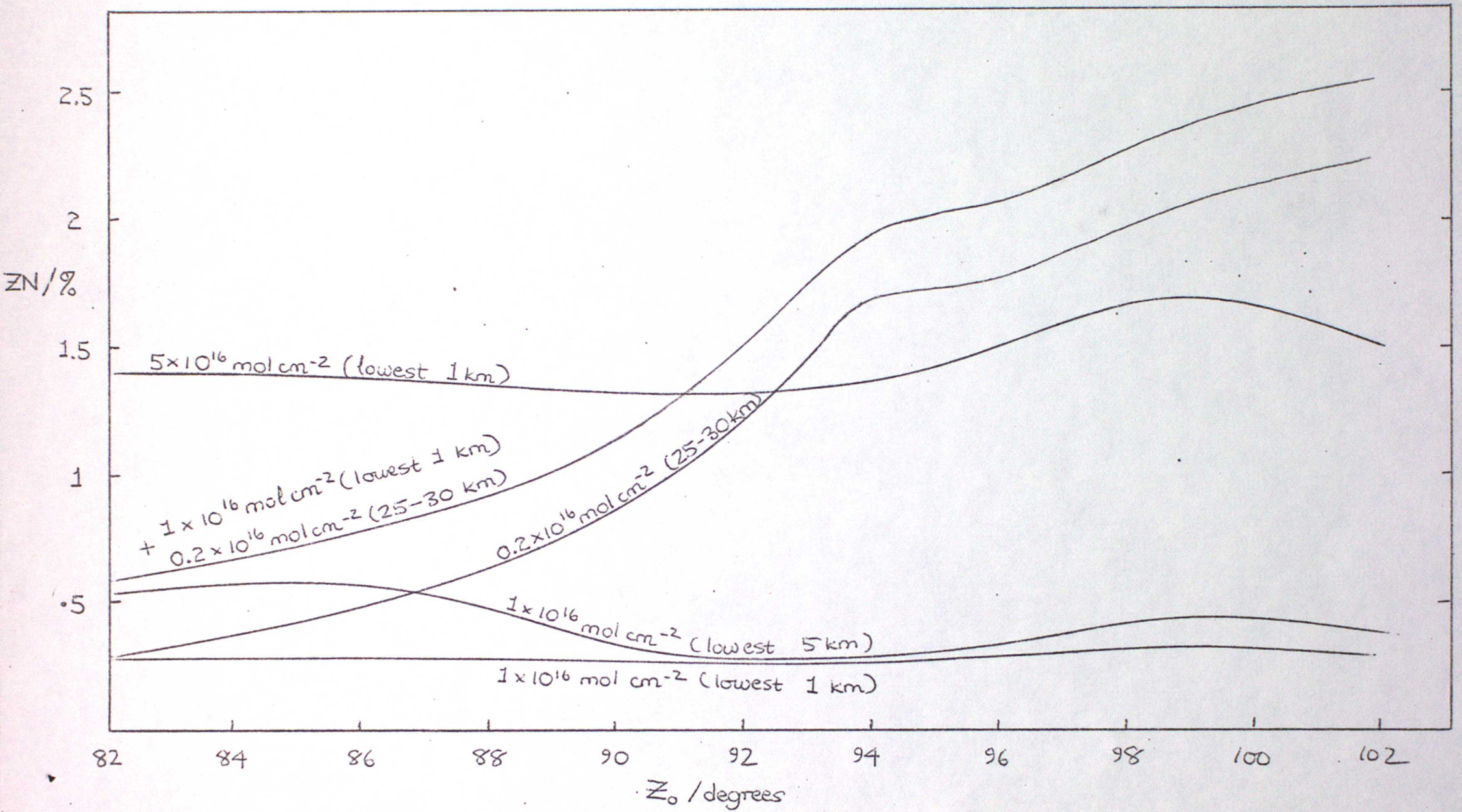

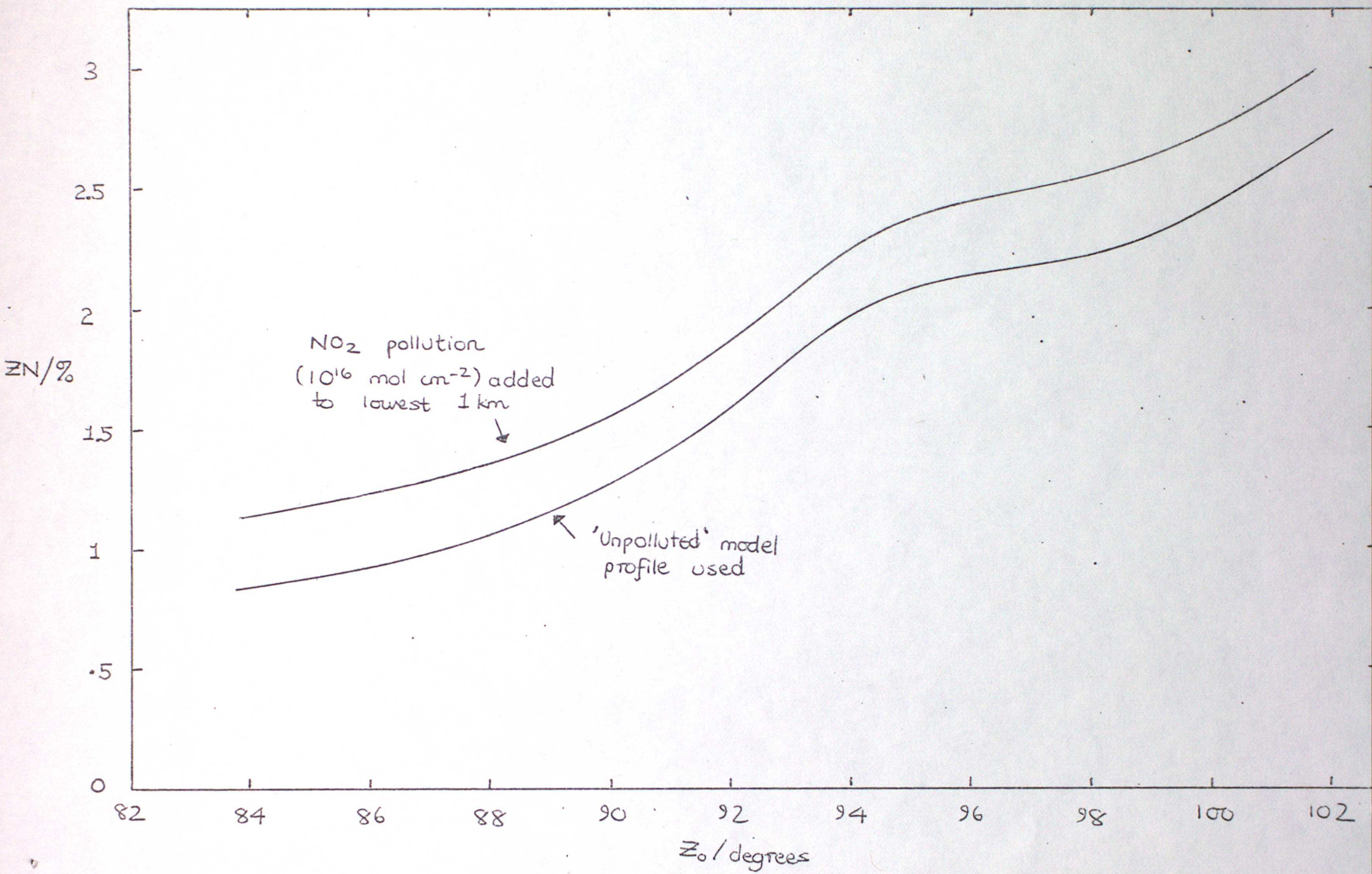

FIG 37 NO_2 ABSORPTION CURVE FOR WARM ATMOSPHERE USING CHEMICAL MODEL NO_2 PROFILE

FIG 38

Ratio spectra obtained using 5/11/81 twilight sky spectra. Scale bar: optical depth of 0.1, relative to reference (14/12/81 midday).

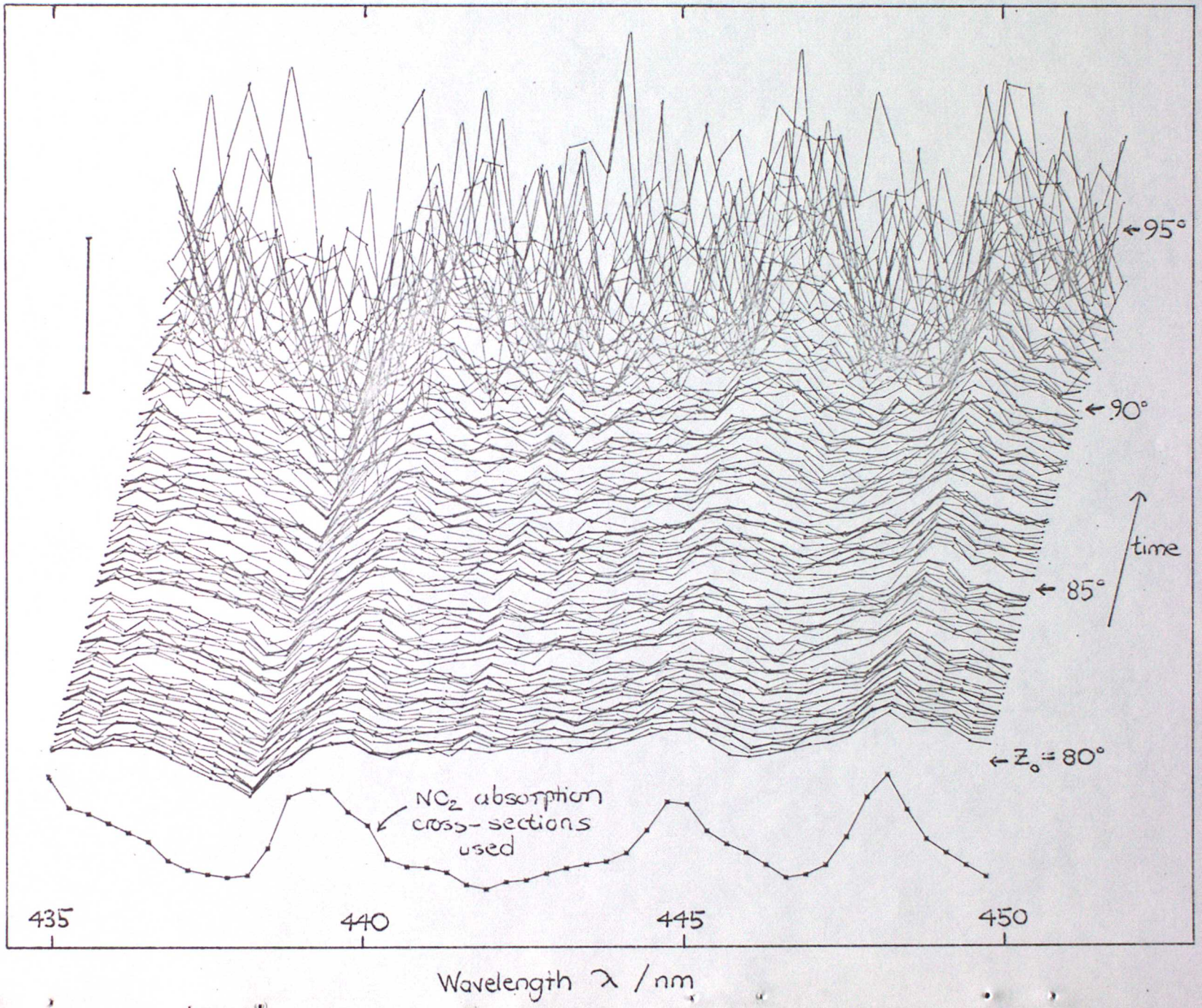

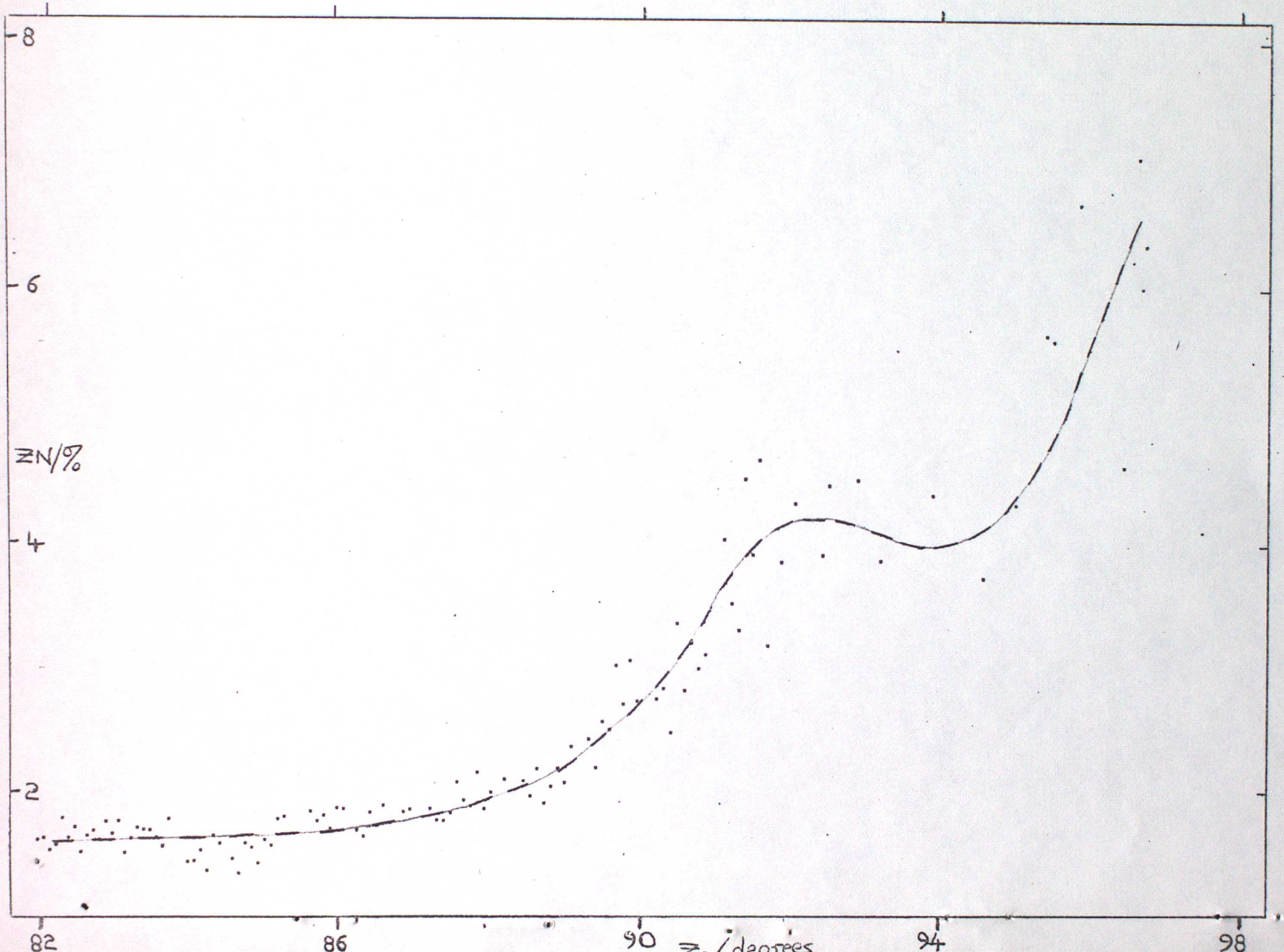

FIG 39.

5/11/81 twilight sky NO_2 absorption, relative to reference (14/12/81).

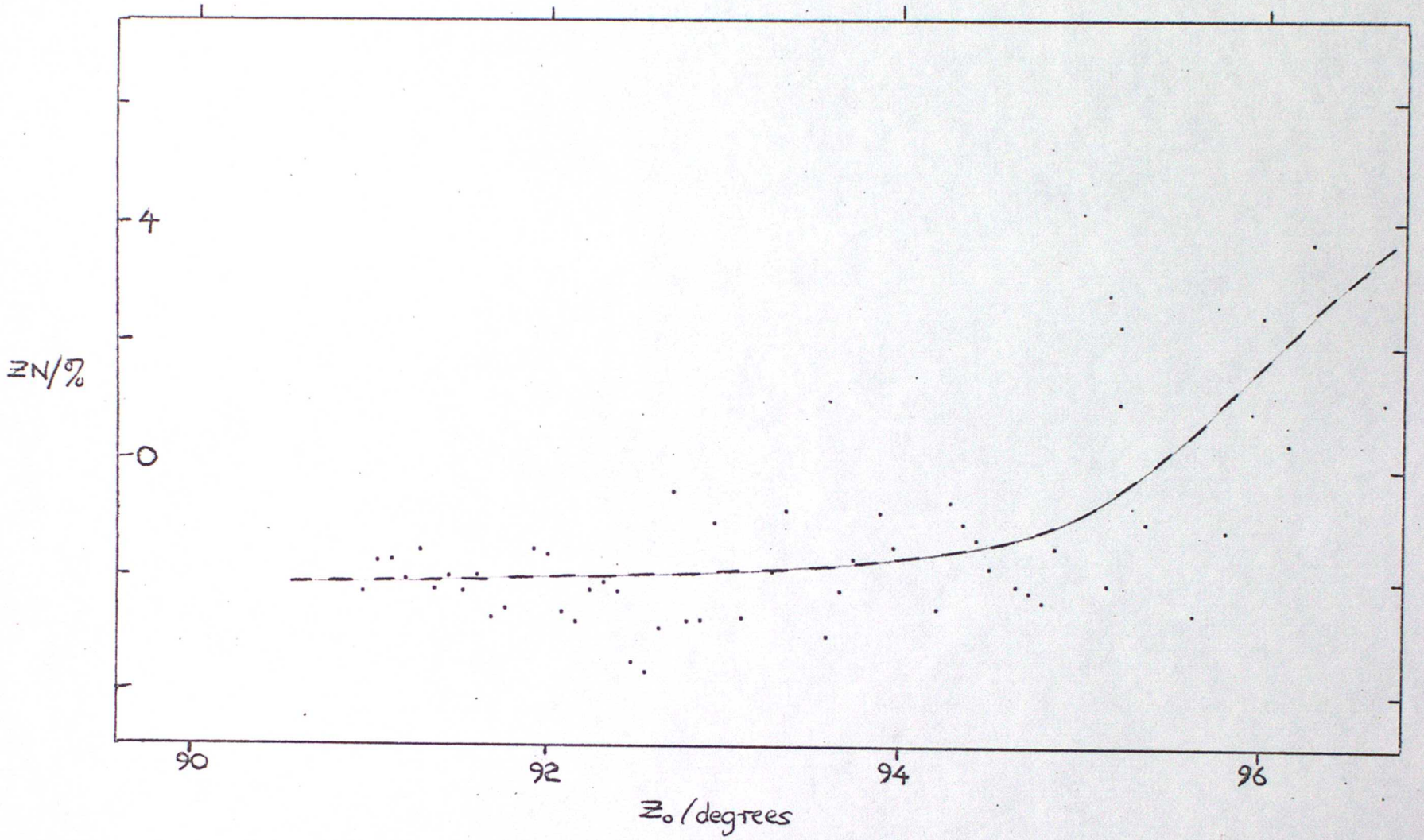

FIG 40 2/6/81 twilight sky NO_2 absorption, relative to reference (22/6/81).

FIG 41 9/11/81 twilight sky NO_2 absorption, relative to reference (14/12/81).

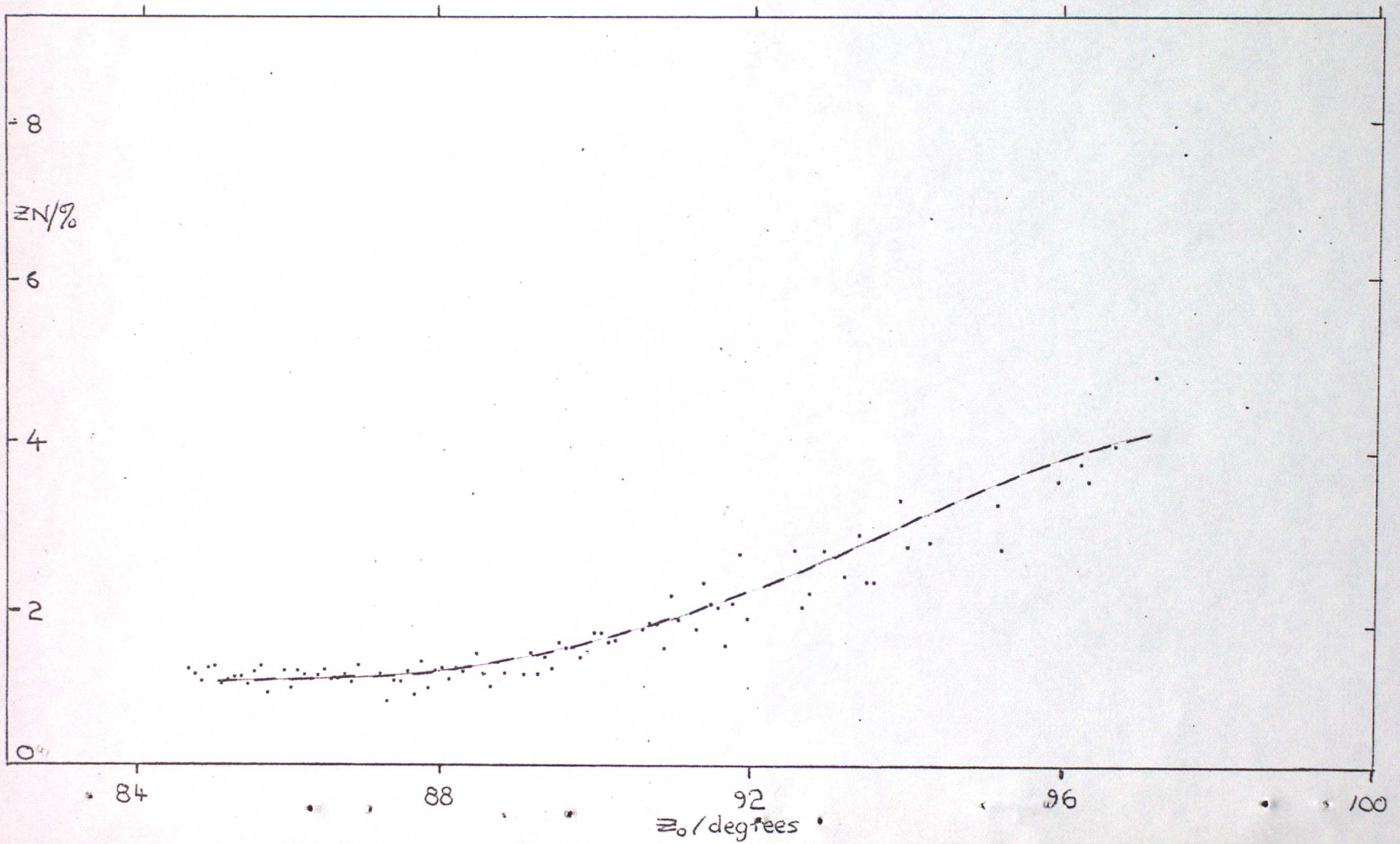

FIG 42 12/12/81 twilight sky NO_2 absorption, relative to reference (14/12/81).

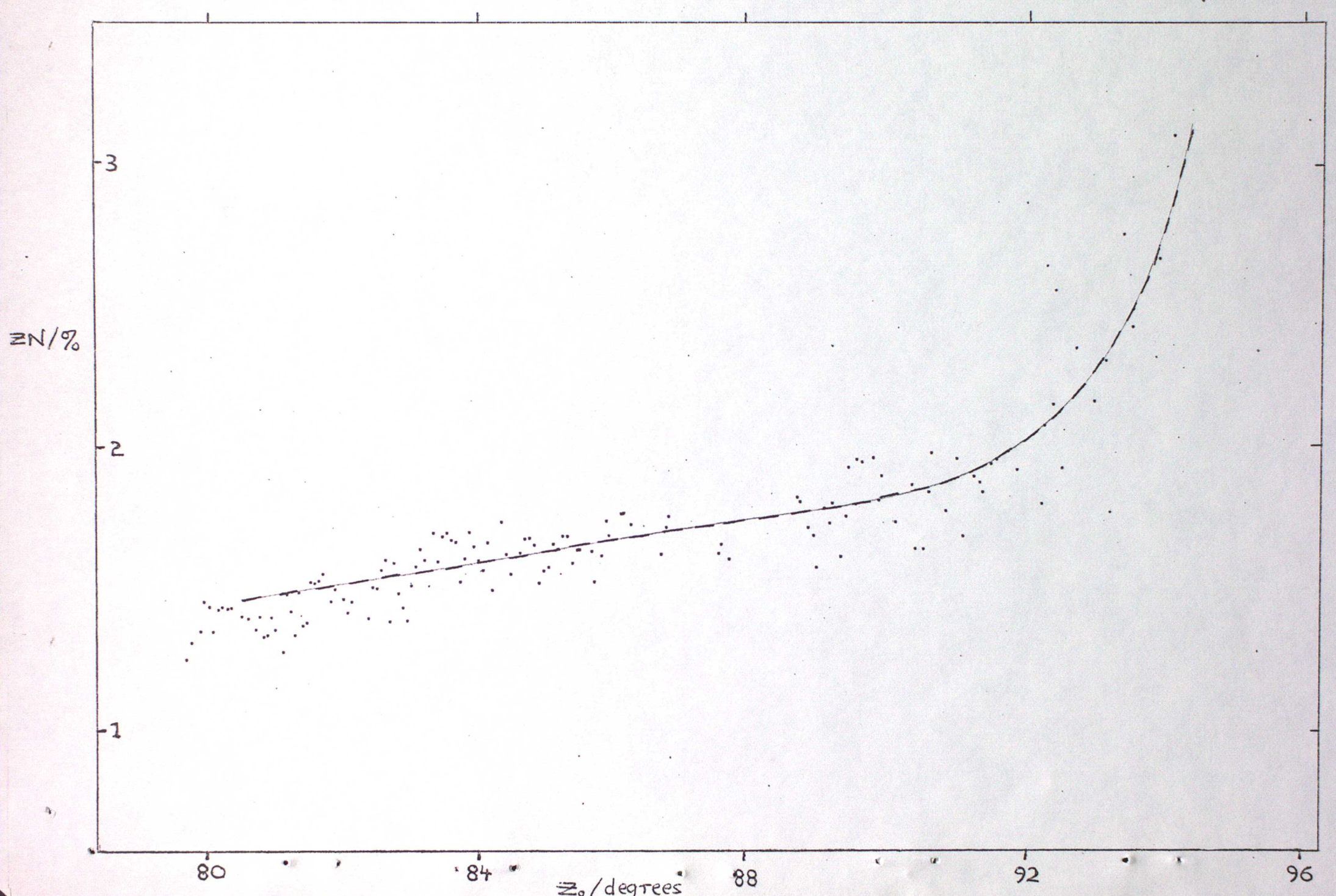

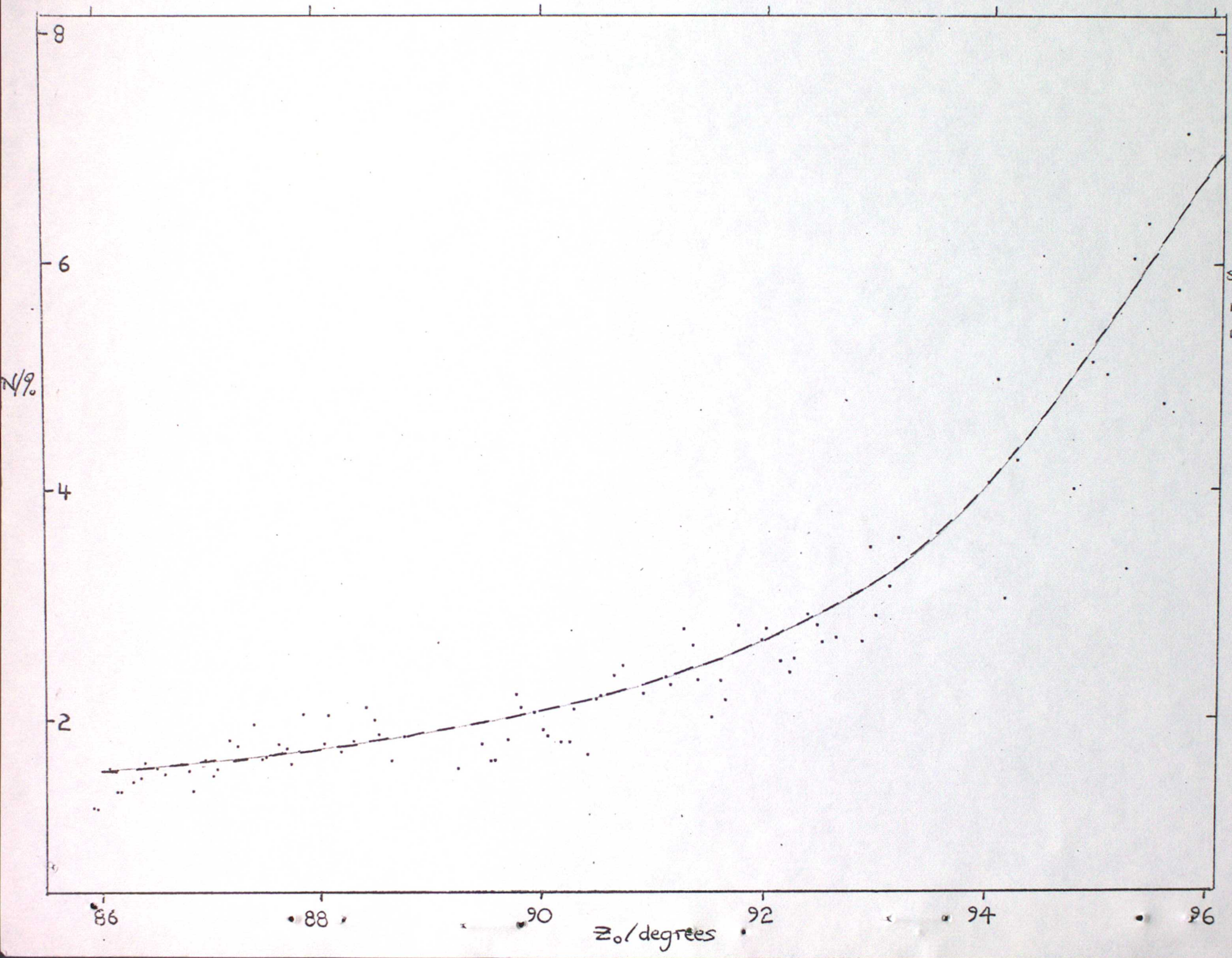

FIG 43

18/12/81 twilight sky NO_2 absorption, relative to reference (14/12/81).

FIG 44 11/1/82 twilight sky NO_2 absorption relative to reference (14/12/81).

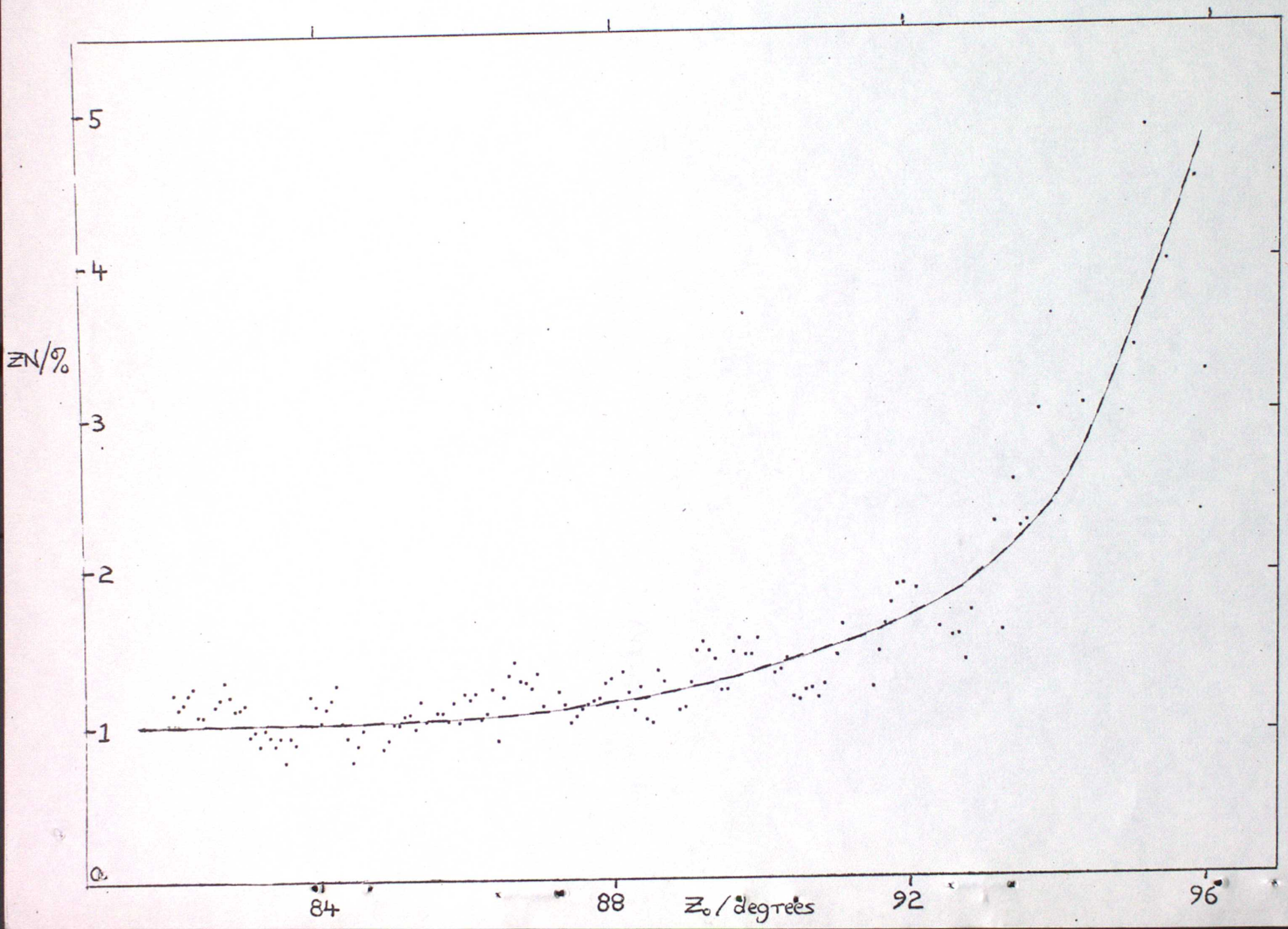

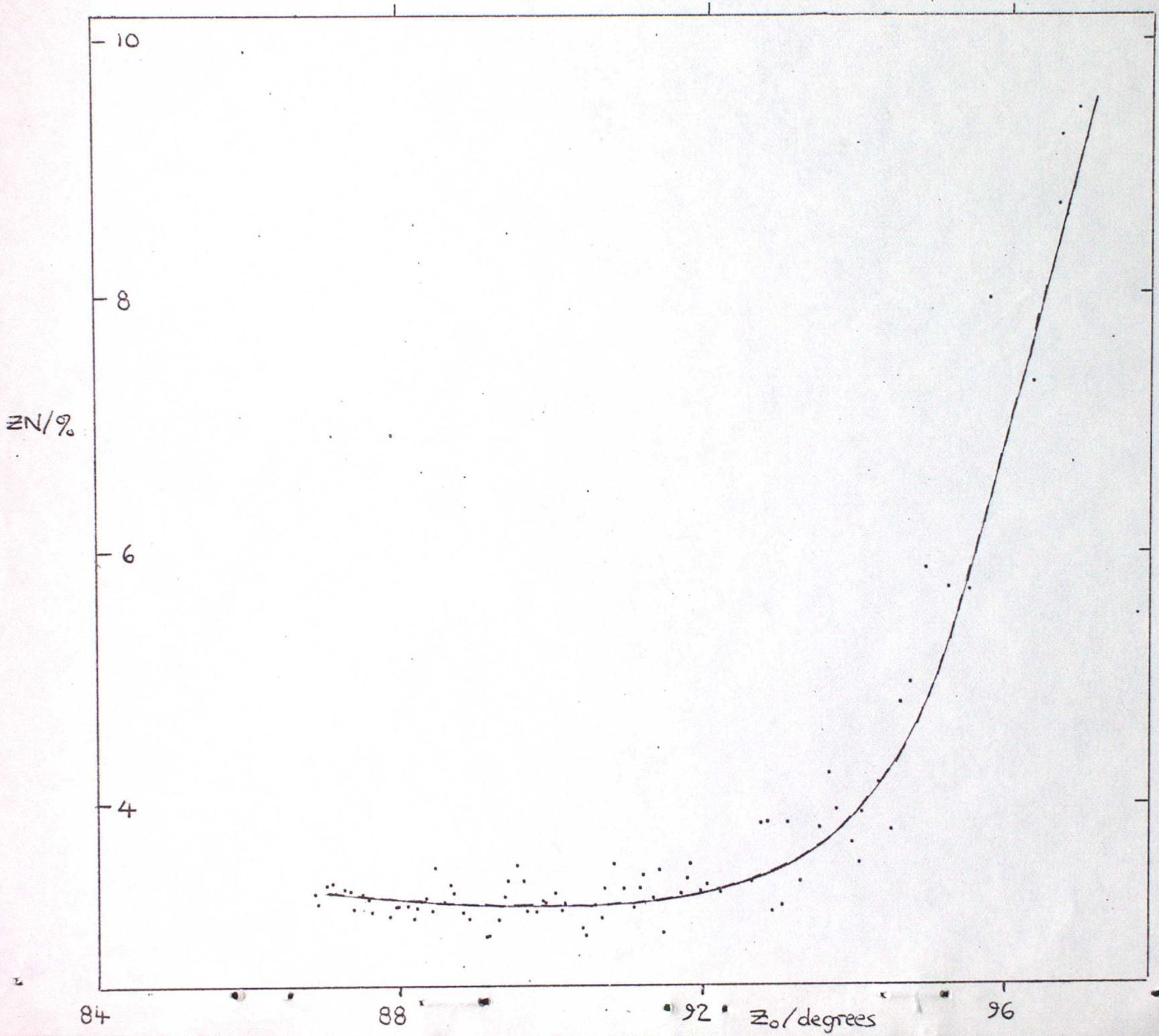

FIG 45.

13/1/82 twilight sky NO_2 absorption, relative to reference (14/12/81).

FIG 46 14/1/82 twilight sky NO_2 absorption, relative to reference (14/12/81).